The Role of HP1α and HP1β in Breast Cancer Progression

A thesis presented to Massey University in partial fulfilment of the requirements for the degree of

Master of Science
in
Biochemistry

at Massey University, Palmerston North,
New Zealand

Tahnee Maree Campbell

2012

Abstract

Breast cancer is the foremost cause of cancer-related deaths in New Zealand women. Metastasis of breast tumours increases the likelihood of fatality of the disease as treatment becomes more difficult and the tumours may interfere with the function of multiple organ systems. Consequently, the identification of biomarkers that may indicate the potential for a tumour to become metastatic are of great importance and may allow for the selection of more targeted treatment regimes.

Heterochromatin Protein 1 (HP1) is a chromatin associating protein that facilitates heterochromatic spreading through its interaction with trimethylated H3K9. There are three HP1 isoforms found in mammals, HP1α, HP1β and HP1γ, each with differing functions and chromatin localisation patterns. Previous research has demonstrated that deregulation of either HP1α or HP1β expression occurs in several types of cancers. Both increases and decreases in HP1α expression have been reported in breast tumour samples, with a decrease in HP1α associated with breast metastases. However, what role loss of HP1α may have in promoting a metastatic phenotype is unclear, and any contribution of HP1β to this process is also explored.

This thesis examined the roles of HP1α and HP1β in breast cancer progression through the creation of breast cancer cell lines with knock-down of either HP1α or HP1β. These cell lines were characterised for changes in proliferation, cell cycle profile, global chromatin compaction, invasive potential and anchorage independence. Though no changes were observed in the majority of these characteristics, a novel role for HP1β as a potential suppressor of anchorage independence was identified. Additionally, it was found that HP1α may act to enhance anchorage independence. This information could help to further knowledge of how breast cancer cells proceed towards metastasis, and provide new avenues of research into the potential for levels of HP1α or HP1β to be used as biomarkers for breast cancer progression.

Foreword and acknowledgements

The Road goes ever on and on
Down from the door where it began.
Now far ahead the Road has gone,
And I must follow, if I can,
Pursuing it with eager feet,
Until it joins some larger way
Where many paths and errands meet.
And whither then? I cannot say.

-J.R.R. Tolkein, *The Fellowship of the Ring*

Just over two yeas ago I began a new phase of my journey, one that has proved to be both more challenging and more rewarding than I could have imagined. The path leading to this point has traversed many twists, turns, rough patches and the occasional dead end, culminating in what felt like an attempt to scale the slippery slopes of Mount Doom while wearing roller blades. However, I had the great fortune of having many more people to provide help and encouragement throughout my journey than just one extremely loyal gardener. I am eternally grateful to the many people who have supported me over the last couple of years; thank you does not seem like enough. You were all integral in strengthening my resolve to keep going, and it is because of you that I can finally say that I have finished.

First and foremost, to my supervisor Dr Tracy Hale, a huge thank you for being my guide, for being so encouraging, for your humour, and for your exceptional tolerance. Thank you for giving me a home in your lab, and for everything you taught me, both science-related and otherwise. This journey has been anything but dull, and I will always look back on my time in your lab with great fondness.

To Sarah Bond, thank you for being such an excellent lab-buddy. Thank you for sharing your knowledge, for being eternally helpful, and for putting up with me for two years!

To Natisha Magan, thank you so very much for your kindness, for all the helpful discussions, for your time, for the excellent chai, and for your tremendous support during the final stages of writing. You are amazing.

To everyone in IMBS: thank you to everyone who answered my questions, let me use equipment or helped to make IMBS a more friendly place. Special thanks to Ann Truter and Cynthia Cresswell, and also to everyone in the MMIC who have helped me with microscopy over the past two years Also thank you to IMBS for financial assistance to attend the 2011 Epigenetics Satellite Meeting in Queenstown. I am also thankful to the Cancer Society of New Zealand for funding this research.

Thank you to all my friends, workmates and extended family for your support and for showing an interest in my research, even if you didn't entirely understand it. Extraordinary thanks go to Mum, Dad, Janae (plus Mark and Brooklyn), Justin, and especially my darling Jeremy for cheering me on, for listening to me whine and for providing the occasional attitude adjustment when I needed it. I will always appreciate the endless love, tolerance and encouragement, especially when times were tough and the end seemed so far away. But what I must thank you for, most of all, is your ability to believe in me when I could not. I love you all very much and know I am incredibly lucky to call you my family.

Abbreviations

°C	Degrees celsius
APS	Ammonium persulfate
BCA	Bicinchoninic acid
BRCA1	Breast cancer type 1 susceptibility protein
BrdU	Bromodeoxyuridine
BSA	Bovine serum albumin
c-Myc	Avian myelocytomatosis virus oncogene cellular homolog
CAF-1	Chromatin assembly factor protein 1
CBX	Chromobox homolog
cDNA	Complementary DNA
CI	Cell index
CP	Crossing point (PCR)
DAPI	4',6-diamidino-2-phenylindole
DCIS	Ductal carcinoma in-situ
dH_2O	Distilled water
DMEM	Dulbecco's modified eagle medium
DMSO	Dimethyl sulfoxide
DNA	Deoxyribose nucleic acid
Dnmt	DNA methyltransferase
dNTP	Deoxyribonucleotide triphosphate
E2F5	E2 transcription factor 5
ECM	Extra cellular matrix proteins
EDTA	Ethylenediaminetetraacetic acid
ER	Estrogen receptor
ERK	Extracellular-signal-regulated kinase
FACS	Fluorescence activated cell sorting
FBS	Foetal bovine serum
GDP	Guanosine diphosphate
GTP	Guanosine triphosphate
GTPase	Guanosine triphosphatase
g	grams
GST	Glutathione S-transferase
H3K9	Lysine 9 of histone H3
HC	Hygromycin control cell line
HCl	Hydrochloric acid
HER2/neu	Human epidermal growth factor 2
hMis12	Human MIND kinetochore complex component factor homolog
HP1	Heterochromatin protein 1
HRP	Horse-radish peroxidase

hTERT	Human telomerase reverse trancriptase
IgG	Immunoglobulin G
INCENP	Inner centromere protein
JAK/STAT	Janus kinase/Signal transducer and activator of transcription
Kap1-Tif1β	Kruppel-associated box (KRAB)-associated protein/transcriptional intermediary factor 1β
Kb	Kilobase
KCl	Potassium chloride
KD	Knock-down
kDa	Kilodaltons
KH_2PO_4	Potassium dihydrogen phosphate
Ku70	Ku autoantigen protein 70
L	Litre
LB	Luria-Bertani bacteriological media
M	Moles per litre
mg	Milligram
Mg	Magnesium
µg	Microgram
µL	Microlitre
mL	Millilitre
mM	Millimoles per litre
mRNA	Message RNA
$Na_2HPO_{4-}7H_2O$	Sodium monohydrogen phosphate heptahydrate
NaCl	Sodium hydroxide
$NaHCO_3$	Sodium bicarbonate
NC	Neomycin control cell line
NF-κB	Nuclear factor kappa-light-chain-enhancer of activated B cells
ng	Nanograms
nm	Nanometres
NP40	Nonyl phenoxypolyethoxylethanol
NRF-1	Nuclear respiratory factor 1
PBS	Phosphate buffered saline
PCR	Polymerase chain reaction
penstrep	Penicillin/streptomycin
PI	Propidium iodide
pmol	Picomole per litre
qRT-PCR	Quantitative reverse transcription polymerase chain reaction
Rac1	Ras-related C3 botulinum toxin substrate 1
RAS	Rat sarcoma protein
RB	Retinoblastoma protein
RIPA	Radioimmunoprecipitation assay buffer
RISC	RNA-induced silencing complex

RLU	Relative light units
RNA	Ribonucleic acid
RNase	Ribonuclease
RT-PCR	Reverse transcription polymerase chain reaction
SDS	Sodium dodecyl sulfate
SDS-PAGE	Sodium dodecyl sulfate polyacrylamide gel electophoresis
shRNA	Short hairpin RNA
siRNA	Small interferring RNA
SUV39HI	Suppressor of variegation 3-9 homolog 1
$TAF_{II}130$	TATA-binding protein associated factor p130
TBE	Tris/borate/EDTA buffer
TBS	Tris-buffered saline
TEMED	Tetramethylethylenediamine
Tris	Tris(hydroxymethyl)aminomethane
U	Units
UV	Ultraviolet
V	Volts
Wnt1	Wingless-integration 1 protein
YY1	Yin-yang 1 transcription factor

List of Figures

List of Tables

Table of Contents

1. Introduction

1.1 Cancer

Cancer is defined as a malignant growth resulting from uncontrolled cell division. The cell cycle is usually a carefully regulated process with a variety of check-points and enzymes that control its progress, and consequently cells will divide only a fixed number of times before becoming senescent (Campisi, 2005). In cancer, however, deregulated cell division enables cells to proliferate unchecked and tumourigenesis begins (Campisi, 2005). In addition to uncontrolled proliferation, tumourigenesis requires other changes in cellular phenotype, such as a loss of contact inhibited growth (Assoian, 1997; Bissell and Radisky, 2001; Freedman and Shin, 1974). As a primary tumour develops it can establish its own blood supply to ensure that it can meet its metabolic needs; this is a process known as angiogenesis (Weidner *et al.*, 1992).

Following tumorigenesis, cancer cells may continue through the sequential series of cellular events that result in metastasis (Bissell and Radisky, 2001; Steeg, 2006). Once new blood vessels have been established, the cells may become anchorage-independent (reduced need to adhere to extracellular matrix) and invade surrounding tissues and move into the blood circulatory system, a process known as intravasion (Wyckoff *et al.*, 2000). Following this, the cells must be able to survive in the circulatory system without being destroyed by immune cells (Chambers *et al.*, 2002). Cells that move from the circulatory system into surrounding tissue must be able to establish and maintain sufficient growth to form metastases (Chambers *et al.*, 2002).

Up-regulation or down-regulation of specific genes have been associated with tumorigenesis. Mutations in proto-oncogenes encoding the signal transduction proteins wingless-integration 1 (Wnt1), avian myelocytomatosis virus oncogene cellular homolog (c-Myc), extracellular-signal-regulated kinase (ERK) and rat sarcoma protein (RAS) may up-regulate their expression (Bos, 1989; Little *et al.*, 1983; Polakis, 2000; Xia *et al.*, 1995). The resulting de-regulated signal transduction can lead to decreased apoptosis or increased proliferation in cancer cells (Cantley *et al.*, 1991). For example,

one or more of the three *ras* genes, H-*ras*, K-*ras*, and N-*ras*, are mutated in many cancer types, including some thyroid, liver and colon cancers (Bos, 1989). *Ras* mutations can be an important step in tumourigenesis as cancer cells must be able to overcome the senescence or apoptosis that normally results from oncogene over-expression (Serrano *et al.*, 1997). Conversely, mutations in tumour suppressor genes results in lost or diminished function of the proteins they encode (Hanahan and Weinberg, 2000). Like oncogenes, the proteins products of tumour suppressor genes are often involved in cell cycle regulation and promoting apoptosis (Hanahan and Weinberg, 2000). The retinoblastoma (RB) and p53 proteins are products of tumour suppressor genes found to be lost in many cancer types, including 70% of colon cancers (RB and p53) and 30-50% of breast cancers (p53) (Friend *et al.*, 1987; Hollstein *et al.*, 1991; Levine *et al.*, 1991; Toguchida *et al.*, 1988).

1.2 Breast cancer

Breast cancer is the most commonly diagnosed form of cancer in women worldwide (Tavassoli, 2003). Significantly, breast cancer is also the greatest cause of cancer-related deaths in New Zealand women (M.O.H, 2004). Metastasis, where cells from the primary tumour gain the ability to detach and spread into other areas of the body, is the leading cause of death resulting from breast cancer (Chambers *et al.*, 2002; Steeg, 2006). This is due to the serious challenge metastasis presents in treatment, as metastatic lesions can continue to grow even after a primary tumour has been removed (Chambers *et al.*, 2002). Due to this, metastatic cells must be carefully targeted during the therapeutic regimen to ensure that recurrence of the disease does not occur (Steeg, 2006).

Between 40% and 75% of all breast cancers diagnosed worldwide are of the ductal sub-type, which arise from mammary ductal epithelial cells (Rakha *et al.*, 2010; Tavassoli, 2003). These cells can undergo changes leading to increased proliferation, which may result in atypical ductal hyperplasia, a benign lesion of the breast that can progress to cancer (Page *et al.*, 1985). Atypical ductal hyperplasias can develop into a ductal carcinoma in-situ (DCIS), a non-invasive breast cancer (Silverstein *et al.*, 1995). DCIS

have the potential to progress to form invasive ductal carcinomas, which invade into the surrounding breast tissue (Oberman, 1987). From here, breast cancer cells may invade the lymph nodes, or may move into the blood stream and metastasise to other organs (Chambers *et al.*, 2002; Weidner *et al.*, 1991). Breast cancer is commonly found to metastasise to areas such as brain, liver, lungs and bone (Paget, 1989).

1.2.1 Staging and clinical markers

Breast cancer is a complex disease with characteristic diagnostic stages. Each stage can be determined by examining tumour size, whether any metastases to the lymph nodes are present, or if any distant metastases are found (Singletary *et al.*, 2002). Stage 0 is defined as a carcinoma in-situ with no metastasis to lymph nodes or more distant sites. Stage I is a tumour smaller than 2cm diameter; where micrometastases may be present in less than three lymph nodes but there are no distant metastases. Stages II-III are both characterised by a tumour that may be larger than 2cm, and micrometastases may be found in four or more lymph nodes, but distant metastases are absent. Stage IV describes breast cancer with distant metastatic tumours. Stages I-III also have a variety of sub-stages dependent on tumour size and which lymph nodes the cancer has spread to (Singletary *et al.*, 2002).

In addition to breast cancer staging, other clinical biomarkers are examined to assess the severity of the disease, to determine a prognosis, and to help to decide upon the optimal treatment regime (Clarke *et al.*, 1998; Yamauchi *et al.*, 2001). The level of the human epidermal growth factor receptor 2 protein (HER2/neu) has been established as an important biomarker (Slamon *et al.*, 2001). Increases in HER2/neu have been shown to occur in around 30% of breast cancers, and this is associated with increased recurrence of the cancer and poor patient prognosis (Slamon *et al.*, 1987; Slamon *et al.*, 1989). Specialised treatments can be administered to reduce HER2/neu activity, currently by using a recombinant monoclonal antibody (Herceptin) that blocks the HER2/neu receptor (Slamon *et al.*, 2001).

Similarly, determining whether breast cancer cells express estrogen receptors (ERs)

is important to establish whether or not treatments that block ER activity will be effective (Clarke *et al.*, 1998). Estrogen stimulates proliferation in mammary cells, and around 70% of breast tumours have been shown to be ER positive (Harvey *et al.*, 1999). Breast cancer cells that do not express ERs are associated with higher disease recurrence rates, a poorer prognosis and increased growth rates (Schottenfeld *et al.*, 1976). For this reason, use of immunohistochemistry to determine ER status can aid in selecting an effective treatment plan, as the ER positive cells can be targeted by ER antagonists such as tamoxifen, but the ER negative cells will be less sensitive to them (Clarke *et al.*, 1998; Harvey *et al.*, 1999).

While the biomarkers and clinical staging of breast cancers mentioned here provide a basis for determining an optimal treatment plan, further characterisation of the molecular mechanisms involved in metastasis and cancer progression would enable treatment to become even more specific. Examining changes in gene expression or post-translational modification of proteins may also allow for better prediction of breast cancer metastasis, and enhanced efficacy of current treatment regimes.

1.2.3 Molecular mechanisms of metastasis

As mentioned earlier, mutations in tumour suppressor genes and proto-oncogenes contribute to tumorigenesis. There are a number of other genes that are important for metastasis, and some of the genes implicated in breast cancer metastasis have been identified. Over-expression of the transcription factor Twist is thought to contribute to metastasis by promoting an epithelial-mesenchymal transition (Yang *et al.*, 2004). Repression of Twist increased metastasis of primary mammary tumours in mice, and was found to be highly expressed in the highly-infiltrating and invasive lobular carcinoma in humans (Yang *et al.*, 2004). Maspin, the product of the *SERPINB5* tumour suppressor gene, has been implicated in preventing metastasis in breast cancer cells (Zou *et al.*, 1994). It was found to inhibit the ability of invasive breast cancer cells to metastasize in mice, and was also shown to be lost in human advanced breast tumour samples (Debies and Welch, 2001). Similarly, the proto-oncogene *ERBB2* gene (encodes the HER2/neu protein) has been found to be important in the progression of certain

types of aggressive breast cancer (Slamon *et al.*, 1987). Additionally, a series of genes known as metastasis suppressors have been found to have the ability to prevent metastasis in breast cancer cells (Hunter *et al.*, 2001). Allelic variation in one of these genes, the *BRMS1* metastasis suppressor gene, has been shown in mice to cause variation in the ability of mammary tumours to metastasise (Hunter *et al.*, 2001).

As already mentioned, some genes have been implicated in breast cancer metastasis, but there is still much that is unknown about the underlying molecular mechanisms of metastasis. In recent years, epigenetics has emerged as a factor in cancer development and progression. Changes in chromatin structure and genomic stability have been observed in breast tumours. Mammary tumour samples with cells displaying larger nuclei have been shown to correlate with an increase in aggression and mortality, and that breast cancer is associated with a loss of specific genomic organisation (Komitowski and Janson, 1990; Komitowski *et al.*, 1993). Large scale changes in chromatin structure have also been observed in breast tumour samples, with aneuploidy and chromosomal rearrangements also not uncommon (Dutrillaux *et al.*, 1990). The changes in chromatin structure and genome stability seen in breast tumours raises the question of whether these changes might be caused by abnormal chromatin regulation. Histone modifications, DNA methylation and chromatin modification need to be further examined to define their potential roles in cancer progression.

1.3 Regulation of chromatin

1.3.1 Chromatin structure and function

DNA is packaged into chromatin, a structure that compacts, constrains and folds strands of DNA using histone and non-histone proteins (Jenuwein and Allis, 2001). Around 147 base pairs of super-helical DNA are wrapped around a histone octomer comprised of two histone H2A/H2B dimers and two histone H3/H4 dimers, forming a nucleosome core structure (Luger *et al.*, 1997; McGhee and Felsenfeld, 1980). This structure is found roughly every 200 ± 40 base pairs in eukaroytic genomes (McGhee and Felsenfeld, 1980). Nucleosomes, which are further stabilised by the linker histone H1,

are coiled together to form 30 nm fibres (Felsenfeld and McGhee, 1986). These can be further packed to form higher order chromatin structures, including chromosomes.

Chromatin can be divided into two sub-categories based on its state of compaction: euchromatin and heterochromatin. Euchromatin is generally less condensed, has a more "open" structure, and is associated with higher transcriptional activity than heterochromatin (Jenuwein and Allis, 2001). Heterochromatin is typically highly condensed and less transcriptionally inactive, owing in part to a greater inaccessibility to transcriptional machinery (Jenuwein and Allis, 2001). Heterochromatin generally contains less protein coding genes than euchromatin. However, it does contain some genes that are important for chromosome structure or functions, including meiotic homologue pairing and maintenance of telomeres and centromeres (de Lange, 2005; Dernburg *et al.*, 1996; Karpen *et al.*, 1996; Yasuhara and Wakimoto, 2006). Transcriptionally silent heterochromatin can be further sub-categorised into facultative and constitutive heterochromatin. Constitutive heterochromatin describes regions of chromosomes that remain condensed in all cell types, such as at telomeres and centromeres (Grewal and Jia, 2007). Facultative heterochromatin, in contrast, has the ability to convert between euchromatin and heterochromatin (Trojer and Reinberg, 2007). This can restrict transcription to specific times, such as during certain developmental states or phases of the cell cycle (Trojer and Reinberg, 2007).

In addition to its roles in gene silencing, heterochromatin also has a role in genomic stability. Studies have found that compromised heterochromatin composition (resulting from mutating genes that regulate heterochromatin structure) caused an increase in spontaneous DNA damage in the heterochromatin of somatic and meiotic cells (Peng and Karpen, 2009). Heterochromatin formation is also necessary to maintain the stability of repeat DNA sequences, potentially by preventing inappropriate homologous recombination (Peng and Karpen, 2007). Decreased levels of heterochromatin in mice and *Drosophila* have also been shown to increase chromosomal instability, generating defects in chromosomal compaction and segregation during mitosis (Peters *et al.*, 2001; Yan *et al.*, 2011).

1.3.2 Histone and DNA modifications

As mentioned, the protein component of a core nucleosome is made up of the H2A, H2B, H3 and H4 histones. These are small basic proteins consisting of a globular domain and a flexible, charged NH_2-terminus (often referred to as the "tail") that projects from the nucleosome (Jenuwein and Allis, 2001). Enzymes such as histone methyl transferases, histone deacetylases and histone acetyl transferases specifically either add or remove post-translational modifications to histone tail amino acid residues (Strahl and Allis, 2000). The resulting methylation, acetylation or phosphorylation marks create a dynamic histone "code" that can be recognised by other proteins (Jenuwein and Allis, 2001).

Specific histone modifications have been associated with cellular functions including transcriptional activation or silencing and chromosome condensation (Strahl and Allis, 2000). Transcriptionally active and "open" euchromatin has been found to be associated with methylation of H3 at lysine four, whereas methylation of H3K9 can be associated with less transcriptionally active and more condensed heterochromatin (Kouzarides, 2007). Histone acetylation is often associated with transcriptional activation, while deacetylation correlates with transcriptional repression (Kouzarides, 2007). Other histone tail modifications, such as phosphorylation of histones H1 and H3, have been implicated in chromosome condensation during mitosis (Bradbury, 1992; Koshland and Strunnikov, 1996). H3 phosphorylation at serine ten, potentially together with phosphorylation of H3 at serine 28, may also be required for correct chromosome condensation and segregation in mitosis (Hendzel, 1997; Wei *et al.*, 1999).

DNA itself can also be modified by the addition or removal of methyl groups to cytosine or adenines by DNA methyl transferases, typically at CpG nucleotide sequences (Bird, 1992, 2002). This form of methylation is generally associated with transcriptional silencing, potentially by physically blocking transcriptional machinery or by recruiting other histone modifying proteins that promote heterochromatin formation (Bird, 2002). Global DNA methylation has been implicated in silencing of certain genes expressed only during particular developmental stages (Jaenisch, 1997).

1.3.3 Epigenetic regulation and cancer

Altered gene expression and mutations have been well-established as contributors to cancer progression. However, changes in DNA methylation and histone modifications have also been implicated in tumourigenesis and cancer progression, possibly through altering gene expression patterns (Jones and Baylin, 2007). DNA methylation-mediated silencing of genes required for normal cell function has been suggested to be an early event during cellular transformation. Loss of these genes can remove the safeguards that prevent abnormal proliferation, allowing tumorigenesis to begin (Jones and Baylin, 2007). Conversely, a decrease in DNA methylation may be an important event in establishing neoplasia, which is the abnormal new growth of cells (Feinberg and Vogelstein, 1983). Hypomethylation of several genes has been observed in cells extracted from tumour samples, but not in the same genes in normal tissue (Feinberg and Vogelstein, 1983).

Changes in histone modifications have also been shown to play a role in cancer. It has been suggested that a global loss of both monoacetylation at lysine 16 and trimethylation at lysine 20 of histone H4 is a hallmark of cancer, as this change is seen in leukaemia and lymphoma cell lines but is not present in normal tissue samples (Fraga *et al.*, 2005). Alterations in other global histone marks have also been associated with a poorer outcome in cancer (Rogenhofer *et al.*, 2012; Schneider *et al.*, 2011). A decrease in global trimethylation of lysine 20 on histone H4 in human bladder cancers has been shown to correspond with increased patient mortality (Schneider *et al.*, 2011). Similarly, renal cell carcinomas show a global decrease in levels of histone H3 lysine 9 mono-methylation compared to benign renal tissue samples, and this decrease correlates with a poor patient prognosis (Rogenhofer *et al.*, 2012). Altered levels of histone modifications such as those mentioned here may disrupt the histone "code" in cancerous cells, potentially impacting the proteins that recognise specific histone marks. One such protein is Heterochromatin Protein 1 (HP1), which interacts with trimethylated lysine 9 of histone H3 (Lachner *et al.*, 2001).

1.4 Heterochromatin Protein 1

1.4.1 Discovery

In 1981, a study by Reuter and Wolff (1981) was carried out to identify genes in *Drosophila* involved in suppressing position-effect variegation. This is a form of mosaic silencing resulting from a euchromatic gene being placed within or next to heterochromatin (Sinclair *et al.*, 1983; Wustmann *et al.*, 1989). Fifty mutations capable of suppressing position-effect variegation were identified (Reuter and Wolff, 1981). One of genes found to suppress position-effect variegation, S*u(var)2-5*, was mapped to the *Drosophila* 2L chromosome and the protein it encoded was identified as a non-histone chromosomal protein that associated with heterochromatin (James and Elgin, 1986). This protein was given the name Heterochromatin Protein 1 (HP1), and mutational analysis confirmed that the mutant form of this protein could no longer suppress position-effect variegation, providing an insight into its role (Eissenberg *et al.*, 1990). HP1 was subsequently shown to be essential in *Drosophila*, as all known mutations in the S*u(var)2-5* gene are recessive lethal (Eissenberg and Elgin, 2000). In the years that followed, homologues of HP1 were found in eukaryotes ranging from *Sacchromyces pombe* to humans (Lorentz *et al.*, 1994; Saunders *et al.*, 1993b; Singh *et al.*, 1991a; Ye and Worman, 1996).

1.4.2 HP1 Isoforms

The HP1 isoforms are largely conserved among metazoans (Lomberk *et al.*, 2006; Singh *et al.*, 1991b). Mammalian cells each contain three HP1 isoforms, in humans these are named HP1α, HP1β and HP1γ (Lomberk *et al.*, 2006). HP1α was the first of the HP1 proteins to be identified in humans through its high DNA sequence homology to *Drosophila* HP1 (Saunders *et al.*, 1993a). The gene encoding human HP1β was initially mistaken for a copy of HP1α, and the human HP1γ protein was identified due to its 98% shared amino acid sequence with the mouse chromodomain protein (Singh *et al.*, 1991b; Ye and Worman, 1996). The three human HP1 proteins are encoded by the *chromobox homolog* (*CBX*) genes; *CBX5* (HP1α), *CBX1* (HP1β) and *CBX3* (HP1γ) (Li *et al.*, 2002;

Ye and Worman, 1996). The translated human HP1α, HP1β, and HP1γ amino acid chains are 191, 185 and 173 residues in length respectively, and sequence homology between these and the *Drosophila* HP1 protein is reasonably high (between 49% and 54% amino acid sequence identity) (Li *et al.*, 2002; Saunders *et al.*, 1993a; Singh *et al.*, 1991b). Each of the three human HP1 proteins are around 25 kDa in molecular weight (Li *et al.*, 2002).

1.4.3 HP1 structure

All HP1 proteins identified in eukaryotes share well-conserved structural characteristics: all are relatively small (15-35 kDa), and each have an amino-terminal chromodomain and an carboxy-terminal chromoshadow domain linked by an unstructured, variable hinge region (Figure 1.1). A 44 amino acid sequence motif within HP1 has been found to be identical to a protein domain in the *Drosophila* homeotic gene silencer *Polycomb* (Paro and Hogness, 1991). This domain was named according to its function as a "chromosome organisation modifier", or "chromodomain" (Paro and Hogness, 1991). Interestingly, the chromodomain of HP1 was shown to be functionally interchangeable with the *Polycomb* chromodomain (Ball *et al.*, 1997). The HP1 chromodomain consists of an α helix packed against a three-stranded β sheet, and has an overall negative surface charge distribution that is well-suited for protein-protein interaction (Ball *et al.*, 1997; Platero *et al.*, 1995). A fusion protein containing only the chromodomain of HP1 has been shown to be sufficient for targeting to heterochromatin. (Ball *et al.*, 1997).

The HP1 chromoshadow domain is similar to the chromodomain in the primary sequence. It forms a hydrophobic binding pocket, and, unlike the chromodomain, forms a tightly associated symmetrical dimer (Brasher *et al.*, 2000; Cowieson *et al.*, 2000). The chromoshadow domain is able to interact with a large variety of proteins, which often contain the PXVXL pentapeptide motif (Li *et al.*, 2002; Thiru *et al.*, 2004). The way it interacts with these proteins can be somewhat unusual; a study examining the binding of HP1β to a peptide containing the PXVXL motif showed that the interacting peptide bound across the dimer interface, and was sandwiched in a β-sheet between

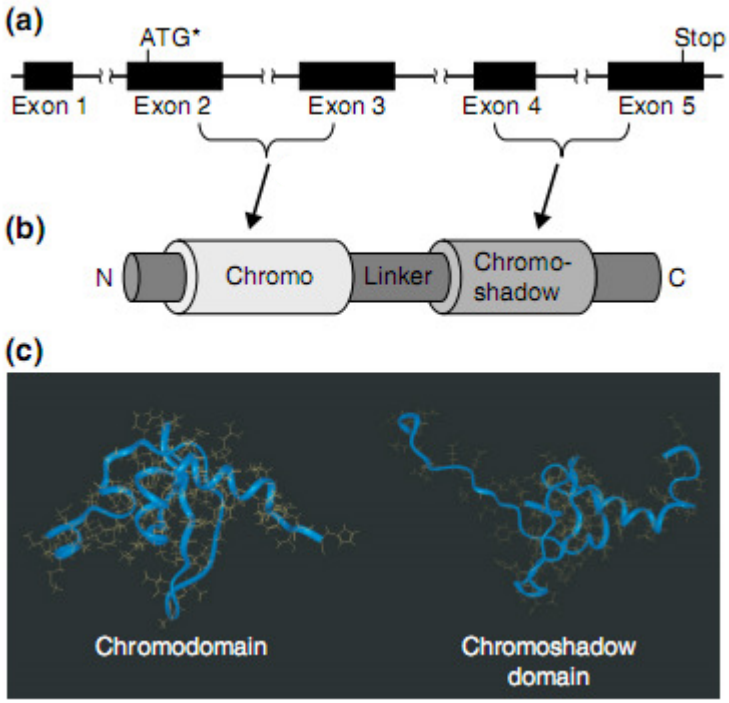

Figure 1.1 General structure of all HP1 proteins and their encoding genes (adapted from Lomberk *et al.*, 2006) **(a)** Conserved genomic structure of all genes encoding HP1 proteins. **(b)** Linear arrangement of the domains of the HP1 proteins. N represents the amino terminus, C the carboxy terminus. **(c)** Three dimensional structures of the murine HP1β chromodomain and chromoshadow domain

strands from each monomer (Thiru *et al.*, 2004).

1.4.4 HP1 localisation

Each HP1 isoforms exhibits distinct localisation pattens on chromatin. HP1α and HP1β are mainly found in constitutive heterochromatin, however their distribution does not entirely overlap, suggesting some unique functions (Bartova *et al.*, 2007; Dialynas *et al.*, 2007). HP1γ, on the other hand, differs from HP1α and HP1β in that it is typically associated with both euchromatin and heterochromatin (Minc *et al.*, 1999; Minc *et al.*, 2000). Yet only a portion of each of the three HP1 isoforms remains bound to chromatin at any given time. Their association with chromatin appears to be dynamic and cell-cycle dependent (Dialynas *et al.*, 2007). Most of the HP1α protein moves into the cytoplasm during mitosis, but some remains associated with pericentric heterochromatin (Schmiedeberg *et al.*, 2004). HP1α has been shown to be the only HP1 isoform that localised to the metaphase centromere, while HP1β localised most strongly to the interphase centromere out of all three isoforms (Hayakawa *et al.*, 2003). The dynamic nature of HP1 binding results may permit the unbound HP1 proteins to participate in other roles such as chromosome segregation and double-stranded break repair (Ainsztein *et al.*, 1998; Obuse *et al.*, 2004; Song *et al.*, 2001).

1.5 The role of HP1 in chromatin

As shown in Figure 1.2, the current model for HP1-mediated spreading of heterochromatic silencing proposes that HP1 binds to trimethylated H3K9, a mark enriched in heterochromatin, and recruits the SUV39HI histone methyl transferase (Bannister *et al.*, 2001; Lachner *et al.*, 2001). SUV39HI then methylates neighbouring H3K9 residues, which recruits more HP1 (Bannister *et al.*, 2001). HP1-mediated heterochromatin spreading is important in mediating silencing and proper chromatin compaction, but HP1 has also been implicated in processes such as telomere stability, chromosome segregation and nucleosome assembly (Ainsztein *et al.*, 1998; Sharma *et al.*, 2003; Vassallo and Tanese, 2002).

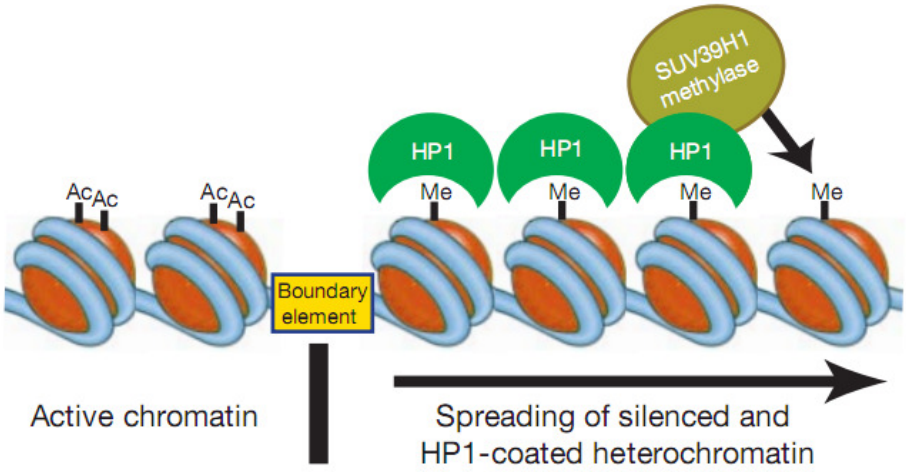

Figure 1.2 Model for heterochromatic spreading carried out by the SUV39H1/HP1 complex (Bannister *et al.,* 2001). Tri-methylated lysine 9 of histone H3 (orange) recruits HP1 (green) which in turn recruits a silencing complex containing the SUV39H1 methylase (brown). Further methylation of H3K9 by SUV39H1 propagates heterochromatic silencing along the DNA strand

1.5.1 Telomere stability and chromosome segregation

HP1 is important for maintaining telomeres, and has a role in chromosome segregation via its association with centromere proteins. HP1 is commonly found at telomeres, and HP1 mutant *Drosophila* larval neuroblasts have been shown to display a high frequency of telomere associations (Fanti *et al.*, 1998). This implies that HP1 had a function in telomere stability, and indeed, over-expression of HP1α and HP1β in human cells correlated with a decrease in associations between telomeres and human telomerase reverse transcriptase hTERT, a a catalytic subunit of telomerase (Sharma *et al.*, 2003). In addition to having abnormal telomeres, *Drosophila* HP1 mutants were found to be deficient in the ability to segregate chromosomes (Kellum and Alberts, 1995; Lu *et al.*, 2000).

A study by De Koning *et al.* (2009) investigated the effects of decreased HP1α on chromosome segregation in HeLa cells. Cells with HP1α knock-down induced via siRNA interference exhibited a greater proportion of chromosomes that were misaligned, lagging, or had bridges between them. This result was not observed when HP1β or HP1γ were knocked down (De Koning *et al.*, 2009). This indicates that HP1α may be important for chromosome segregation, a function that could be mediated through the proteins HP1α interacts with. A specific kinetochore protein, hMis12, specifically associates with HP1α (Obuse *et al.*, 2004). This protein is conserved in eukaryotes, and is essential for correct chromosome segregation (Obuse *et al.*, 2004). Similarly, the inner centromere protein (INCENP) also interacts with HP1α during centrosomal targeting and this aids in readying INCENP for its other cystoskeleton-based mitotic functions (Ainsztein *et al.*, 1998).

HP1β has also been shown to play a role in chromosome segregation (Aucott *et al.*, 2008). Cells isolated from the brains of mice with a null homozygous *CBX1* mutation exhibited profound genomic instability, including a significant increase in unpaired sister chromatids, premature centromere division, miconuclei formation, ploidy and the formation of diplochromosomes (chromosomes with four chromatids) compared to wild type mice (Aucott *et al.*, 2008). These events signifying genomic instability

occurred at a rate of less than 5% in wild type cells but increased to at least 38% in the *CBX1* null mice, emphasising a critical role for HP1β in maintaining genomic stability in mice (Aucott *et al.*, 2008).

1.5.2 Duplication of heterochromatin

HP1 has been implicated in nucleosome assembly during DNA replication through its interaction with a PXVXL motif in the p150 subunit of the chromatin assembly factor 1 protein (CAF-1) (Lechner *et al.*, 2000; Murzina *et al.*, 1999). The CAF-1 complex facilitates deposition of histone H3 and H4 onto newly replicated DNA at the replication fork (Kaufman *et al.*, 1995). The association of HP1 with CAF-1 at the replication fork provides a potential mechanism for re-establishing disrupted HP1-H3K9 binding during nucleosome assembly (Kaufman *et al.*, 1995). HP1 may then recruit other proteins involved in heterochromatin formation, thus ensuring proper duplication of heterochromatin during DNA replication (Maison and Almouzni, 2004).

1.6 Other functions of HP1

1.6.1 HP1 and DNA repair

Roles for the HP1 proteins in several DNA repair pathways have been proposed. HP1α interacts with Ku70, a protein that binds to DNA double-stranded break ends and that is necessary for the non-homologous end-joining repair pathway (Song *et al.*, 2001). BRCA1 is a second DNA repair protein that associates with HP1α, but is involved in the homologous recombination repair pathway (Maul *et al.*, 1998). All three human HP1 isoforms were shown to be recruited to UV-induced DNA lesions in a study carried out by Luijsterburg *et al.* (2011). They also concluded that the HP1 chromodomain was the most important for this function, and that *Caenorhabditis elegans* with HP1α knock-out were more susceptible to DNA damage caused by UV (Luijsterburg and van Attikum, 2011).

1.6.2 HP1 in transcriptional regulation

Each of the three HP1 isoforms may have roles in regulating transcription. HP1α has been found to directly associate with proteins that modify DNA or regulate transcription. These include the transcriptional co-repressor Kap1-Tif1β (Kruppel-associated box (KRAB)-associated protein/transcriptional intermediary factor 1β) and $TAF_{II}130$ (TATA-binding protein associated factor p130, a co-activator for multiple proteins that regulate transcription) (Nielsen *et al.*, 1999; Vassallo and Tanese, 2002). Both HP1α and HP1β interact with DNA methyl transferase-3a (Dnmt3a), and HP1β also binds to the DNA methyl transferase Dnmt1 (Bachman *et al.*, 2001; Fuks *et al.*, 2003). As both Dnmt1 and Dmnt3a possess transcriptional regulation activity independent of their methylation activity, an interaction of HP1α and HP1β with these proteins represents another mechanism through which HP1 may participate in gene regulation (Fuks *et al.*, 2003).

HP1β can act as a negative regulator of the HIV1 long terminal repeat promoter, and is present at the promoter with a non-processive RNA polymerase II prior to activation (Mateescu *et al.*, 2008). Post-activation, however, HP1β is replaced by HP1γ which then localises inside the coding region with a processive RNA polymerase II (Mateescu *et al.*, 2008). Another study has shown that HP1γ can a bind to the $TAF_{II}130$ transcriptional regulator protein, further demonstrating that HP1y has a role in transcriptional regulation (Vassallo and Tanese, 2002).

In order for specific proteins to effectively bind to DNA, an interaction with HP1β may be required (Shiota *et al.*, 2010). The androgen receptor (AR) is a member of the class I subgroup of the nuclear receptor family, and also a ligand dependent transcription factor (Fujimoto *et al.*, 1999). This receptor has been shown in a GST pull-down assay to interact with HP1β, but not HP1α or HP1γ (Shiota *et al.*, 2010). This interaction was found to be mediated through the HP1β chromodomain and DNA binding of AR was decreased when HP1β was knocked down through siRNA targeting (Shiota *et al.*, 2010).

1.6.3 HP1 as a tumour suppressor

Evidence that HP1 may have a role in tumorigenesis has been revealed using a JAK/STAT overexpression model. Over-expression of the JAK/STAT pathway contributes to the establishment of several types of cancer in humans and this pathway also contributes to tumorigenesis in *Drosophila* (Bromberg, 2001; Shi *et al.*, 2006). A study using *Drosophila* has demonstrated that when the JAK/STAT pathway was over-expressed, tumour-like lesions were observed (Shi *et al.*, 2006). However, loss of the HP1 protein through mutation of the HP1 gene caused an increase in the number of lesions. Correspondingly, an increase in wild-type HP1 expression lead to a reduction in lesion numbers (Shi *et al.*, 2006). This collectively demonstrates that HP1 may be capable of acting as a tumour suppressor in *Drosophila*.

1.7 Transcriptional regulation of HP1

Significant advances have been made in revealing how expression of HP1α could be regulated. The invasive breast cancer cell line MDA-MB-231 exhibits decreased levels of HP1α protein and mRNA compared to the non-invasive MCF-7 breast cell line (Kirschmann *et al.*, 1999; Thomsen *et al.*, 2011). Thomsen *et al.* (2011) examined levels of tri-methylated lysine 36 on histone H3 (a mark that indicates transcriptional activity) at the *CBX5* promoter, and found these to be decreased in the MDA-MB-231 cells. This decrease also correlated with lower levels of basal transcription factors bound at the *CBX5* promoter in the MDA-MB-231 cells (Thomsen *et al.*, 2011). The differences in HP1α expression between MCF-7 and MDA-MB-231 cells were not found to be due to differences in DNA methylation of the *CBX5* gene. However, several protein binding sites were identified within the promoter that may be involved in regulating HP1α expression (Norwood *et al.*, 2004).

A study conducted by Lieberthal *et al.* (2009) further characterised transcription factor binding sites within the *CBX5* promoter. Several DNA binding sites for the yin-yang1 (YY1) transcriptional regulator, nuclear respiratory factor-1 (NRF-1) and also a site for E2F were found in the *CBX5* promoter (Lieberthal *et al.*, 2009). The YY1 sites initially

appeared to be important for regulating *CBX5* promoter, but further investigation revealed that HP1α expression did not appear to change if YY1 levels were decreased (Lieberthal *et al.*, 2009). However, another study has shown that the E2F5 transcription factor may regulate transcription of the *CBX5* gene, as HP1α mRNA decreased in cells with reduced levels of E2F5 (Thomsen *et al.*, 2011). Further research is required to fully define the transcriptional regulation of HP1α, as well as that of HP1β and HP1γ.

1.8 Human HP1 expression

Ritou *et al.* (2007) have investigated levels of HP1 isoforms in a comprehensive range of human tissues. During initial microarray analysis, HP1γ mRNA levels were found to vary little between different tissue types (Ritou *et al.*, 2007). Consequently, only HP1α and HP1β protein levels were examined using immunohistochemical staining. A summary of the staining results for each tissue type can be seen in Table 1.1. Additionally, levels of all three HP1 isoforms were investigated in blood cells. Down-regulated HP1β and HP1α expression were observed during erythropoesis, but also that all three isoforms were present in peripheral blood leukocytes (Ritou *et al.*, 2007). The tissue-dependent expression of HP1α and HP1β seen in this study suggests that these isoforms are not essential in all human cell types.

1.9 HP1 expression in cancer

Decreased expression of a specific HP1 isoform has been reported in several cancer types. Studies using microarray analysis have demonstrated that reduced HP1α mRNA levels can be found in metastatic colon cancer cell lines, and also in 83% of papillary thyroid tumours compared to normal thyroid tissue samples (De Lange *et al.*, 2001; Wasenius *et al.*, 2003). A third microarray study was conducted using medulloblastoma tumours, which also showed down-regulation of HP1α mRNA expression (Pomeroy *et al.*, 2002). Immunohistochemical staining of a thyroid tissue microarray containing samples ranging from normal tissue to advanced thyroid tumours showed that a decrease in HP1β staining correlated with cancer progression (Contreras *et al.*, 2009). Lastly, HP1γ expression is down-regulated in some ovarian

Tissue/cell type	HP1α	HP1β
Skin		
Stratum basalis	+	+
Stratum spinosum	+	+
Stratum granulosum	+	+
Stratum lucidum	-/+	+
Stratum corncum	-/+	+
Sebaseous glands	+/-	+
Sweat glands	+	+
Liver		
Hepatocytes	-	-
Kupffer cells	-	+
Bile duct cells	+	+
Marrow		
Megakaryocytes	+	-
Proerthryblasts	+	+
Basophilic erythroblasts	-/+	-/+
Normoblasts	-	-
Promyelocytes	+	+
Early myelocytes	-	-/+
Metamyelocytes	-/+	-
Seminiferous tubules		
Sertoli cells	+	-/+
Spermatogonia	-	+
Primary spermatocytes	+	+
Secondary spermatocytes	-/+	+
Spermatazoa	-	-
Stomach		
Smooth muscle fibres	+/-	+
Gastric gland (surface)	+/-	+
Gastric gland (deep position)	+/-	-/+
Skeletal muscle		
Muscle fibres	+/-	+/-
Fibroblasts	+/-	+
Adipocytes	+/-	ND
Mammary gland		
Epithelial cells	+/-	+
Myoepithelial cells	+/-	+

Table 1.1 Summarised results of immunohistochemical staining of HP1α and HP1β in human tissues (Ritou *et al.* 2007).+ indicates strong staining, - indicates undetectable staining, +/- denotes weak staining in most cells of this type, and -/+ indicates that there was no staining in most cells of this type. ND is not determined.

cancer cell lines relative to control cell lines (Maloney *et al.*, 2007).

Enhanced expression of the HP1 isofoms have also been seen in some cancer types. A study by Popova *et al.* (2006) demonstrated that HP1α, HP1β and HP1γ protein levels were significantly increased in peripheral blood leukocytes of patients with advanced leukaemia compared to peripheral blood leukocytes from normal donors or chronic myeloid leukaemia patients (Popova *et al.*, 2006). Similar increases in HP1γ protein were observed in seminoma tumours, which are germ cell cancers of the testes, and increased HP1α levels have also been seen in teratomas (encapsulated tumours containing several types of tissues that are not native to the tumour location) with epithelial and neuronal differentiation (Bartkova *et al.*, 2011). Up-regulated HP1β expression has been correlated with an increased likelihood of cancer progression in prostate tumour samples (Shiota *et al.*, 2010).

The studies mentioned here demonstrate that HP1 isoforms in cancer may be either up-regulated or down-regulated in specific tumour varieties. As altered HP1 isoform levels are seen in such a variety of tumour types and cancer cell lines, this may suggest that deregulation of the normal expression patterns of the HP1 proteins contributes to cancer progression.

1.9.1 HP1α in breast cancer

HP1α expression is also altered in breast cancer cell lines and tumours (De Koning *et al.*, 2009; Kirschmann *et al.*, 1999). Reverse transcriptase polymerase chain reaction was used to demonstrate that the invasive breast cancer cell lines HS578T and MDA-MB-231 exhibited little HP1α expression and no decrease in either HP1β or HP1γ when compared with the non-invasive (HP1α-expressing) breast cancer cell lines MCF-7 and T47D (Kirschmann *et al.*, 1999). A second study by De Koning *et al.* (2009) examined protein levels of HP1α, HP1β and HP1γ in two breast cell lines, Hs578T and Hs578Bst. These cell lines were originally derived from the same patient, Hs578T from a carcinosarcoma of epithelial origin, and Hs578Bst from normal tissue peripheral to the tumour (Hackett *et al.*, 1977). The Hs578T cells were

shown to have increased HP1α mRNA and protein levels from both chromatin bound and soluble fractions, compared to the Hs578Bst cells (De Koning *et al.*, 2009). HP1β and HP1γ levels were reported to be the same in both cell lines (De Koning *et al.*, 2009). Collectively this evidence indicates that deregulation of normal HP1α expression patterns may be an important biomarker in defining breast cancer progression.

Studies have established a correlation between decreased HP1α and enhanced invasive potential in breast cancer cell lines. Norwoord *et al.* (2006) created MCF-7 cell lines with stable HP1α knock-down which were assayed for changes in invasive potential. This was measured by determining the percentage of cells able to pass through pores in a plastic membrane that had been coated with extracellular matrix proteins (Kirschmann *et al.*, 2000). It was found that MCF-7 cells with decreased HP1α were up to 50% more invasive than the MCF-7 control cell lines (Norwood *et al.*, 2006). Additionally, studies have examined whether re-introducing HP1α could "rescue" invasive MDA-MB-231 cells. The MDA-MB-231 cells with re-introduced HP1α did in fact become up to 30% less invasive; further supporting the idea that HP1α has a causal role in invasion (Kirschmann *et al.*, 2000).

Altered levels of HP1α have also been observed in breast malignancies compared to normal tissue, although contrasting results have been reported. One specific study by Kirschmann *et al.* (2000) examined normal breast tissue, primary mammary tumours and breast metastases using immunohistochemical staining with an antibody raised against HP1α. This study demonstrated that seven out of nine breast metastases displayed a decrease in HP1α when compared to primary breast tumours and normal breast tissues. HP1α staining in the normal breast tissues and in the primary tumours was shown to be similar (Kirschmann *et al.*, 2000).

A second study carried out by De Koning *et al.* (2009) also examined HP1α levels in breast tumours and normal tissue samples using immunohistochemical staining with antibodies raised against HP1α. Interestingly, this study observed an increase in HP1α levels in pancreatic, uterine, prostate and breast tumours compared with

normal tissue samples (De Koning *et al.*, 2009). HP1α protein levels were further examined specifically in breast tumour samples, and 64 out of 86 primary breast tumours were reported to have increased HP1α staining compared to matched normal breast tissue samples. De Koning *et al.* (2009) also stained breast tumour and normal breast tissue samples for HP1β and HP1γ protein, but reported these two isoforms were unchanged between the samples.

The differences in HP1α levels observed in breast tumour samples in the De Koning *et al.* (2009) and Kirschmann *et al.* (2000) studies may be attributed to several factors. First, these studies used different HP1α antibodies for the immunohistochemical staining. The Kirschmann *et al.* (2000) study used a mouse polyclonal human HP1α antibody, whereas De Koning *et al.* (2009) used a mouse monoclonal human HP1α antibody and also a rabbit polyclonal human HP1α antibody. Second, these studies used different methods for fixing and staining the breast tumour or normal tissue samples. These variations in both antibodies and in the procedures used could result in different levels of HP1α staining that is not reflective of increased or decreased HP1α in the tissue samples. Further studies exploring immunohistochemical staining in breast tumour samples is needed to clarify whether this is the case.

The study carried out by De Koning *et al.* (2009) also investigated the prognostic value of HP1α over-expression in breast tumours. This was carried out by examining HP1α mRNA levels in primary breast tumour samples and correlating these with patient outcomes. Twenty-two patients with increased HP1α mRNA were found to have, on average, decreased survival times, disease-free intervals and metastasis-free intervals compared to 64 patients with lower HP1α mRNA levels (De Koning *et al.*, 2009).

Overall, the studies described highlight an interesting trend in HP1α levels during breast cancer progression; a potential increase in HP1α levels in primary breast tumours, followed by a decrease in metastatic tumours (De Koning *et al.*, 2009; Kirschmann *et al.*, 2000; Norwood *et al.*, 2006). Further research is needed to

determine how HP1α expression fluctuates during breast cancer progression, focussing on how de-regulated HP1α expression could be established.

1.10 Exploring the consequences of HP1α and HP1β reduction in breast cancer cell lines

Altered levels of one or more of the three human HP1 isoforms have been demonstrated in several tumour types, including in breast neoplasms (Bartkova *et al.*, 2011; De Koning *et al.*, 2009; Pomeroy *et al.*, 2002). Decreased HP1α levels were were seen in breast metastases in one study, but a second study has reported that primary breast tumours have increased HP1α compared to normal tissue samples (De Koning *et al.*, 2009; Kirschmann *et al.*, 2000). A causal role for HP1α as a suppressor of invasion has also been established in breast cancer cell lines (Kirschmann *et al.*, 2000; Kirschmann *et al.*, 1999). Collectively this evidence suggests that HP1α has a role in breast cancer progression, potentially in preventing invasion. However, other roles are also possible as HP1α has been implicated in processes such as DNA repair and telomere stability (Sharma *et al.*, 2003; Song *et al.*, 2001). Altered levels of HP1β have also been reported in tumour types such as thyroid and prostate, but levels of HP1β in breast tumours have not been examined in detail (Contreras *et al.*, 2009; Shapiro *et al.*, 2008). Additionally, any role that HP1β has in breast cancer progression is yet to be investigated.

This study plans to establish non-invasive MCF-7 breast cancer cell lines with decreased HP1α or HP1β expression to be able to characterise them for changes in processes such as growth, anchorage independence and invasive potential. It is envisaged that more can be learned about the role of HP1α in breast cancer progression, and also whether HP1β is involved. This research will contribute to our knowledge of the molecular basis of breast cancer progression, and could potentially pave the way for more effective treatments to be developed.

1.10.1 Specific research aims

Specific research objectives to further define the role of HP1 in breast cancer

progression are as follows:

- ⇧ To establish non-invasive MCF-7 breast cell lines with stable knock-down of HP1α or HP1β
- ⇧ To characterise the MCF-7 HP1α or HP1β knock-down cell lines for changes in growth
- ⇧ To characterise the MCF-7 HP1α or HP1β knock-down cell lines for altered *in vitro* metastatic potential
- ⇧ To establish a MDA-MB-231 (invasive breast cell line) cell line with enhanced expression of HP1α

These objectives will be achieved using a range of molecular techniques and cell-based assays, including transfection of shRNA expressing plasmids, anchorage independence assays, proliferation assays, and through transfection of an inducible expression system.

2. Materials and Methods

2.1 Materials

2.1.1 Cell culture

Dulbecco's Modified Eagle Medium (DMEM, high glucose), Opti-MEM, foetal bovine serum (FBS), 0.05% trypsin-EDTA, phosphate buffered saline (PBS), penicillin/streptomycin (penstrep, 100x), geneticin, Zeocin™ and hygromycin were purchased from Life Technologies, Carlsbad, CA, USA. Cell culture flasks (75 cm^2 and 25 cm^2), 96 well plates, six well plates and 24 well plates were all purchased from Becton Dickinson, Franklin Lakes, USA. Ten centimetre tissue culture dishes were obtained from Thermo Fisher Scientific, Waltham, MA, USA. Dimethyl sulfoxide (DMSO), β-estradiol, doxycycline and bovine insulin were purchased from Sigma Aldrich, St Louis, MO, USA. Millicell invasion plates, receiving plates and extracellular matrix solution were obtained from EMD Millipore, Billerica, MA, USA. E-plates for real-time cell monitoring and Fugene 6 and XtremeGene 9 transfection reagents were purchased from Roche, Mount Wellington, NZ. SeaPlaque® agarose (low melting temperature) was purchased from Lonza, Basel, Switzerland. The SureSilencing™ shRNA Plasmids (targeting the *CBX1* and *CBX5* genes) were purchased from SABiosciences (Frederick, MD, USA).

2.1.2 DNA manipulation

Agarose powder was purchased from Bio-Rad, Hercules, CA, USA. Ethidium bromide (10 mg/mL solution) and deoxynucleotides (dNTPs) were acquired from Sigma-Aldrich, St Louis, MO, USA. Ten kb Plus ladder, TrackIt™ Loading Buffer, $MgCl_2$, 10x PCR Buffer, ChargeSwitch Plasmid Purification Kit, PureLink PCR Purification Kit and the Platinum® Taq DNA Polymerase were purchased from Life Technologies, Carlsbad, CA, USA. The High Pure RNA Isolation Kit, Transcriptor First Strand Synthesis Kit and 10x SYBR® Green PCR Master Mix were obtained from Roche Applied Science, Indianapolis, IN, USA.

2.1.3 Protein manipulation

The following antibodies were supplied by Cell Signalling Technologies, Danvers, MA, USA: monoclonal rabbit antibody raised against HP1α (catalogue number C7F11), and a rabbit anti-HP1β antibody (catalogue number 2613). Acrylamide was purchased from Bio-Rad Laboratories, Hercules, CA, USA. Anti-mouse Cy3 antibody (catalogue number A10521), anti-rabbit Cy5 antibody (catalogue number A10523) and anti-tubulin mouse monoclonal antibody (catalogue number A11126), 4',6-diamidino-2-phenylindole (DAPI), acridine orange staining solution (10 mg/mL) and SlowFade® Gold Antifade Reagent were obtained from Life Technologies, Carlsbad, CA, USA. Pierce ECM Plus Western Blotting Substrate was purchased from Thermo Fisher Scientific. The anti-rabbit horse radish peroxidase conjugated antibody (catalogue number NA934VS) and 0.2 μm Protran nitrocellulose membrane were obtained from GE Healthcare, Little Chalfont, Buckinghamshire, United Kingdom. Tetramethylethylenediamine (TEMED) was purchased from Sigma-Aldrich.

2.1.4 General lab materials

The following were purchased from Axygen, Union City, CA, USA: 10 μL, 20 μL, 200 μL and 1000 μL aseptic barrier pipette tips, and also 1.5 mL and 0.2 mL microcentrifuge and PCR tubes. Sodium dodecyl sulfate (SDS), Triton X-100™, Tween® 20, glycine, crystal violet, Tris base, sodium deoxycholate, bacteriological agar, boric acid, Ethylenediaminetetraacetic acid (EDTA), paraformaldehyde and ammonium persulfate (APS) were all supplied by Sigma-Aldrich. RNase H and cOmplete Mini Protease Inhibitor Cocktail tablets were obtained from Life Technologies and Roche Applied Science respectively. Luria-Bertani broth (1.0% tryptone, 0.5% yeast extract, 1.0% Sodium Chloride at pH 7.0) was puchased from Sigma-Aldrich.

2.2 Methods

2.2.1 Cell culture

All handling of mammalian cells was carried out aseptically in a class II biohazard hood (LA2-4A1, ESCO). MDA-MB-231 and MCF-7 cells were cultured in DMEM media containing 10% FBS and 1% penstrep. MCF-7 cells were also grown in the presence of 20 μg/mL bovine insulin. Cells were grown in 15 mL of DMEM in 75 cm² cell culture flasks in a humidified 37°C incubator (HERAcell 150, Heraeus, Kendro) with 5% CO_2. MCF-7 or MDA-MB-231 cells started from frozen were removed from liquid nitrogen storage, defrosted in a 37°C water bath with agitation, and grown in DMEM containing 10% FBS and 1% penstrep. Spent media was exchanged for fresh media 18 hours later to remove the DMSO left over from freezing.

Passaging of cells was carried out once cells reached 90% confluency after around three days' growth. Old media was removed and the cells washed twice with sterile PBS (1.54 mM KH_2PO_4, 155.17 mM NaCl, 2.71 mM $Na_2HPO_4.7H_2O$, pH 7.2) and incubated in 0.05% trypsin EDTA (5.33 mM KCl, 0.441 mM KH_2PO_4, 4.17 mM $NaHCO_3$, 137.93 mM NaCl, 0.336 mM $Na_2HPO_4.7H_2O$, 5.56 mM dextrose, 0.0251 mM phenol red, 0.481 mM Na_2-EDTA, 0.021 mM trypsin) for five minutes. Cells were then re-suspended in fresh media and placed in new 75 cm² flasks for further growth. Before the cells had been passaged three times after starting them from frozen, cells were washed with PBS and re-suspended in DMEM containing 10% FBS, 1% penstrep and 5% DMSO, then aliquoted into 1.5 mL cryovials. The cells were frozen overnight in a "Mr. Frosty" freezing container (Thermo Fisher Scientific) at -80°C, before being moved to liquid nitrogen storage.

2.2.2 MCF-7 transient transfections

MCF-7 cells were seeded into 6 well plates at a concentration of $1.5x10^5$ cells/well, transfected 24 hours later with 1 μg of plasmid in the presence of Fugene 6 at a ratio of 3:1 of transfection reagent:plasmid according to manufacturer's instructions. Forty-eight

hours after transfection, the cells were washed with PBS and scraped from the plates, pelleted by centrifugation for five minutes at 1000 rpm, re-suspended in PBS, and centrifuged again. The PBS was then removed and the cell pellets were frozen at -80°C for later analysis.

2.2.3 MCF-7 stable transfections

MCF-7 cells were seeded at a concentration of $1x10^5$ cells/well into 6 well plates. Transfection was carried out 24 hours later using 1 μg of plasmid in the presence of Fugene 6 at a 3:1 ratio of transfection reagent:plasmid according to manufacturer's instructions. After 24 hours, the media was removed and replaced with media containing antibiotics. Media was replaced every three days, and the antibiotic-resistant monoclonal colonies combined and expanded before being frozen for storage in 5% DMSO, or pelleted as in section 2.2.3 for later RNA extraction.

2.2.4 MDA-MB-231 stable transfections

Approximately $7.5x10^4$ cells/well MDA-MB-231 cells were seeded into six well plates and grown for 24 hours prior to transfection. Transfections were carried out using 1 μg of plasmid and the X-tremeGene™ 9 in a 3:1 ratio of transfection reagent:plasmid according to the manufacturer's instructions. Forty-eight hours after transfection, the cells were trypsinised and re-seeded into ten centimetre dishes, where DMEM containing antibiotics was added to select for plasmid expression. MDA-MB-231 cells that were transfected with X-tremeGene™ 9 but no plasmid were used as a control to show that the antibiotic could kill the cells. A control for transfection reagent toxicity was carried out using cells exposed to transfection reagent and plasmid, but not antibiotics.

Media containing geneticin was replenished every two to three days until resistant colonies were visible. When the colonies were large enough, media was removed and the plate washed twice with PBS before trypsin-soaked cloning disks with a 5mm diameter were placed on top of each colony. After a five minute incubation, the colonies

had adhered to the disks and were relocated into the wells of a 24 well plate containing selective media. Media was again replenished every three days until the colonies were large enough to be relocated into six well plates and subsequently frozen as in section 2.2.1, or subjected to further analysis.

2.2.5 Transient transfection of MDA-MB-231 Tet-On cells

MDA-MB-231 Tet-On clones obtained in section 2.2.6 were seeded in duplicate into six well plates and grown to around 80% confluency. These cells were then transfected with a total of 1 μg of plasmid using a 3:1 ratio of X-tremeGene 9 transfection reagent: plasmid according to manufacturer's instructions. If being used, doxycycline was added to the wells twenty-four hours post-transfection when the media was replenished.

2.2.6 Luciferase assays

Cells were harvested 48 hours post doxycycline addition, and the lysates prepared according to the manufacturer's instructions for the Dual-Luciferase® Reporter Assay System (Promega, Madison, WI). This system allows for sequential measurement of both firefly and renilla luciferase activity in the same sample. Twenty microlitres of lysate from each transfection assayed was each aliquoted into a 96 well plate in duplicate, and the assay performed according to the manufacturer's instructions. A FLUOStar Galaxy 96 well plate reader equipped with a chemiluminescence detection system (BMG Labtech, Offenburg, Germany) was used to record the intensity of the light given off by each well as Relative Light Units (RLU). Readings of a well containing lysis buffer only were taken to use as a blank; these were subtracted from all other readings to give corrected readings. Firefly luciferase activity was normalised to renilla activity by dividing the corrected firefly RLU readings by the corrected renilla RLU readings. Duplicate readings were averaged. Calculations were carried out in Microsoft Excel.

2.2.7 RNA and cDNA preparation

Cells pellets containing $1x10^6$ cells were obtained through centrifugation at 0.8 rpm for five minutes and RNA was extracted from them using the High Pure RNA Isolation Kit (Roche, Mount Wellington) according to the manufacturer's instructions. The resulting RNA was quantified by reading the absorbance at 260 nm and 280 nm using a NanoDrop 1000 Spectrophotometer (Thermo Scientific). An A260/280 ratio of approximately 2 was expected for each RNA sample (Wilfinger *et al.*, 1997).

Synthesis of cDNA was carried out using the Transcriptor First Strand Synthesis Kit (Roche, Mount Wellington). Reactions contain the Transcriptor Reverse Transcriptase, a recombinant enzyme with RNA-dependent DNA polymerase activity and also RNase H activity, which degrades RNA in RNA/DNA hybrids. Consequently, the need for an additional RNase H incubation after reverse transcription was eliminated. One microgram of RNA and anchored Oligo (dT) primers were used to create cDNA using the reaction and protocol described in Table 2.1 and 2.2 respectively. The reactions were set up in 0.2 mL PCR tubes with a total reaction volume of 20 µL, and the reaction was carried out on an Eppendorf Mastercycler® thermocycler (Eppendorf South Pacific, Sydney).

2.2.8 Semi-quantitative reverse transcriptase polymerase chain reaction

Polymerase chain reaction (PCR) is a process that allows the specific amplification of short DNA sequences by using thermal cycling, primer pairs designed to amplify a particular product, and a thermostable polymerase. This reaction uses cDNA synthesised from mRNA according to section 2.2.7. These PCR reactions were amplified for 27 cycles only, as this number of cycles was just under the 28 amplification cycles found to be optimal to show differences in HP1α, HP1β and HP1γ mRNA expression levels (Kirschmann *et al.*, 1999). Consequently, differences in amplification caused by variable amounts of the cDNA template are visible when the PCR products are subjected to agarose electrophoresis and stained with ethidium bromide. In this way, the RT-PCR method used was semi-quantitative as levels of PCR product are still in the

Component	**Amount (µL)**	**Final concentration**
Anchored oligo dT (50 pmol/µL)	1	2.5 pmol/µL
5 x reaction buffer	4	1x
Protector RNase inhibitor (40 U/µL)	0.5	20 U
Deoxynucleotide mix (10 mM each)	2	1 mM
Transcriptor reverse transcriptase (20 U/µL)	0.5	10 U
dH_2O	to make up to 20 µL	-
RNA (1 µg total)	*	50 ng/µL

Table 2.1 Reaction mix for cDNA synthesis using the Transcriptor First Strand Synthesis Kit. * indicates that the volume of RNA added varied depending on its concentration.

50°C	60 minutes
85°C	5 minutes
4°C	HOLD (optional)

Table 2.2 Reaction protocol for cDNA synthesis using the Transcriptor First Strand Synthesis Kit

exponential phase and have not reached a plateau. The Platinum® Taq DNA Polymerase, a recombinant Taq polymerase activated at 94°C, was used to examine the expression of HP1α, HP1β and β-actin in the MCF-7 HP1α and HP1β knock-down cell lines.

Reactions were set up in 0.2 mL thin-walled PCR tubes with a total reaction volume of 50 µL and carried out on an Eppendorf Mastercycler® thermocycler (Eppendorf South Pacific, Sydney) as outlined in Table 2.3 and 2.4 respectively. A non-template control lacking DNA was included in each set of PCR reactions.

2.2.9 Primer design and optimisation

The HP1α, HP1β, HP1γ and actin primers were designed by either the PrimerBlast designed to span exon-exon boundaries of *CBX5*, *CBX1*, *CBX3* and β-actin cDNA website (NCBI) or LightCycler Probe Design Software 2.0 (Roche). The primers were sequences to specifically amplify targets from mRNA only, minimizing amplification of genomic DNA (see Appendix 1 for primer sequences).

Optimisation of the primer annealing temperatures was carried out using the same reaction set up as in section 2.2.13, but was instead performed using a Mastercycler™ Gradient thermocycler providing a range of annealing temperatures from 55°C-65°C for 27 cycles. Agarose gel electrophoresis was carried out as in section 2.2.10.

2.2.10 Agarose gel electrophoresis

Agarose gel electrophoresis is a technique that allows PCR products to be visualised by the use of ethidium bromide, an UV fluorescent compound that intercalates into DNA. Two percent agarose gels were made by dissolving 6 g of agarose powder into 300 mL of 1x tris-borate-EDTA (TBE; 89 mM Tris base, 89 mM boric acid, 2 mM EDTA, pH 8) buffer by heating in a microwave, and adding 15 µL ethidium bromide (10 mg/mL original concentration, final concentration 0.5 µg/mL). After pouring, the gel was allowed to solidify, and 1x TBE containing ethidium bromide at a concentration of 0.5

Component	Amount (µL)	Final concentration
10x PCR buffer (-Mg)	5	1x
100 mM dNTP mix	0.4	0.2 mM
50 mM $MgCl_2$	1.5	1.5 mM
Forward primer (500 pmol/µL)	1	0.2 µM
Reverse primer (500 pmol/µL)	1	0.2 µM
Platinum® Taq DNA Polymerase	0.2	1 unit
dH_2O	38.9	-
cDNA	2	-

Table 2.3 Reaction components for semi-quantitative RT-PCR

94°C	1 minute		Initial denaturation
94°C	30 seconds	27 cycles	Denaturation
60°C	30 seconds		Annealing
72°C	1 minute		Extension
72°C	10 minutes		Final Extension

Table 2.4 Reaction protocol for semi-quantitative RT-PCR

μg/mL was poured over the gel. Twenty microlitres of each PCR reaction were mixed with 4 μL of 0.6x TrackIt™ loading dye and dispensed into the wells of the gel. Five microlitres of a 1 Kb Plus DNA Ladder (1 μg/μL) was also added to aid in determining DNA fragment sizes, and electrophoresis was carried out at 90 V for approximately one hour. DNA was visualised using UV illumination on a Gel-doc™ (Biorad).

2.2.11 Quantitative real-time polymerase chain reaction

Traditional PCR reactions are end-point assays, meaning that levels of PCR product can be examined at the end of the reaction only. Real-time PCR, however, enables detection of PCR products over the course of the entire reaction, which allows for much greater sensitivity when determining differences in amounts of PCR product. This detection is made possible by monitoring the fluorescence of a fluorescent dye, in this case SYBR® green, which intercalates into double stranded DNA.

The standard curves for HP1α, HP1β, HP1γ, and actin were created by running four identical PCR reactions set up as in 2.2.8, but carrying out amplification for 45 cycles instead of 27. Electrophoresis was performed as in 2.2.10 to check for amplification. Then identical PCR reactions were pooled together and purified using a PureLink™ PCR Purification kit according to the manufacturer's instructions (Life Technologies, Carlsbad). These pooled PCR products were diluted in dH_2O to give five 10-fold dilutions ranging in concentration from $2x10^{-4}$ ng/μL to $2x10^{-8}$ ng/μL to give the range required for standard curve generation.

A reaction mix containing 7 μL of dH_2O, 1 μL each of forward and reverse primers (final concentration of 0.2 μM each) and 10 μL of 10x SYBR® Green PCR Master Mix (final concentration 1x) was added to the wells of a white 96 well multi-well plate, primers were added to a final concentration of then 2 μL of cDNA (1 μg) added for a final volume of 20 μL. The plate was sealed and centrifuged at 2000 x g for two minutes before being subjected to the program laid out in Table 2.5 on a Lightcycler® 480 real-time PCR instrument (Roche, Mount Wellington). All reactions were carried out in triplicate. Primer pairs used were the same as those described in section 2.2.9.

Target (°C)	Acquisition mode	Hold (mm : ss)	Ramp Rate (°C/s)	Acquisitions per °C
Program name: Denature Number of cycles: 1				
95	None	10 : 00	4.40	-
Program name: Amplification Number of cycles: 45				
95	None	00 : 10	4.40	-
60	None	00 : 20	2.20	-
72	Single	00 : 30	4.40	-
Program name: Melt Number of cycles: 1				
95	None	00 : 05	4.40	-
65	None	01 : 00	2.20	-
97	Continuous		0.11	5
Program name: Cool Number of cycles: 1				
40	None	00 : 10	1.50	-

Table 2.5 Reaction protocol used for qRT-PCR

2.2.12 Topo cloning and sequencing

Topo cloning and sequencing was carried out to confirm the identity of the PCR products of the HP1α, HP1β, HP1γ and β-actin primer pairs. PCR products were incorporated into the Topo vector according to the manufacturer's instructions using the Topo Cloning kit (Life Technologies). A selection of bacterial colonies positive for both the Topo vector and the PCR product insert under blue-white selection were grown overnight in 2 mL of LB broth (10 g/L tryptone, 5 g/L yeast extract, 5 g/L NaCl) containing 100 μg/mL of ampicillin, then centrifuged at 2500 rpm for ten minutes. The pellets were processed using the ChargeSwitch Plasmid Prep Kit (Life Technologies), and 300 ng of the resulting RNA sent to the Allan Wilson Centre Sequencing service for sequencing using the BigDye Terminator 3.1 reaction and the T7 primer. The resulting sequences were BLAST searched using the NCBI Nucleotide Blast search engine to confirm the presence of the correct amplicon as targeted by the primers. A 100% match in all four amplicons was obtained between at least a portion of the searched sequence and the desired gene, indicating that these primers amplify the expected product. Chromatograms of the sequences obtained from sequencing can be seen in Appendix 2.

2.2.13 Extraction of whole cell lysate

MCF-7 cells were overlaid with 200 μL of cold RIPA buffer (10 mM NaCl, 1% NP40, 0.5% deoxycholate, 0.1% SDS, 50 mM Tris pH 8 and one cOmplete Mini Protease Inhibitor Cocktail tablet) and scraped from the tissue culture plates using a cell scraper.

The cells were then placed into a 1.5 mL tube and incubated on ice for 30 minutes with vortex mixing at five minute intervals. This was followed by centrifugation at 12000 rpm for 10 minutes at 4°C to remove any cell debris, at which point the supernatant was placed in a new 1.5 mL tube.

2.2.14 Protein quantification

Cell lysate concentrations were determined using a bicinchoninic acid (BCA) Protein

Assay Kit (Thermo Scientific). Ten microlitres of whole cell lysate from each cell line were aliquoted into a 96 well plate in duplicate, along with duplicates of bovine serum albumin (BSA) standards containing 0, 25, 125, 250, 500, 750, 1000 or 2000 µg of protein. Two hundred microlitres of BCA reagent was added to each well and the plate incubated at 37°C for one hour. Once the plate had cooled to room temperature, the absorbance at 560 nm of the wells was read on a PowerWave XS plate reader (Biotek). A protein standard curve was plotted using the absorbances of the BSA standards, and the concentrations of the whole cell lysates calculated using the equation calculated from the standard curve using Microsoft Excel.

2.2.15 Sodium dodecylsulfate polyacrylamide gel electrophoresis

Sodium dodecylsulfate polyacrylamide gel electrophoresis (SDS-PAGE) was used to separate whole cell lysate proteins in preparation for immunoblotting according to a previously established protocol (Laemmli *et al.*, 1970). Twenty micrograms of lysate was combined with 6x loading buffer (containing 375 mM Tris-HCl pH 6.8, 6% SDS, 48% glycerol, 9% 2-Mercaptoethanol, and 0.03% bromophenol blue) and RIPA buffer for a final concentration of 1X loading buffer. The samples were denatured at 99°C for five minutes. Electrophoresis was carried out on a 1.5 mm thick 12% resolving polyacrylamide gel with a 5% stacking gel at 80 V for approximately an hour and a half using a SE400 Sturdier Vertical Electrophoresis system (Hoefer).

2.2.16 Immunoblotting

Following protein separation with SDS-PAGE, protein samples were transferred to a 0.2 µm nitrocellulose membrane at 4°C in cold towbin buffer (12.12 g Tris, 57.6 g Glycine and 800 mL methanol made up to 4 L with distilled water) for two-three hours at 100 V in a Transblot Cell apparatus (BioRad). The membrane was then blocked for one hour in blocking buffer containing 5% IgG free BSA, 0.1% Tween-20 and 1x TBS. After blocking, the membrane was incubated on a rocker at 4°C overnight in blocking buffer containing primary antibody (HP1α and HP1β antibodies were each diluted 1:1000, anti-tubulin antibody was diluted 1:1500). The following day the membrane was rinsed

in wash buffer containing 1x TBS and 0.1% Tween-20, then placed in fresh wash buffer at room temperature on the rocker for two intervals of 5 minutes and two intervals of ten minutes. Secondary antibody (conjugated to a horseradish peroxidase (HRP) enzyme) diluted in blocking buffer was then added to the membrane and incubated for one hour on the rocker. The washes carried out after removing the primary antibody were then repeated, and the membrane was covered with ECM Plus Detection Reagent (GE Healthcare) for five minutes. Protein bands were visualised via chemiluminescence and imaged using an Intelligent Dark Box (GE Healthcare).

2.2.17 Immunofluorescent staining

Cells were seeded at $1x10^5$ cells/well on to glass cover slips in 6 well plates. Forty-eight hours later the cover slips were washed three times for five minutes in 2 mL PBS, fixed in 2% paraformaldehyde for two minutes, washed for ten minutes twice in PBS, then permeabilized with 0.2% Triton X-100 in PBS for five minutes. The cover-slips were then transferred to one well each of a 24 well plate and blocked with PBS containing 5% BSA and 0.5% Tween-20 for 30 minutes at room temperature while rocking. After blocking, the cells were incubated overnight at 4°C with two antibodies, one a monoclonal mouse antibody targeting α-tubulin (catalogue number A11126, Life Technologies) diluted 1/400, the other a rabbit antibody targeting HP1β (catalogue number 2613, Cell Signalling Technologies, Danvers, Massachussetts) diluted to 1/100. The cover-slips were again washed three times for five minutes in PBS containing 0.15 Triton X-100, then incubated for one hour with a 1/650 dilution of anti-rabbit Cy5 antibody (catalogue number A10523, Life Technologies, Carlsbad) and also a 1/1000 dilution of an anti-mouse Cy3 antibody (catalogue number A10521, Life Technologies, Carlsbad) in blocking buffer. After three more five minute washes in PBS with 0.1% Triton X-100, the cover-slips were washed once for five minutes in PBS and then fixed again for 15 minutes with 2% paraformaldehyde in PBS. Two more washes were then carried out with PBS and one more with PBS containing 0.1% Triton X-100, before the cells were counter-stained for one minute in 300 mM DAPI diluted in PBS. Following two more washes in PBS, the cover-slips were dried and mounted onto slides in SlowFade (Life Technologies). Cells were imaged using a Leica SP5 DM6000B under

40x magnification. Identical conditions were used for each image.

2.2.18 Invasion assay

This assay is based upon an invasion assay described previously (Albini *et al.*, 1987). Twenty-four well tissue culture plates (Millipore) comprised of an upper chamber and a lower chamber separated by a porous plastic membrane were used for the invasion assays. The membrane had 0.2 μM pores, and provided an interface for the media contained in the upper and lower wells. A solution of extracellular matrix (ECM) proteins (Millipore) was diluted to 0.5 mg/mL with sterile dH_2O and 100 uL dispensed onto some of the upper membranes to give 50 μg/well total ECM. The membranes was allowed to dry overnight in a laminar flow hood. Cells at 80-90% confluency were also serum starved on the day of membrane coating. This was accomplished by washing the cells twice with PBS and incubating the cells in media containing 1% penstrep and 0.2% BSA overnight.

The following day, the cells were trypsinised as in section 2.2.1, then counted using a haemocytometer and re-suspended in media containing 0.2% BSA , and seeded into the upper wells at a density of $1.5x10^5$ cells/well. The membranes were re-hydrated in DMEM for 30 minutes prior to adding the cells, while DMEM containing either 10% FBS and 1% penstrep or 0.2% BSA and 1% penstrep was aliquoted into the lower wells as shown in Figure 2.1. The cells were then left to invade for five days. Non-invading cells were removed from the upper surface of the membrane using a cotton swab. The membrane was fixed in methanol for ten minutes, then stained with 0.4 mg/mL crystal violet in 20% methanol. Cells were imaged using a Zeiss Axiophot Light microscope.

2.2.19 Bromodeoxyuridine (BrdU) incorporation assay

Cells were seeded in triplicate at a density of $1x10^3$ cells/well into six 96 well plates. On each of the five days following seeding, including day zero, BrdU (100 μM, final concentration 10 μM in each well) was added to one of the plates for six hours. The media was removed and the cells were processed using the Cell Proliferation ELISA,

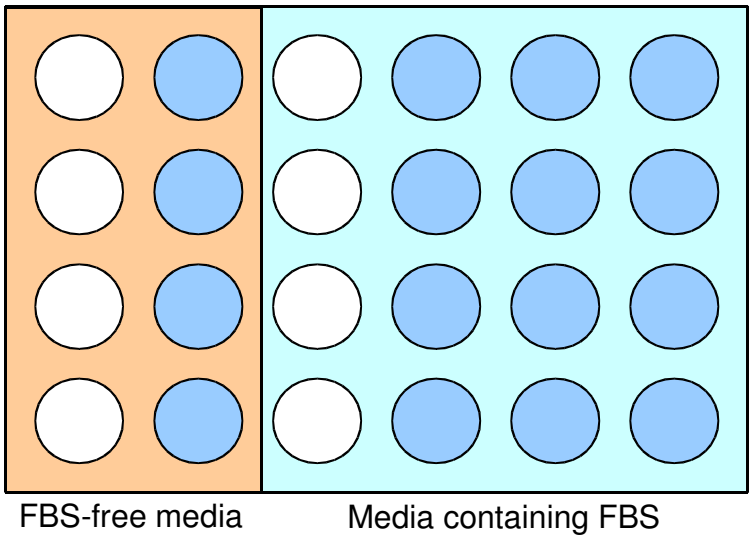

Figure 2.1 Invasion assay plate layout. Wells are coated with either 100μL of ECM (blue) or left uncoated (white). Media containing 1% penstrep and either 0.2% BSA (orange) or 10% FBS (green) is used to fill the lower wells.

BrdU (colourimetric) kit (Roche, Mt Wellington) according to the manufacturer's instructions. Briefly, fixation was carried out with the FixDenat solution for 30 minutes, followed by a 90 minute incubation with the diluted anti-BrdU-POD. The plate was washed three times with PBS and incubated for 25 minutes with substrate solution. Absorbances were read at 370 nm and 492 nm on a PowerWave XS Plate Reader (Biotek, Vermont). The 492 nm readings were subtracted from the 370 nm readings to give corrected absorbances. Wells containing only media were used as a negative control. The corrected blank absorbance readings obtained from the negative control wells were subtracted from all the other corrected absorbance readings.

2.2.20 Real-time cell monitoring

The xCELLigence™ System (Roche, Mount Wellington) was used to monitor real-time cellular proliferation. This system measures impedence generated by cells growing on electrode coated plates. Impedence is recorded as a parameterless value known as a Cell Index (CI) value. CI is a measurement of cellular morphology, cell spreading and the degree of adherence to the plates and also correlates with cell number (Atienzar *et al.*, 2011). By normalising CI readings to the time of cellular adherence to the wells, CI values representing a trend of cellular proliferation can be obtained. Prior to adding the cells, a background measurement of the culture media was taken. This was subtracted from all subsequent readings. The cells were seeded in triplicate into 96 well electrode covered cell culture plates (E-Plates) at a density of $1x10^3$ cells/well. Cellular index readings were taken every 15 minutes for 118 hours. The triplicate CI readings were averaged, and normalised cell index readings were calculated by dividing the CI readings by those obtained at a nominated time point of adherence.

2.2.21 Fluorescence activated cell sorting

Sub-confluent cells were washed twice with PBS, trypsinised and counted using a haemocytometer, then centrifuged at 1300 rpm for 5 minutes. The media was aspirated and the cell pellets re-suspended in PBS containing 10% FBS. The centrifuging step was then repeated, and the resulting cell pellets re-suspended in PBS/10% FBS to give a

final concentration of $1x10^6$ cells/mL. One millilitre of cells were then aliquoted into polypropylene tubes, and 2.5 mL of cold ethanol added drop-wise while vortexing. After one hour at 4°C, the cells were washed twice by centrifuging the cells at 1800 rpm, aspirating the supernatant and re-suspending the pellet in 3 mL of PBS. After washing, the cells were re-suspended in 1 mL of a solution containing 10 μg/mL of propidium iodide (PI) in PBS, with the exception of a no-PI control which was instead re-suspend in PBS. RNase A was added to a final concentration of 50 μg/mL, though one tube was left as an RNase-free control. The cells were incubated at 37°C for 30 minutes, then the cell cycle profiles and forward/side scatters of $1x10^4$ nuclei were examined using a FACScalibur™ flow cytometer (Becton-Dickinson, East Rutherford, NJ, USA). Triplicate samples of each cell line were analysed.

2.2.22 Soft agar colony formation assay

This assay was based on a soft agar colony formation that had been developed previously (Hurlin *et al.*, 1987). Two thousand two hundred and fifty MCF-7 cells per well were combined with 1 mL of 0.35% Seaplaque low melting temperature agarose in 1x DMEM, and overlaid onto 1 mL of previously set 0.5% agarose in 1x DMEM. The plate was refrigerated for ten minutes to set the agarose. Plates were incubated in a humidified 37°C incubator with 5% CO_2 for nineteen days. One hundred microlitres of media was added to each well every three days to prevent the agarose from drying out. At the conclusion of the assay, the wells were stained with 0.5 mL 0.005% crystal violet in PBS for one hour, then visualised using a dissecting microscope. The number of spherical colonies from triplicate wells for each cell line were averaged. Wells containing only agarose and DMEM were used as negative controls.

2.2.23 Acridine orange staining

MCF-7 cells were seeded onto cover-slips at a density of $1.5x10^5$ cells/well and allowed to adhere and grow for 24 hours. Fixation was then carried out with methanol and acetone, and the cells were treated with RNase A for 30 minutes at 37°C. Staining with a solution containing $2.5x10^{-5}$ M acridine orange in PBS was carried out for 20 minutes,

before the cells were washed in PBS and mounted onto slides. Visualisation and imaging was carried out using a Leica SP5 DM6000B confocal microscope using an excitation maxima of 502 nm and an emission maxima of 525 nm. Analysis of staining intensity was undertaken using the Leica LAS AF software.

3. Creation of shRNA MCF-7 stable cell lines with reduced expression of HP1α or HP1β

3.1 Introduction

Studies have identified a link between HP1α protein levels and the invasive potential of breast cancer cell lines and metastatic tumours (Kirschmann *et al.*, 2000; Norwood *et al.*, 2006). However, as yet alternative consequences of HP1α loss in breast cancer progression remain undefined. This study examines the role of HP1α or HP1β loss in breast cancer progression. To achieve this, breast cancer lines were artificially manipulated to have decreased levels of HP1α or HP1β protein.

Modified cell lines were created by transfecting MCF-7 cells (a non-invasive epithelial breast cell line widely used as a model for breast cancer) with plasmids encoding short hairpin RNAs (shRNAs). These shRNAs were designed to target mRNA sequences encoding either the HP1α or HP1β proteins and result in degradation of the *CBX5* or *CBX1* mRNA. This is due to digestion of double-stranded shRNA by the enzyme Dicer, and the loading of the resulting small interfering RNA (siRNA) fragments onto the RNA-induced silencing complex (RISC) (Tomari and Zamore, 2005). Depending on which of these small RNA fragments binds to the RISC protein complex, the gene of interest will be silenced either through sequence-specific degradation, or through inhibiting translation of the mRNA (Chiu and Rana, 2003). Initially, knock-down conditions were tested using transient transfections, and then stably transfected MCF-7 knock-down cell lines were created to undergo characterisation.

As a means of determining whether stable knock-down cell lines were produced using this method, the mRNA levels of the genes encoding HP1α and HP1β were examined using quantitative reverse transcriptase PCR (qRT-PCR). Whole cell mRNA was reverse transcribed into cDNA, which was then used as a template in PCR reactions. The PCR products provided an indirect means of monitoring changes in reverse transcribed cellular mRNA.

This chapter describes the creation of MCF-7 cell lines with reduced HP1α or HP1β expression using shRNA plasmids, and confirmation of knock-down using qRT-PCR.

3.2 Results

3.2.1 Testing of the CBX5 and CBX1 shRNA plasmids

Four SureSilencing® shRNA plasmids (CBX5 ID1-4) each expressing a shRNA that targeted a unique region of the *CBX5* mRNA were used to achieve HP1α knock-down. A plasmid expressing a non-targeting shRNA (scrambled shRNA plasmid) was also used as a control. To initially confirm that the CBX5 shRNAs targeted *CBX5* mRNA, MCF-7 cells were transiently transfected with one of the five shRNA plasmids (outlined in Table 3.1) and whole cell RNA was extracted from the transfected cells and subjected to cDNA synthesis (Methods 2.2.2 and 2.2.7). Semi-quantitative RT-PCR (described in 2.2.8) was performed using primers that were designed to amplify regions of the synthesised cDNA corresponding to HP1α or β-actin. The products of these reactions were subjected to agarose gel electrophoresis (see section 2.2.10) and are shown in Figure 3.1. This figure shows that each CBX5 ID1-4 cell line has a reduction in the amount of HP1α amplicon compared to the hygromycin control (HC). This indicates that the HP1α mRNA levels are decreased in the knock-down cell lines compared to the HC control. β-actin was used as an internal reference (control) to normalise for the amount of RNA, hence cDNA, present in each PCR reaction. As the actin amplicons for the five transfections and the untransfected sample have comparable levels in all transfected cell lines (Figure 3.1B), the difference that are observed in HP1α across the cell lines are not due to unequal RNA content. The untransfected control cells appear to have increased HP1α cDNA compared to the shRNA transfected cells, but β-actin levels also appear to be increased in these cells. This may indicate a variation in the amount of RNA used in cDNA synthesis for the untransfected cells.

Four plasmids targeting CBX1 (ID1, ID2, ID3 and ID4) were similarly used to knock-down HP1β along with a plasmid expressing a non-targeting scrambled shRNA. These shRNA plasmids contained a geneticin resistance gene, as opposed to the hygromycin

Name	Cell Line	Plasmid Transfected (1 µg)	Target	Antibiotic Selection
CBX5 ID1	MCF-7	CBX5 ID1 shRNA plasmid	HP1α	Hygromycin-B
CBX5 ID2	MCF-7	CBX5 ID2 shRNA plasmid	HP1α	Hygromycin-B
CBX5 ID3	MCF-7	CBX5 ID3 shRNA plasmid	HP1α	Hygromycin-B
CBX5 ID4	MCF-7	CBX5 ID4 shRNA plasmid	HP1α	Hygromycin-B
HC Control	MCF-7	Scrambled shRNA plasmid	None	Hygromycin-B
CBX1 ID1	MCF-7	CBX1 ID1 shRNA plasmid	HP1β	Geneticin
CBX1 ID2	MCF-7	CBX1 ID2 shRNA plasmid	HP1β	Geneticin
CBX1 ID3	MCF-7	CBX1 ID3 shRNA plasmid	HP1β	Geneticin
CBX1 ID4	MCF-7	CBX1 ID4 shRNA plasmid	HP1β	Geneticin
NC Control	MCF-7	Scrambled shRNA plasmid	None	Geneticin

Table 3.1 Summary of the shRNA plasmids used to create the MCF-7 HP1α or HP1β knock-down and control cell lines

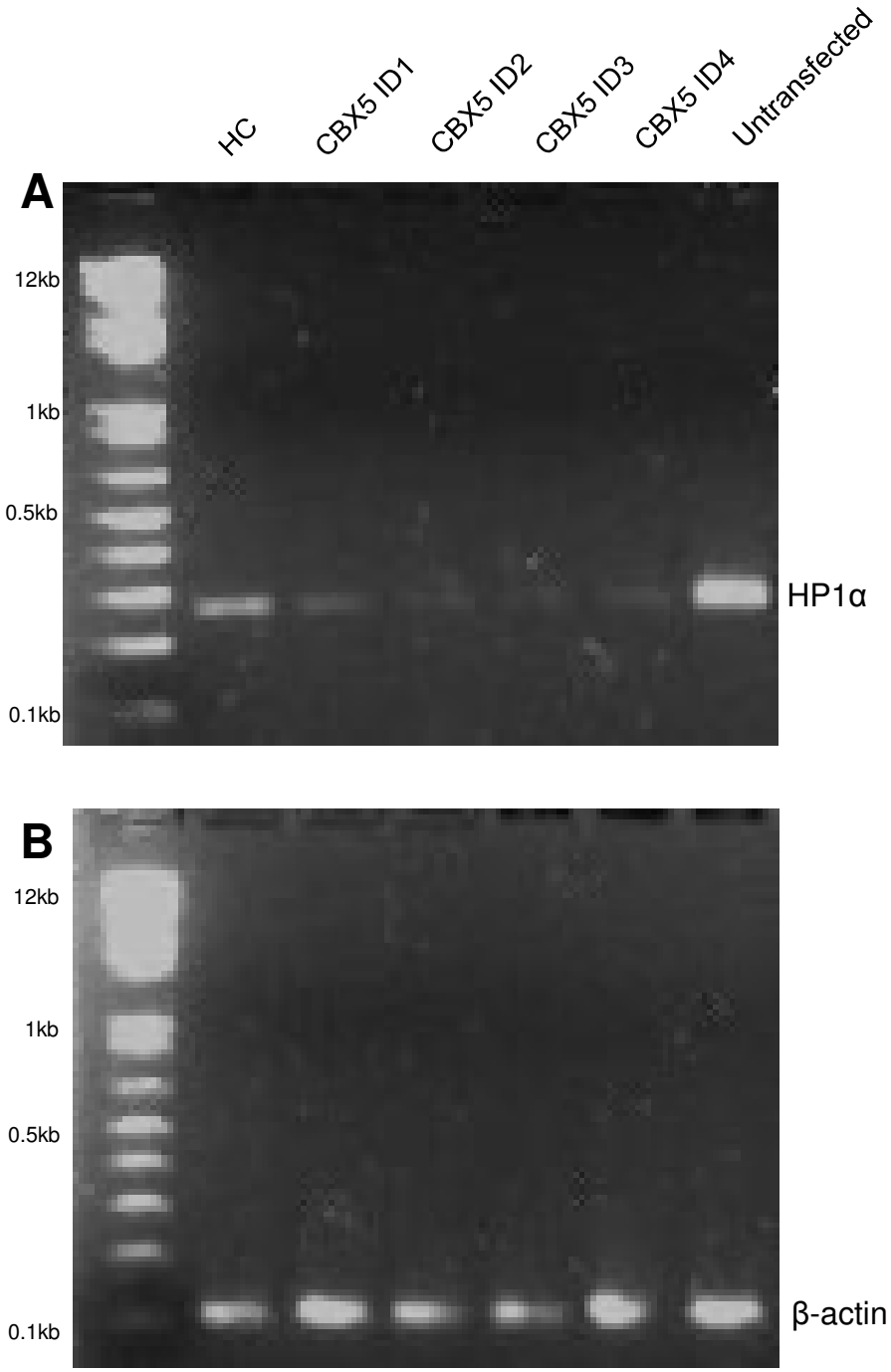

Figure 3.1. MCF-7 cells transiently transfected with CBX5 shRNA plasmids show decreased HP1α mRNA levels**.** Whole cell RNA was extracted from MCF7 cells either untransfected or transiently transfected with either one of shRNA plasmids CBX5 ID1-4 or hygromycin control (HC), subjected to semi-quantitative RT-PCR analysis using primers targeting HP1α cDNA (outlined in section 2.2.8). Primers specific to β-actin were used as a control and molecular size markers were used to determine PCR product sizes.

resistance gene in the HP1α shRNA plasmids.

3.2.2 Creation of MCF-7 stable HP1α or HP1β knock-down shRNA cell lines

Once the CBX1 and CBX5 shRNA plasmids were confirmed to target HP1β or HP1α respectively, they were used to create MCF-7 knock-down cell lines. Stable transfection of MCF-7 cells was carried out as described in section 2.2.3, using the plasmids described in Table 3.1. As the CBX5 shRNA plasmids also expressed a gene encoding for a kinase that deactivates hygromycin, 200 μg/mL of hygromycin-B was used to select for the uptake of shRNA plasmid. Similarly, the CBX1 shRNA plasmids expressed the gene for the aminoglycoside 3‘-phosphotransferase APH 3‘ II, which confers resistance to geneticin. Consequently, 600 μg/mL of geneticin was used to select for expression of the CBX1 shRNA plasmids.

Two weeks after transfection, the MCF-7 cells transfected with one of the ten shRNA plasmids had formed colonies that had each developed from a single antibiotic resistant cell. All colonies expressing the same shRNA plasmid were trypsinised and pooled, resulting in ten polyclonal cell lines. This was desirable as polyclonal cell lines will have different shRNA plasmid insertion sites, compared with monoclonal cell lines where all cells will have the same shRNA plasmid insertion site. Consequently, creating polyclonal cell lines reduced the chances of any phenotypic differences between the cell lines being attributable to genes other than HP1α or HP1β being disrupted by the shRNA plasmid insertion.

Semi-quantitative RT-PCR was again used to initially observe changes in HP1α or HP1β levels in transfected cell lines (described in 2.2.8). The resulting PCR reactions were subjected to agarose gel electrophoresis (outlined in 2.2.10) and are shown in Figure 3.2. HP1α cDNA levels in the CBX5 ID3 and ID4 cell lines were decreased compared to the HC cell line (Figure 3.2A). Decreases in HP1α amplicons in the CBX5 ID1 and ID2 cell lines appeared negligible compared to the HC cell line. This indicated that the CBX5 ID3 and ID4 cell lines had greater HP1α knock-down than the ID1 and ID2 cell lines. β-actin mRNA levels remain fairly consistent across all five cell lines (Figure

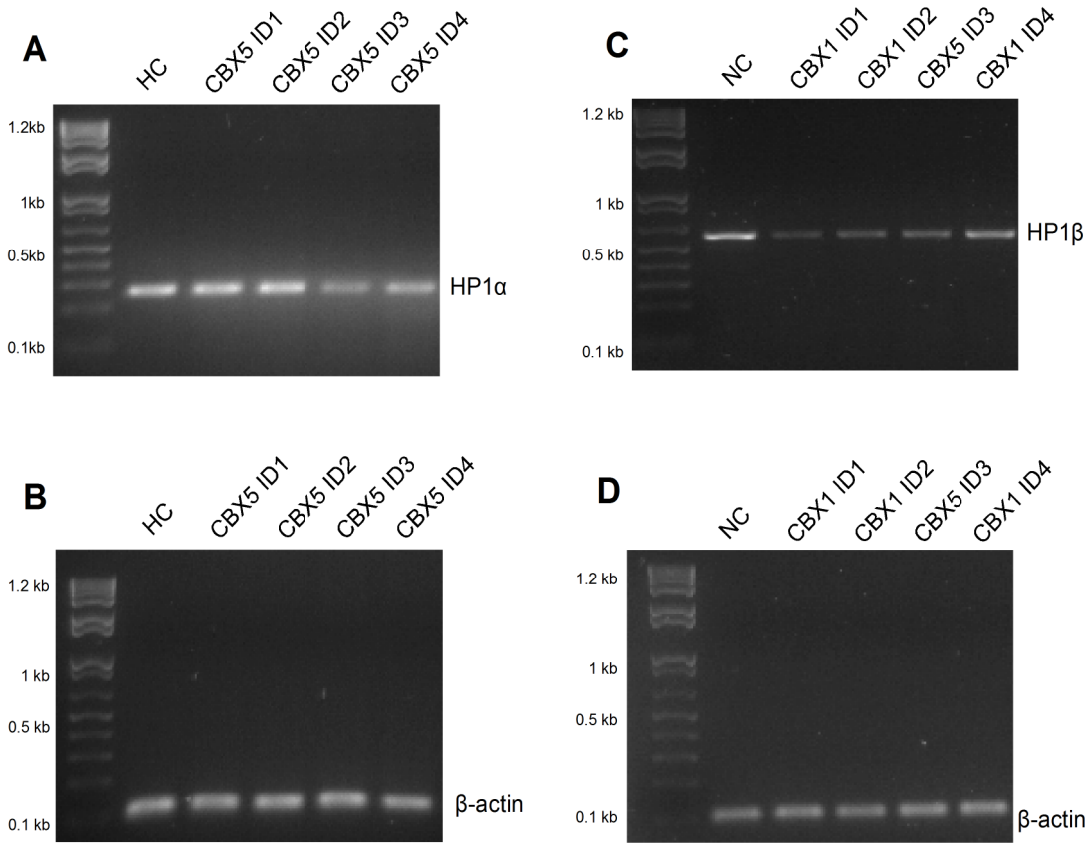

Figure 3.2. Stable transfection of MCF-7 cells with CBX1 or CBX5 shRNA plasmids results in HP1β or HP1α knock-down respectively. Whole cell RNA was extracted from MCF7 cells transfected with one of the shRNA plasmids described in Table 3.1 and subjected to RT-PCR analysis using primers targeting cDNA sequences HP1α (**A**) or HP1β (C) followed by gel electrophoresis. Reactions containing β-actin primers (**B** and **D**) were used as an expression control, and and molecular size markers (kb) were used to determine PCR product sizes.

3.2B), indicating that differences in HP1α are not likely due to variations in the amount of cDNA present in each PCR reaction.

Similarly, Figure 3.2C shows that HP1β cDNA levels in the CBX1 ID1-4 knock-down cell lines were markedly decreased compared to the neomycin control, particularly in the ID1 cells. This shows that the CBX1 ID1-4 shRNA plasmids effectively produced a reduction in HP1β mRNA. Levels of β-actin are unchanged between the five cell lines (Figure 3.2D). Collectively, these results provided an initial insight that the method used to create the stable HP1α or HP1β knock-down cell lines had been successful.

3.2.3 Quantification of HP1 mRNA expression in CBX1 and CBX5 shRNA stable MCF-7 cell lines using qRT-PCR

To accurately determine the extent of change in each HP1 isoform due to knock-down of HP1α or HP1β in MCF-7 shRNA cell lines, qRT-PCR was performed. This would enable determination of whether a specific shRNA exhibited any cross-targeting between the HP1 isoforms. As before, β-actin mRNA was used as an internal reference control.

3.2.3.1 Optimisation of HP1 primers

Optimal annealing temperatures had previously been determined for the HP1α, HP1β and β-actin primers, but not for the HP1γ primers (primer sequences can be found in Appendix 1). To find the optimal primer annealing temperature, PCR reactions containing cDNA from MCF-7 cells and the HP1γ primers were performed at a range of five annealing temperatures between 55°C and 62°C (as described in section 2.2.9). The resulting PCR products were analysed using agarose gel electrophoresis and are shown in Figure 3.3. A single band was seen in each of the five lanes, indicating a single PCR product and that the HP1γ cDNA target had successfully amplified. The temperature that facilitated optimal primer annealing (and was chosen for subsequent qRT-PCR reactions) was 60°C, as the HP1γ amplicon was present in the greatest abundance at this temperature.

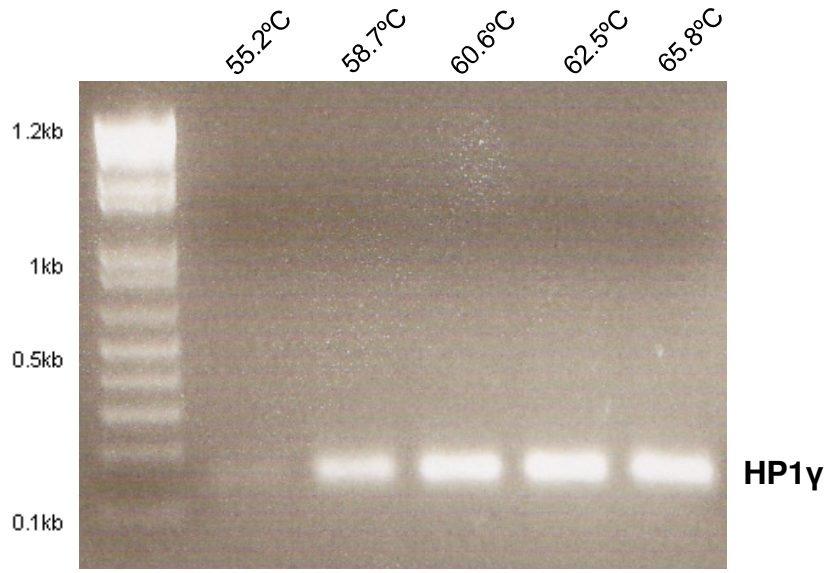

Figure 3.3. Optimising HP1γ primers for RT-PCR**.** Five PCR reactions were set up using MCF-7 cDNA and HP1γ primers and subjected to PCR at five annealing temperatures between 55.2ºC and 65.8ºC (as described in section 2.2.9). Molecular size markers were used to determine PCR product sizes.

Each primer pair for HP1α, HP1β, HP1γ and β-actin was also confirmed to amplify the correct target through sequencing the corresponding PCR products (described in section 2.2.12) and the resulting sequence chromatograms can be found in Appendix 2.

3.2.3.2 Establishment of qRT-PCR standard curves and reaction efficiencies

Quantitative real-time PCR was carried out using the LightCycler® 480 System (Roche). The PCR method used a non-saturating dye which binds to double stranded PCR products and enables quantification of the PCR product levels during the entire reaction. This makes qRT-PCR substantially more sensitive than traditional PCR, which can only detect the amount of PCR product at the plateau phase of the reaction. This method was used to examine levels of each HP1 isoform and β-actin in the various MCF-7 HP1 knock-down cell lines.

Absolute quantification is a qRT-PCR method used to determine the concentration of a specific cDNA amplicon. This is achieved by using pooled traditional PCR reactions that have used specific primers to amplify a cDNA target (carried out as described in Methods 2.2.8). The concentration of the target amplicon is determined using spectrophotometry, and a series of dilutions are carried out to give PCR standards containing between $2x10^{-4}$ ng/μL to $2x10^{-8}$ ng/μL of the target amplicon. These standards are then amplified using a LightCycler® 480 System, which uses the known concentrations and the crossing-point values of the standards to construct a standard curve (reaction described in 2.2.11). Crossing-point values from samples containing an unknown concentration of the target cDNA amplicon can then be compared to the standard curve by the LightCycler® 480 software, and the concentration of the target amplicons can be calculated.

To construct the standard curves for the HP1α, HP1β, HP1γ and β-actin primers, qRT-PCR reactions were carried out using five standards. These five standards contained a known concentration of the PCR products amplified using these primers. The HP1α panel of Figure 3.4 shows that duplicate samples of each HP1α standard gave identical sigmoidal amplification curves that reached plateaus as maximum SYBR green

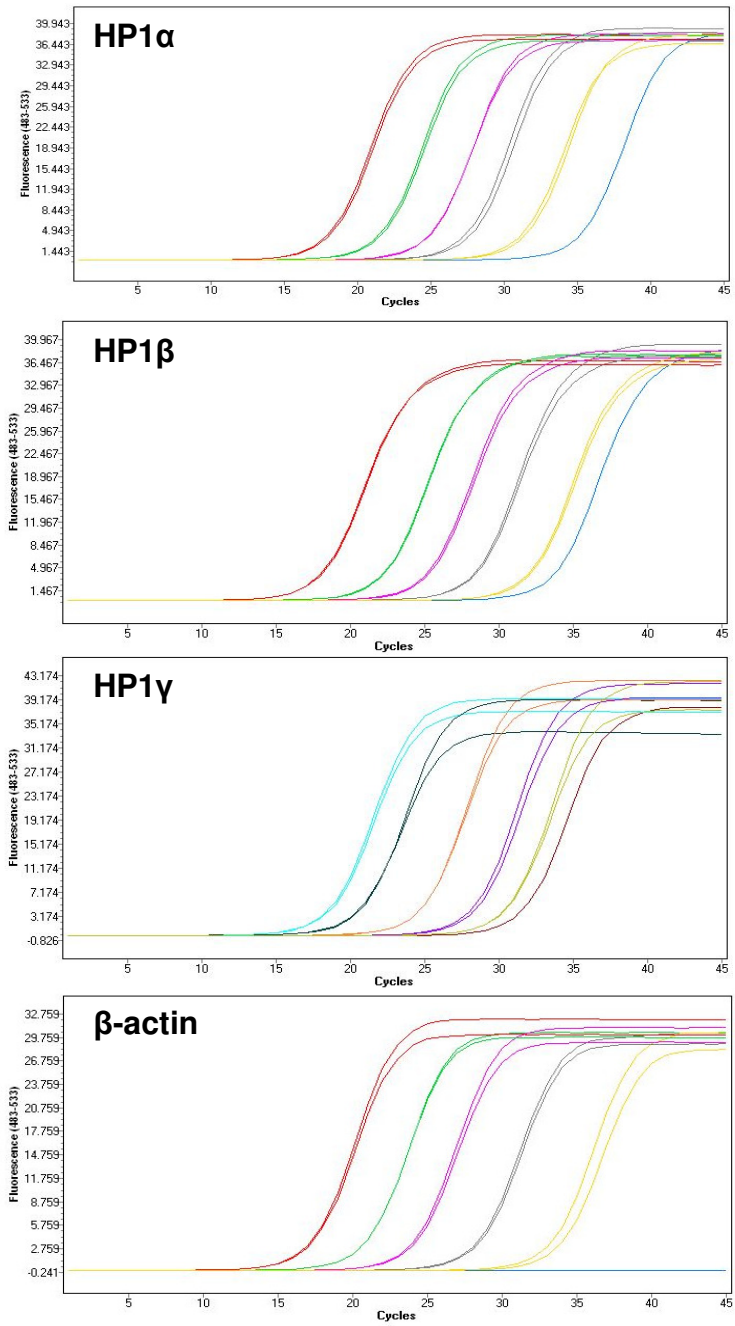

Figure 3.4. Amplification curves for HP1α, HP1β, HP1γ and β-actin standards. RNA extracted from MCF-7 cells was subjected to cDNA synthesis and PCR carried out using either HP1α, HP1β, HP1γ or β-actin primers as outlined in sections 2.2.7 and 2.2.8. The resulting PCR standards were run as duplicate samples in qRT-PCR reactions. Amplification curves for ten fold dilutions of HP1α, HP1β and β-actin are shown in red, green, pink, grey and yellow, and turquoise, dark green, orange, purple and lime for the amplification curves of the ten-fold dilutions of HP1γ. Non-template controls are shown in blue for HP1α, HP1β and β-actin, and brown for HP1γ.

incorporation was achieved. The evenly spaced amplification curves from each concentration in the dilution series show that the amount of amplification is proportional to the amount of PCR product present in each reaction and that a good range of crossing points are covered by the dilution series. A similar result is also seen when the HP1β, HP1γ, and β-actin standards were amplified. A non-template control containing only primers, water and SYBR Green I Master reagent was analysed along with each run of standards to ensure there was no genomic DNA contamination present. Each non-template control displayed either no amplification or only slight amplification after cycle 35, which is not uncommon in qRT-PCR and not an issue as it is after cycle 35.

The HP1α panel of Figure 3.5 shows the HP1α standard curve constructed by the LightCycler® 480 software. Five standards were used to ensure that a wide range of CP values were included in the standard curve, which improves accuracy in determining the concentrations of unknown samples. The reaction efficiency and the slope of the standard curve was calculated from data generated in Figure 3.4 by the LightCycler® software. The HP1α standard curve had a slope of -3.374 and an efficiency of 1.979. A slope of approximately -3.32 in conjunction with an amplification efficiency of 2 is indicative that the template is doubling in each cycle (Bustin, 2000). The standard curves used to determine concentrations of HP1β, HP1γ and β-actin cDNA in the knock-down cell lines also had amplification efficiency values as close as possible to 2±10%, and standard curve slopes of between -3.1 and -3.6. This indicated that the standards and primers for each sample produced standard curve data that were reliable, reproducible and suitable to use for subsequent absolute quantification of unknown samples.

Melt curve analysis of the HP1α, HP1β, HP1γ and β-actin standards and primers was carried out using the LightCycler® software. This ensured that each primer pair specifically amplified a single target and did not produce primer dimers. Figure 3.6 (panel HP1α) shows a single peak melting curve, which indicates that the HP1α primers do not amplify more than one specific target and also do not dimerise. This was also true for the HP1β, HP1γ and β-actin primers, which also had single melting peaks.

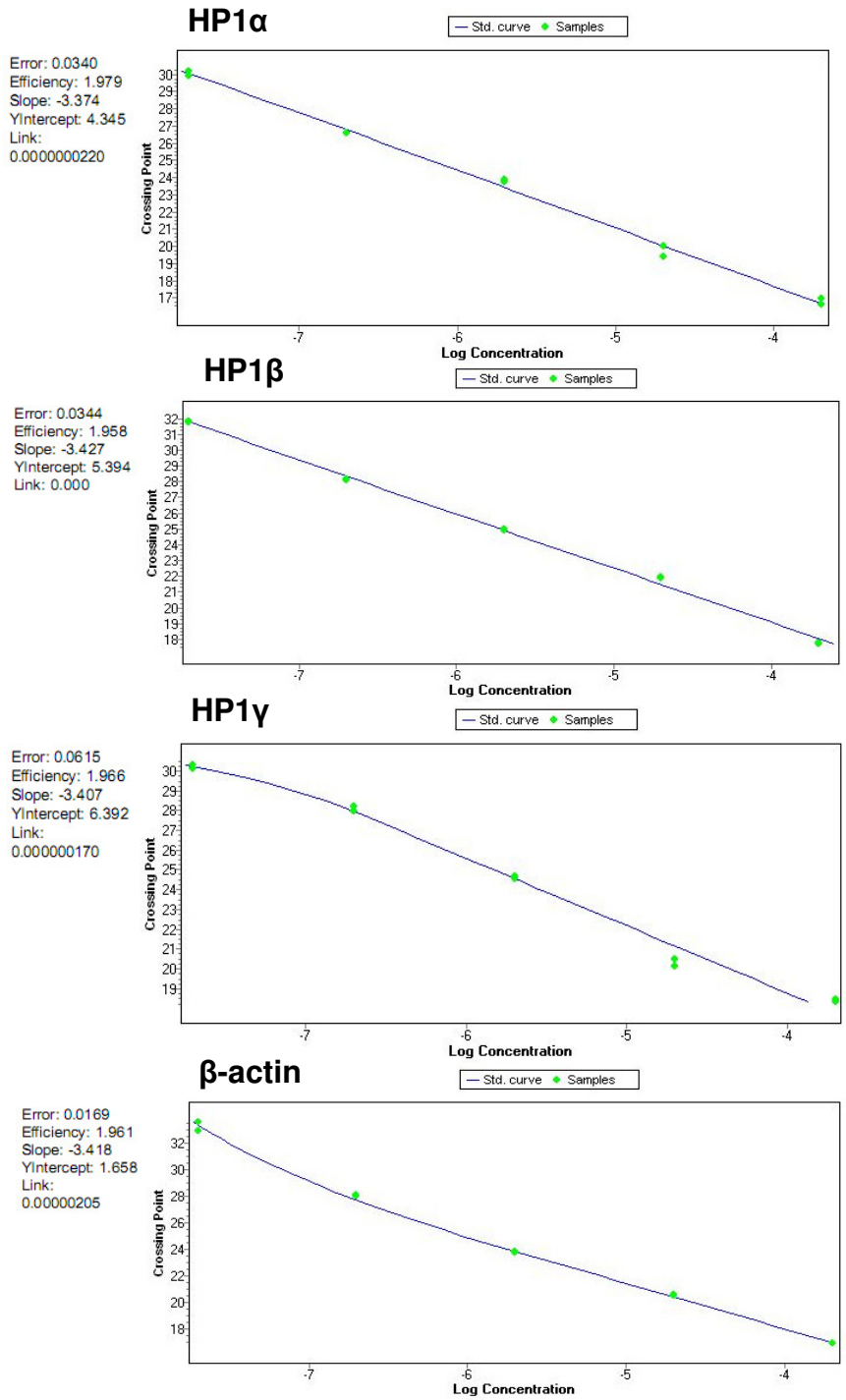

Figure 3.5. Standard curves used to determine HP1α, HP1β, HP1γ and β-actin levels in MCF-7 shRNA cell lines. RNA extracted from MCF-7 cells was subjected to cDNA synthesis and PCR carried out using either HP1α, HP1β, HP1γ or β-actin primers as outlined in sections 2.2.7 and 2.2.8. The resulting PCR standards were run as duplicate samples in qRT-PCR along side the unknown samples as in 2.2.11. Standard curves were constructed by the LightCycler 2.0 Software.

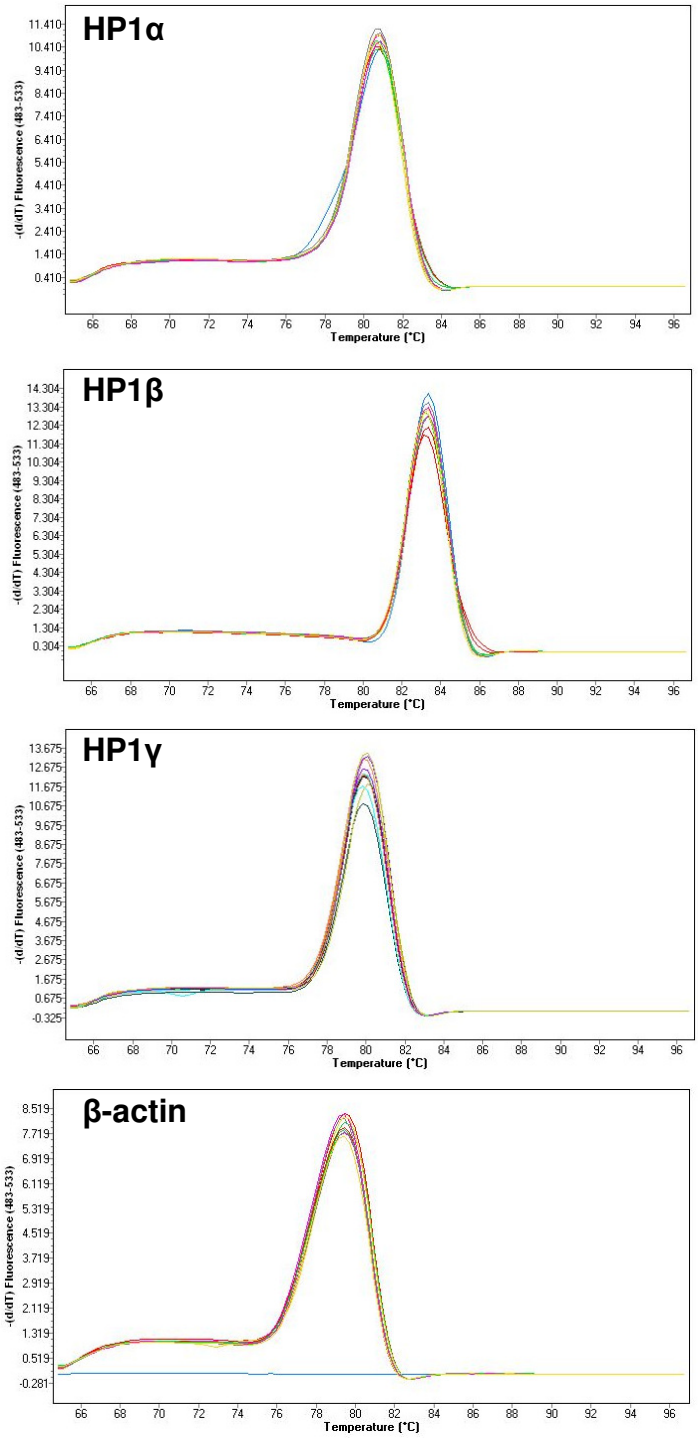

Figure 3.6. Melting curves for HP1α, HP1β, HP1γ and β-actin standards. RNA extracted from MCF-7 cells was subjected to cDNA synthesis and PCR carried out using either HP1α, HP1β, HP1γ or β-actin primers. The resulting PCR standards were run as duplicate samples in qRT-PCR along side the unknown samples as in 2.2.11. Amplification curves for ten fold dilutions of HP1α, HP1β, HP1γ and β-actin are shown in red, green, pink, grey and yellow. Non-template controls are shown in blue.

3.2.3.3 Levels of HP1 isoforms are reduced in corresponding MCF-7 stable shRNA cell lines

To quantify HP1α, HP1β and HP1γ mRNA expression in the HP1α or HP1β knock-down and control cell lines quantitative RT-PCR was performed. The cDNA used in the triplicate qRT-PCR reactions was synthesised from RNA extracted from passage two HP1α KD, HP1β KD or the two control cell lines. Primers targeting either HP1α, HP1β, HP1γ or β-actin were used (protocol described in section 2.2.11). Concentrations of the HP1 cDNA were normalised for differences in expression between the cell lines. Normalised HP1 cDNA levels for each cell line were calculated by dividing the cDNA concentration of each HP1 isoform by the concentration of β-actin cDNA. The normalised cDNA concentration of a specific HP1 isoform from the knock-down cell lines was divided by the normalised cDNA concentration of the same HP1 isoform from the respective control cell line to calculate relative expression of the knock-down cell lines. The control cell lines were set as one, and the relative HP1α, HP1β, and HP1γ cDNA levels were graphed for the HP1α or HP1β knock-down cell lines (Figure 3.7).

The CBX5 ID1, ID2, ID3 and ID4 show 80%, 55%, 10% and 20% of the level of HP1α cDNA seen in the HC cell line. All four CBX5 shRNA cell lines also had between a 200% and 250% of the HC HP1β cDNA levels. HP1γ expression was between 15% and 45% higher in the CBX5 ID1-4 cells than the HP1γ level in the HC cell line. These results indicate that the CBX5 ID3 cell line had the greatest reduction in HP1α expression, but that all the HP1α knock-down cell lines had increased HP1β, and to a lesser extent, enhanced HP1γ expression.

Figure 3.8 shows that the HP1β cDNA levels in the CBX1 ID1-4 shRNA cells were between 10% (ID3) and 30% (ID2) of the HP1β levels in the NC cells. HP1α expression was also reduced by varying degrees; the CBX1 ID 1-4 cells had decreases of 30%, 40%, 64% and 78% relative to the NC cells respectively. Levels of HP1γ were between 42% and 78% of those seen in the NC cell line. Together, these results indicate that the CBX1 ID3 cell line had the greatest reduction in HP1β cDNA, but that all the HP1β cell lines showed varying levels of HP1α and HP1γ expression.

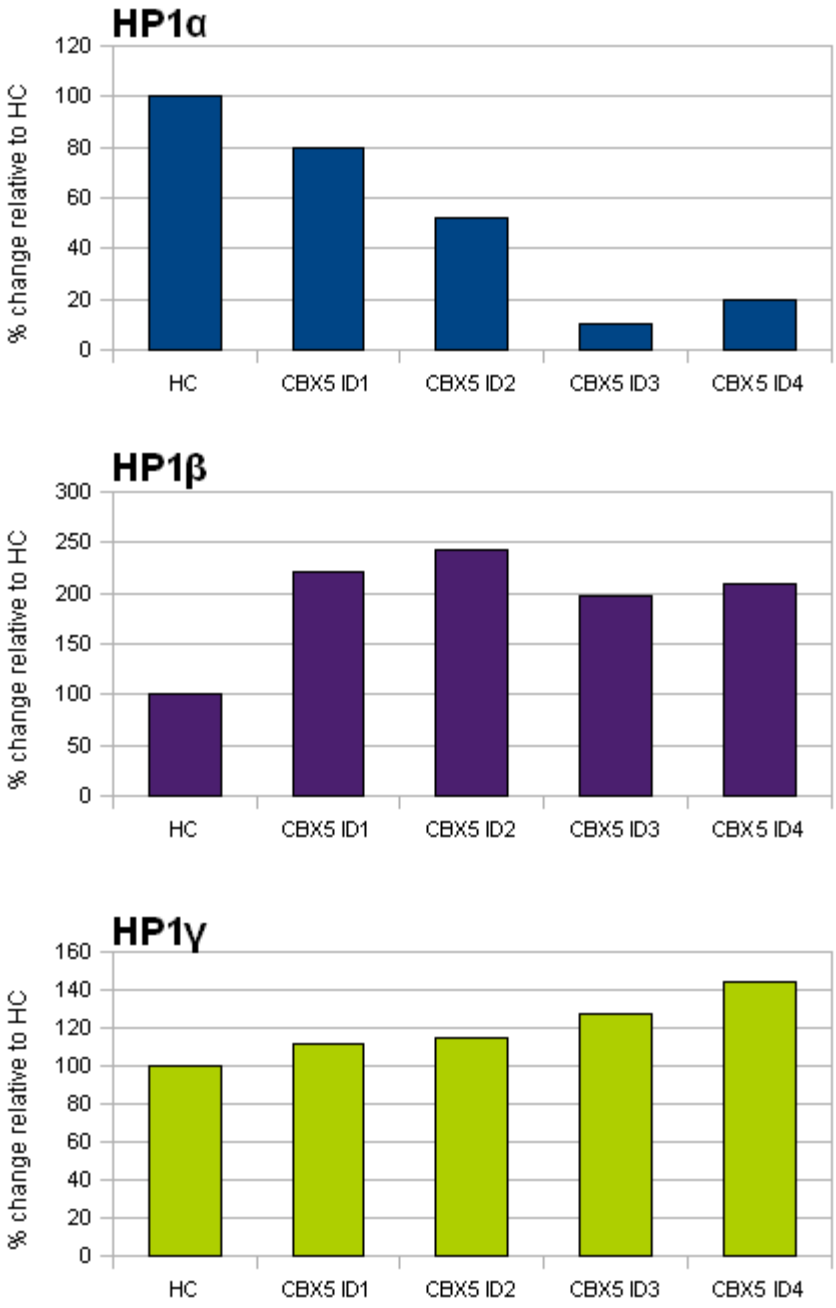

Figure 3.7 HP1 isoform mRNA expression in CBX5 shRNA cell lines. RNA extracted from four CBX5 shRNA MCF-7 cell lines or the hygromycin control (HC) cell line and subjected to qRT-PCR in triplicate reactions with primers targeting HP1α, HP1β, HP1γ or and β-actin as in 2.2.11. Relative expression was determined by normalising HP1α, HP1β and HP1γ cDNA levels to β-actin cDNA and then calculating the percentage change relative to the HC expression levels.

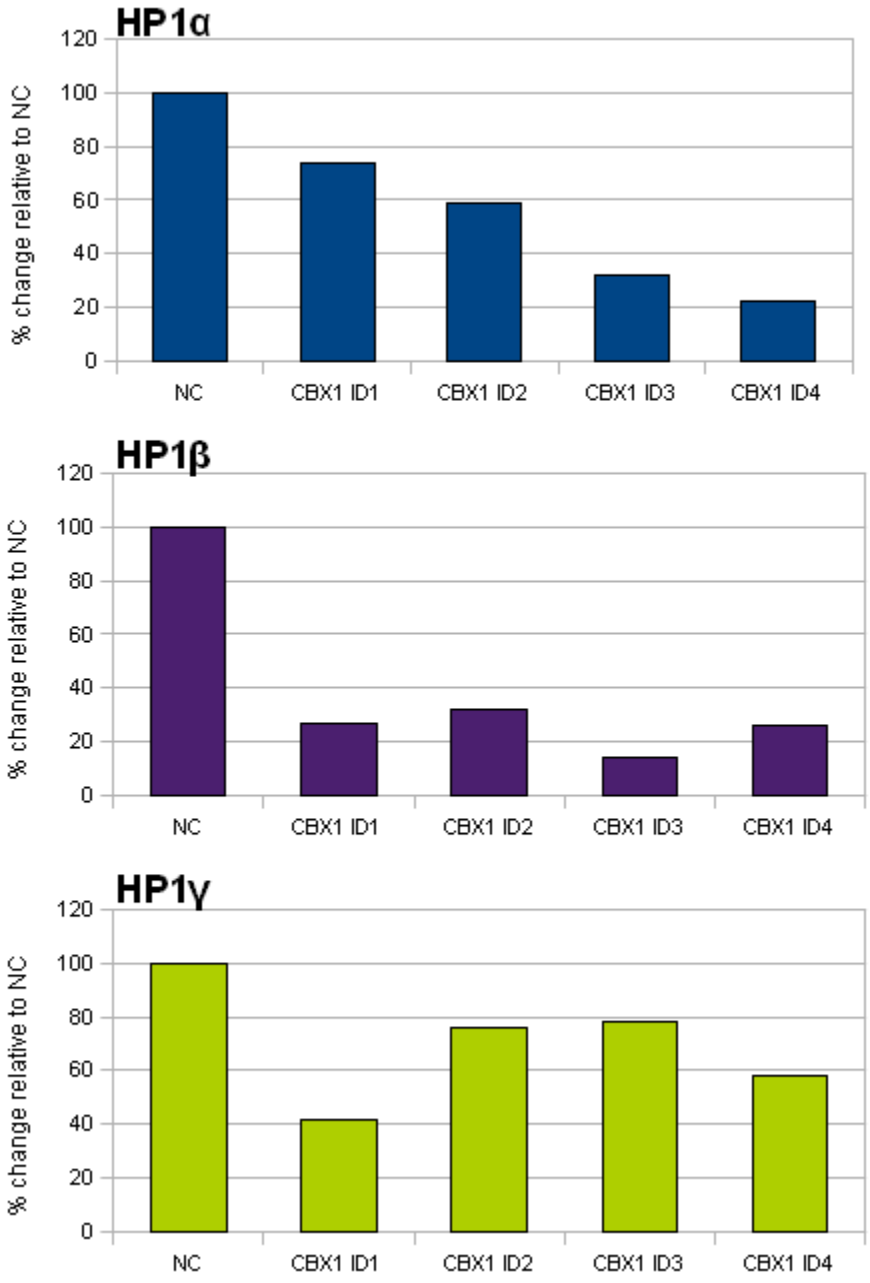

Figure 3.8. HP1 isoform mRNA expression in CBX1 shRNA cell lines. RNA extracted from four CBX1 shRNA MCF-7 cell lines or the neomycin control (NC) cell line and subjected to qRT-PCR in triplicate reactions with primers targeting HP1α, HP1β, HP1γ or β-actin as in 2.2.11. Relative expression was determined by normalising HP1α, HP1β and HP1γ cDNA levels to β-actin cDNA levels and then calculating the percentage change relative to the NC cell line.

Overall, these results indicated that MCF-7 cell lines with stable reduction in either HP1α or HP1β had been successfully created, although the many of the cell lines also showed changes in other HP1 isoforms.

3.2.4 Examining levels of HP1α and HP1β protein in the HP1α or HP1β KD MCF-7 shRNA cell lines

To confirm that altered levels of HP1α and HP1β mRNA correlated with protein levels, the HP1α KD and HP1β KD cell lines selected for further analysis (CBX5 ID3 for HP1α KD and CBX1 ID3 for HP1β KD) were examined. HP1α KD and HP1β KD cell lysates were prepared, quantified and subjected to SDS-PAGE as described in section 2.2.13-2.2.15. Immunoblotting was then performed as described in section 2.2.16 using antibodies raised against either HP1α, HP1β or tubulin and the results can be seen in Figure 3.9. The immunoblot shows that the amount of HP1α protein is reduced in the HP1α KD cell line compared to the HC cell lines, and the same is true of the amount of HP1β protein in the HP1β KD cell line relative to the NC cell line. However, the HP1β protein in the HP1α KD cell line appeared to be increased. In addition, the amount of HP1α protein was reduced slightly in the HP1β KD cell line. Tubulin levels in the HP1α KD, HP1β KD, NC and HC lanes were similar, indicating that the differences seen in the levels of HP1α and HP1β protein were not due to unequal gel loading.

Taken together, these results confirm that HP1α protein was decreased in the HP1α KD cell line compared to the HC cell line, but that HP1β protein levels appear to be increased. HP1β levels were reduced in the HP1β KD cells, but HP1α levels were also slightly reduced. These results confirm that altered HP1 mRNA levels seen in section 3.2.3.3 also extend to changes in protein levels in the HP1α KD and HP1β KD cell lines. HP1γ protein levels will need to be examined in these cell lines to confirm whether they are similar to HP1γ mRNA levels.

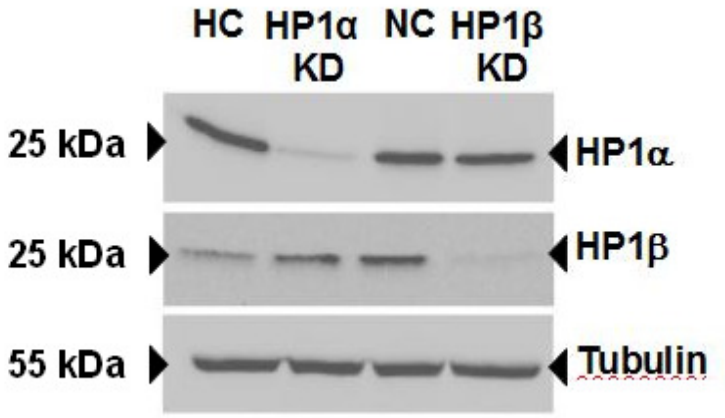

Figure 3.9. Levels of HP1α and HP1β protein are altered in the HP1α KD and HP1β KD cell lines. Whole cell lysate was extracted from the four cell lines above and subjected to SDS-PAGE and immunoblot using antibodies against HP1α and HP1β (described in sections 2.2.13-2.2.16). An antibody against tubulin was used as a loading control. Sizes of the proteins as determined using molecular size markers are indicated on the left hand side.

3.3 Chapter discussion

Several MCF-7 cell lines were created that exhibited decreased expression of either HP1α or HP1β mRNA. While the CBX5 ID3 cell line that was selected for further analysis had an expected decrease in HP1α of 90% relative to the control cell line, qRT-PCR showed that there was also an increase in HP1β mRNA. The altered levels of HP1α and HP1β mRNA were also shown to extend to HP1α and HP1β protein. The increase in HP1α suggests that there may be some form of cross-regulatory or compensatory effects at play between the HP1α and HP1β isoforms. Repeated qRT-PCR reactions with later passage cells showed that the CBX5 ID3 cells continued to have low HP1α mRNA expression and increased HP1β mRNA expression compared to the HC cells (data not shown). This demonstrates that the stable HP1α knock-down remains constant and that the increase in HP1β is not a transient effect.

However, the cell lines created with the CBX1 shRNA plasmids were found to have partially reduced expression of HP1α mRNA as well as an 85% reduction in HP1β mRNA levels. While this could potentially be the outcome of the CBX1 shRNA plasmids cross-targeting to reduce HP1α expression, BLAST searching carried out by the shRNA plasmids' manufacturer has indicated that these shRNAs should not also target the CBX5 mRNA. As a result, it is a possibility that this partial decrease in HP1α is due to HP1β playing a role in the regulation of HP1α expression, and could highlight an explanation for the concurrent loss of both HP1α and HP1β that has been observed previously in several tumour types (T. Hale and A Contreras, unpublished data).

The CBX1 ID3 cell line chosen for further characterisation had the greatest decrease in HP1β mRNA compared to the NC cell line (85% reduction in expression), but the partial HP1α knock-down (expressed 30% of the NC HP1α level, slight decrease in HP1α protein seen) it also exhibits could also provide some insight into the consequences of a concurrent decrease in both HP1α and HP1β in MCF-7 cells. Like the HP1α KD cells, the HP1β KD cells also maintained low HP1 mRNA expression compared to the NC cell line when later passage cells were again examined with qRT-PCR, indicating that the decrease in HP1α is a change that is maintained over time (data

not shown).

Any changes observed during the characterisation of the HP1β KD cell line could attributed to either a decrease in HP1β, or a concurrent decrease in both HP1α and HP1β. Similarly, any altered phenotype in the HP1α KD cells could potentially be due to increased HP1β rather than decreased HP1α. This potential interplay between the different HP1 isoforms cannot be disregarded, and will need to be considered when analysing data generated from charactering these cell lines. Consequently, it will be necessary in the future to characterise cell lines with reduced HP1β expression only to determine whether this is sufficient to cause these changes, or if a decrease in HP1α is also needed. Additionally, characterisation of cell lines with decreased HP1α but no increases in HP1β will be needed to confirm that any changes are due to HP1α knock-down only.

4. Growth analysis of HP1α or HP1β knock-down MCF-7 cell lines

4.1 Introduction

MCF-7 cell lines with reduced expression of HP1α or HP1β had been created to explore the role of HP1α and HP1β in breast cancer progression. These cell lines had been examined for changes in HP1 mRNA expression and two cell lines were selected for further analysis on the basis of these results.

Given that HP1α has been shown to be expressed in a cell cycle dependent manner and that the HP1 isoforms have a role in chromatin segregation (De Koning *et al.*, 2009), it is possible that a decrease in HP1α or HP1β could result affect the cell cycle profile of MCF-7 cells. Previous research had shown that siRNA targeting of any of the three HP1 isoforms in HeLa cells did not alter cell cycle profiles (De Koning *et al.*, 2009). In this study, the cell cycle profiles of the HP1α KD and HP1β KD MCF-7 cell lines were compared to the control cell lines. This was carried out using fluorescent activated cell sorting (FACS).

As HP1α and HP1β have been implicated in regulating transcription, reducing their levels in MCF-7 cells may impact the expression of proteins that regulate basic cell functions such as proliferation (Bachman *et al.*, 2001; Fuks *et al.*, 2003). Two approaches were taken to investigate the proliferation of the HP1α KD and HP1β KD cell lines: a bromodeoxyuridine (BrdU) incorporation assay and real-time cell monitoring.

The HP1 isoforms also play an important role in the formation of heterochromatin (Lachner *et al.*, 2001). To explore whether reducing the levels of HP1α or HP1β in MCF-7 cells had impacted global chromatin compaction, the cells were treated with a fluorescent DNA intercalating stain and the intensity of the staining was measured.

This chapter describes the analysis of proliferation, cell cycle profiles and global chromatin compaction of the HP1α KD and HP1β KD cell lines using the assays mentioned here.

4.2 Results

4.2.2 Growth analysis of HP1α and HP1β KD cells using a bromodeoxyuridine incorporation assay

To determine if decreased HP1 levels affected the growth of MCF-7 cells, growth patterns for the HP1α KD and HP1β KD cell lines were established. BrdU is a synthetic nucleoside that can be incorporated into replicating DNA in the place of thymidine during the S-phase of the cell cycle (Gratzner, 1982). By using an antibody against BrdU along with a secondary antibody conjugated to a peroxidase enzyme, the appropriate colourimetric peroxidase substrate can be used to determine BrdU that is incorporated using spectrophotometry. The amount of BrdU incorporated will be relative to the number of cells present. Therefore, by BrdU-treating cells that have been seeded at the same density but which have been allowed to grow for different lengths of time it is possible to establish a growth pattern. This type of assay is an endpoint assay, meaning that the cells are harvested and tested for BrdU incorporation after a specific length of time, as opposed to being monitored continuously throughout the assay.

4.2.2.1 Optimisation of seeding density for the BrdU incorporation assay

Before the BrdU incorporation assay could be carried out using the HP1 knock-down MCF-7 cells, the appropriate seeding density had to be determined. Insufficient cell numbers would lead to the levels of BrdU being below the detection threshold for the assay. Conversely, too many cells would cause saturation of the assay, and data would be inaccurate. The NC and HP1β KD cell lines were selected to optimise seeding density.

The four cell lines were seeded in triplicate at five seeding densities ranging from $6x10^2$ cells/well to $1x10^4$ cells/well. Cells were allowed to grow for 24 hours before being exposed to BrdU for 18 hours. The cells were then processed as in 2.2.19 and the resulting corrected absorbance values are presented in Figure 4.1. Gradual increases in absorbances are seen for both cell lines as the seeding density increases up to $2.5x10^3$

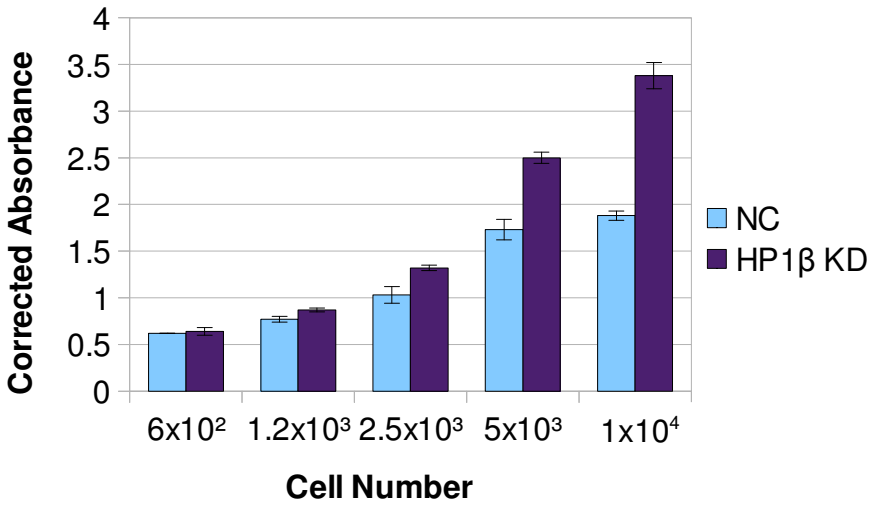

Figure 4.1 Optimising cell number for a BrdU incorporation assay. NC and HP1β KD MCF-7 cells were seeded in triplicate at five concentrations, exposed to BrdU for 18 hours and then subjected to a colourmetric assay (described in section 2.2.24) to determine the amount of BrdU incorporated. Corrected absorbance was calculated by subtracting the absorbance reading at 492 nm from the absorbance reading at 370 nm for each well. Error bars represent the standard error of the mean of triplicate wells.

cells/well. However, at the $5x10^3$ cells/well and $1x10^4$ cells/well seeding densities the HP1β KD cells exhibited a higher absorbance readings compared to the the NC cells. When the cells were viewed under an inverted light microscope just prior to harvesting, the cells seeded at $5x10^3$ cells/well and $1x10^4$ cells/well were at around 80% and 90% confluency respectively. This may indicate that the growth of the NC cells were inhibited at these higher seeding densities due to over-crowding.

Collectively, these results suggest that seeding densities of more than $2.5x10^3$ cells/well may show differences in growth between the HP1β KD and NC cells after 33 hours. However, the proliferation assays used to generate growth curves were to be carried out for a longer time period. As a result, the seeding density needed to be lower than $2.5x10^3$ cells/well to avoid the cells becoming over-confluent by the end of the assay. Consequently, a seeding concentration of $1x10^3$ cells/well was selected to carry out the assays used to construct growth curves for the HP1α KD and HP1β KD cell lines. This seeding concentration had resulted in absorbance readings that showed minor variation in the NC and HP1β KD cells 33 hours after seeding, so it was deemed that this would be sufficient cells for the BrdU assay to display any differences in proliferation between the four cell lines.

4.2.2.2 Growth patterns of HP1α KD and HP1β KD MCF-7 stable cell lines are similar

Growth patterns for the HP1α KD and HP1β KD MCF-7 cell lines were constructed using absorbance values obtained from a BrdU incorporation assay as described in section 2.2.19. The media of the cells grown for four or five days was replenished at the day three mark to prevent media exhaustion. Corrected absorbance values for each of the four cell lines taken over five days were used to construct the graph depicted in Figure 4.2.

Corrected absorbance values for the HP1α KD and HC cell lines remain similar over the course of the experiment, increasing slowly up to day two and then sharply between days two and three. The corrected absorbance values for both cell lines appear to reach a

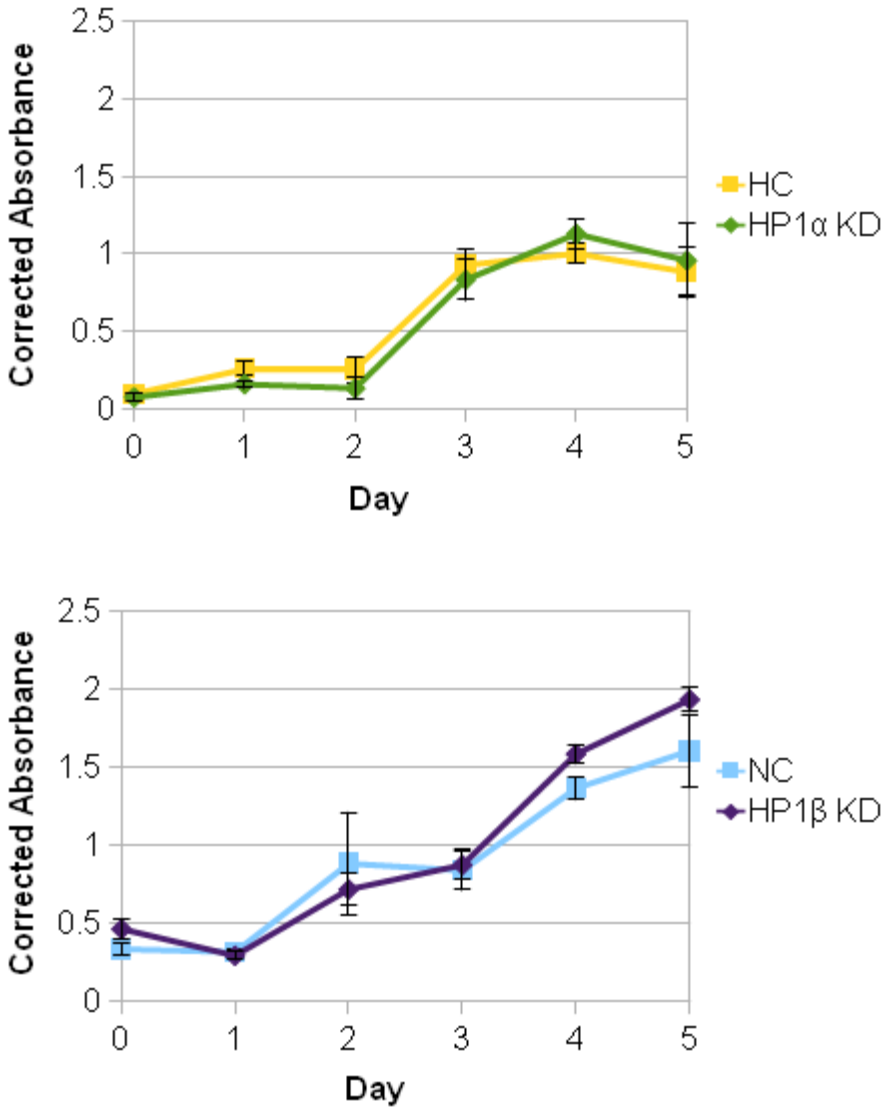

Figure 4.2 HP1α KD and HP1β KD MCF-7 cells show unaltered growth patterns in a BrdU incorporation assay. HC, HP1α KD, NC and HP1β KD MCF-7 cells were seeded in triplicate into six plates and one plate was exposed to BrdU and processed (as in section 2.2.19) at 24 hour intervals. Corrected absorbance was calculated by subtracting the absorbance reading at 492 nm from the absorbance reading at 370nm for each well. Error bars represent the standard error of the mean of triplicate wells.

plateau between days four and five. Similarly, the corrected absorbance values for the HP1β KD and NC cell lines follow a similar pattern of gradual increase between days zero and five. Together, these results suggest that decreasing HP1α or HP1β does not alter proliferation in MCF-7 cells.

When assaying the HC and HP1α KD cells, the greatest difference between the highest and lowest absorbance values was 1.1, whereas the maximum absorbance change from the proliferation assays carried out on the NC and HP1β KD cells was 1.9. This could have been due to an increase in sensitivity of the MCF-7 cells to the hygromycin compared to the geneticin, as the cells grown in hygromycin typically were observed to grow more slowly than the cells treated with geneticin when cultivated for use in assays. Alternatively, it may have been due to errors in seeding density; this assay could be repeated to confirm this.

4.2.3 Real-time cell monitoring demonstrates unchanged proliferation in HP1α KD and HP1β KD MCF-7 cell lines

One of the limitations of end-point proliferation assays is that cell growth can only be examined at a single time point. The growth of two cell lines may appear identical using an end-point assay, but it is possible that differences in the proliferation rates are being missed due to errors in time point selection or seeding densities. These problems can be minimised using the xCelligence™ (Roche) real-time cell monitoring, a system that uses specialised electrode coated cell culture plates to measure the impedence generated by the cells as they adhere and spread on the plate surface (Atienzar *et al.*, 2011). This data is recorded as the Cell Index (CI), and by normalising this data to the point at which cells are adherent a pattern of cell growth can be determined. Additionally, the xCelligence System™ is also able to calculate doubling times (the length of time taken for CI to increase two-fold) and dose responses to any compounds we might wish to expose the cells to.

The HP1α KD and HP1β KD MCF-7 cell lines and the controls were subjected to real-time cell monitoring as described in section 2.2.20. The CI data was normalised to the

16 hour time point, as this was when the cells were visually confirmed to be adherent. Figure 4.3A shows that the HP1α KD cell line showed the same gradual rise in normalised CI (NCI) as the HC cells over 119 hours. Similarly, the HP1β KD cells also had a similar gradual rise in NCI as the NC cell line (Figure 4.3B). The doubling times for each cell line were also calculated by the xCelligence™ software using the NCI readings for each cell line. As none of the four cell lines showed a plateau in NCI towards the end of the experiment, the cells were still viable and proliferating right up to 119 hours and had not arrested due to growth restrictive conditions. Therefore it was appropriate to calculate doubling times over the course of the entire 119 hours. All four cell lines were found to have a doubling time of roughly 25 hours (Figure 4.3C). These results indicate that there was no difference in proliferation between the four MCF-7 cell lines examined.

4.2.3.1 Response to β-estradiol is unaltered in HP1α KD and HP1β KD MCF-7 cells

MCF-7 possess cytoplasmic estrogen receptors, and typically show an increased growth response when treated with estrogen (Wiese *et al.*, 1992). However, whether levels of HP1α or HP1β affected this growth response in MCF-7 cells was unknown. Real-time cell monitoring was used to assess how the HP1α KD and HP1β KD cells responded to estrogen. The four cell lines were seeded in triplicate onto E-plates and 24 hours later were treated with 1 μM of β-estradiol or left untreated and monitored for four days (as in section 2.2.20). The resulting CI values were normalised to the 16 hour time point, averaged across triplicate wells and graphed against time (Figure 4.4).

The untreated cells for all four cell lines showed a gradual increase in NCI over the course of the 119 hours. In contrast, NCI values for the β-estradiol treated cells rapidly increased from 64 hours until the conclusion of the assay. This demonstrated an increased growth response in the presence of estrogen. However, when the doubling times of all the growth curves were calculated and compared there was again very little difference between them (data not shown). Therefore, this indicated that the HP1α KD and HP1β KD cells did not show different proliferation responses to β-estradiol compared to the control cell lines. Nevertheless, as this experiment was only carried out

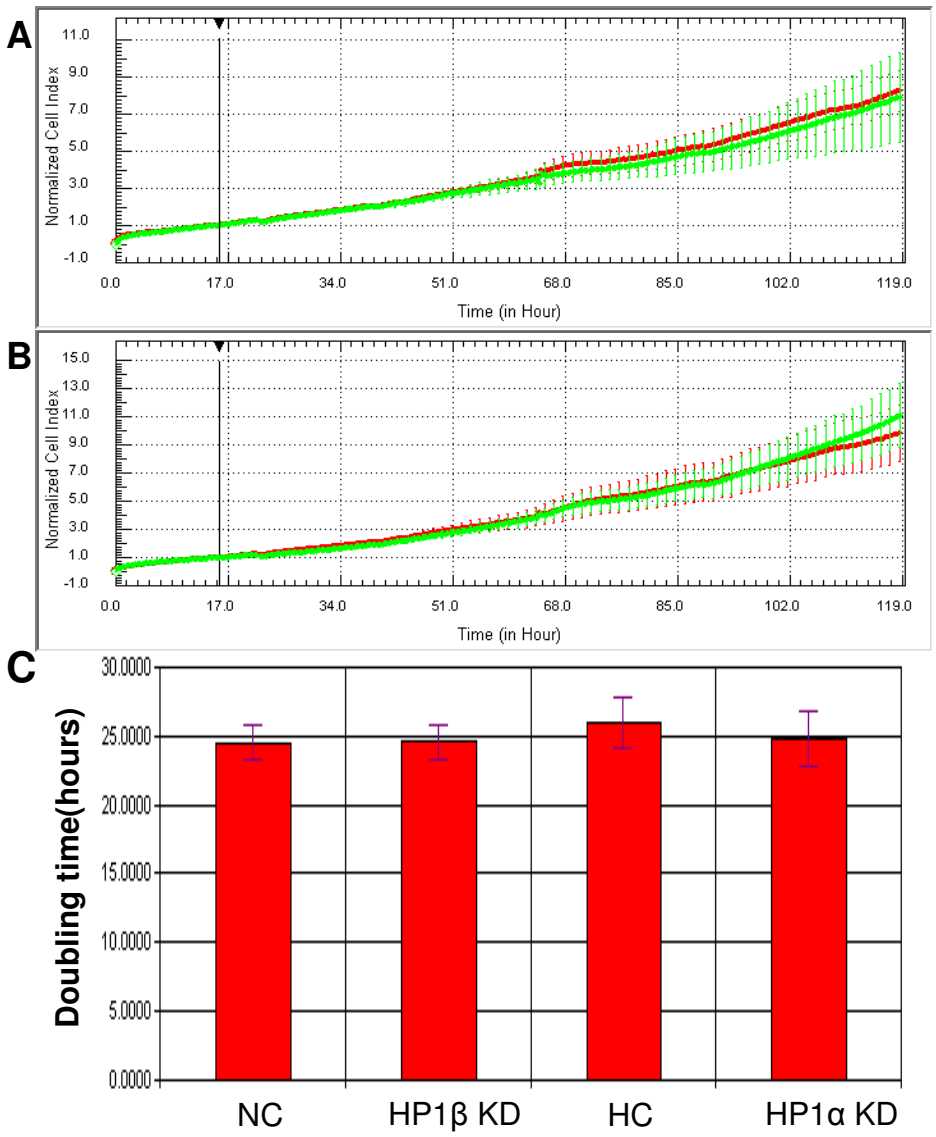

Figure 4.3 HP1α and HP1β KD cells show identical growth curves compared to their respective controls when examined using real-time cell monitoring. HC (**A**, red), HP1α KD (**A**, green), NC (**B**, red) and HP1β KD (**B**, green) cells were seeded in triplicate into electrode coated plates (section 2.2.20) and cell index readings were taken by the xCelligence™ software at 15 minute intervals for 119 hours. Triplicate cell index readings for each cell line were averaged, and the values normalised to the time of adherence (black arrow) and graphed. The xCelligence™ software was also used to determine the average doubling times from the triplicate CI vs. time plot of each cell line (**C**). Error bars represent the standard deviation of the mean.

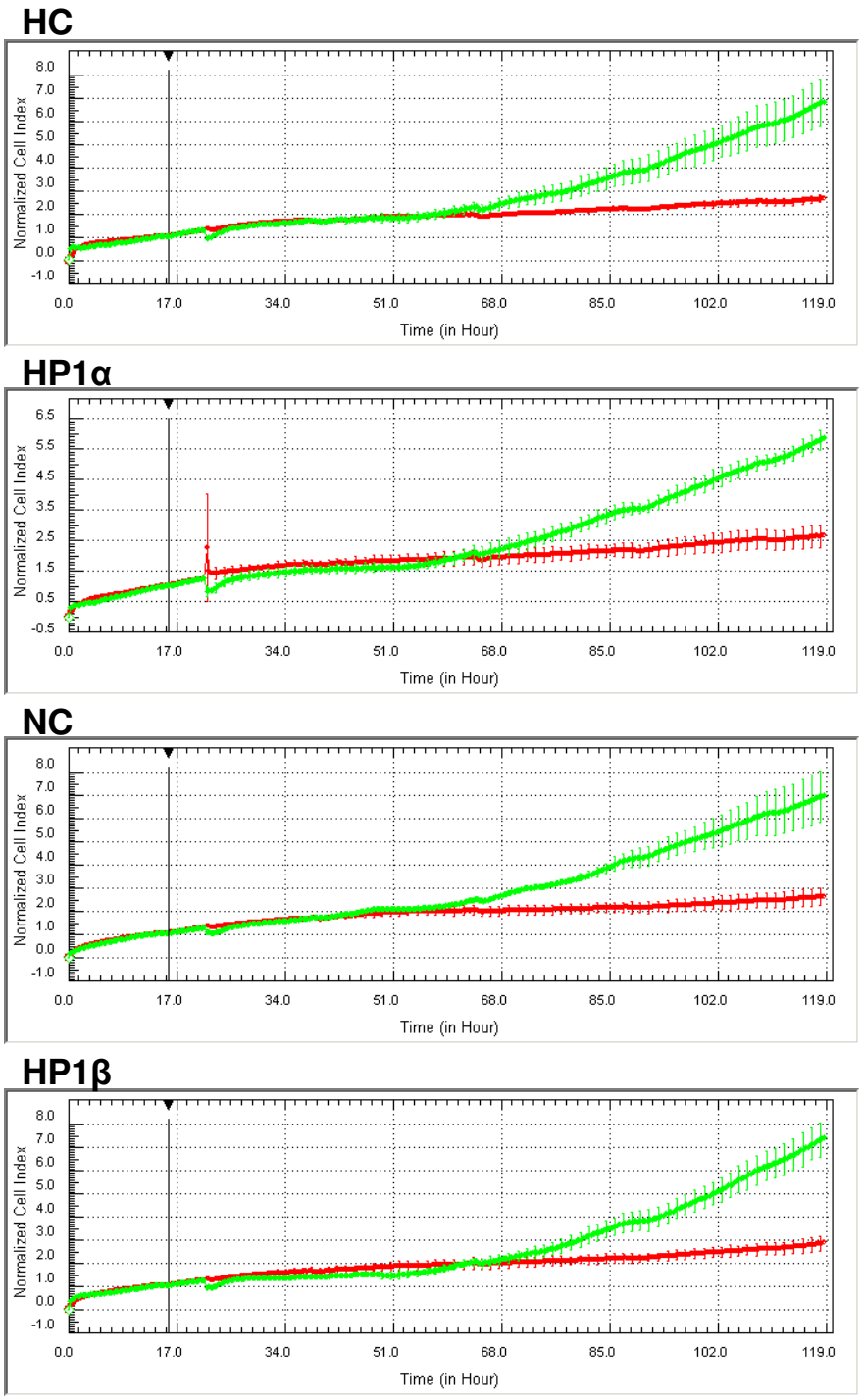

Figure 4.4 MCF-7 cells with stable HP1α or HP1β knock-down do not have an altered response to estrogen. The four cell lines above were seeded in triplicate into E-plates and treated after 24 hours with media containing either no estrogen (red) or 1μM β-estradiol (green) for four days (described in 2.2.20). The CI values of triplicate wells were normalised for time of adherence (black arrow), averaged and plotted against time. Error bars represent the standard deviation of the mean.

once due to time constraints it should be repeated to confirm this result.

4.2.2 Analysis of HP1α KD and HP1β KD cells with fluorescence activated cell sorting demonstrates unchanged cell cycle profiles

Fluorescence activated cell sorting (FACS) was the method chosen to examine the cell cycle profiles of the HP1α KD and HP1β KD cell lines (method outlined in 2.2.21). This method utilised a flow cytometer to sort the cells into three populations according to DNA content. DNA content was determined by intensity of staining with propidium iodide, a fluorescent molecule that can intercalate within the DNA. The populations of cells were G0/G1(2n DNA, cells are quiescent or preparing to begin cell division), S (increased DNA staining, synthesis of DNA is occurring in preparation for mitosis), and G2/M (4n DNA, cells just prior to entering or undergoing mitosis).

The cells were treated with RNase prior to sorting to ensure that propidium iodide fluorescence was due to the presence of DNA only. Samples from each cell line were also left unstained as a control for propidium iodide staining; these cells had cell cycle profiles that were shifted to the left with a single peak (data not shown). This is because the flow cytometer was still able to count the cells, but they could not be sorted into the different phases of the cell cycle due to the lack of propidium iodide. An RNase A control was also included, using cells from each cell line that were not treated with RNase A. As expected, these cells had cell cycle profiles that were shifted to the right as the result of increased propidium iodide staining (data not shown). Cell cycle profiles for the HP1α KD, HP1β KD cell lines and control cell lines were constructed using cell counts at each propidium iodide (PI) intensity (Figure 4.5).

The HP1α KD cells had cells distributed across the PI intensities similarly to the HC cells, with a large peak corresponding to the G0/G1 cells (M1) and a much smaller peak corresponding to the G2/M cells (M3). The percentages of cells sorted into G0/G1, S and G2/M were similar in the HP1α KD and HC cells (Table 4.1).

The cell cycle profiles of the HP1β KD cell line also had cells distributed over the

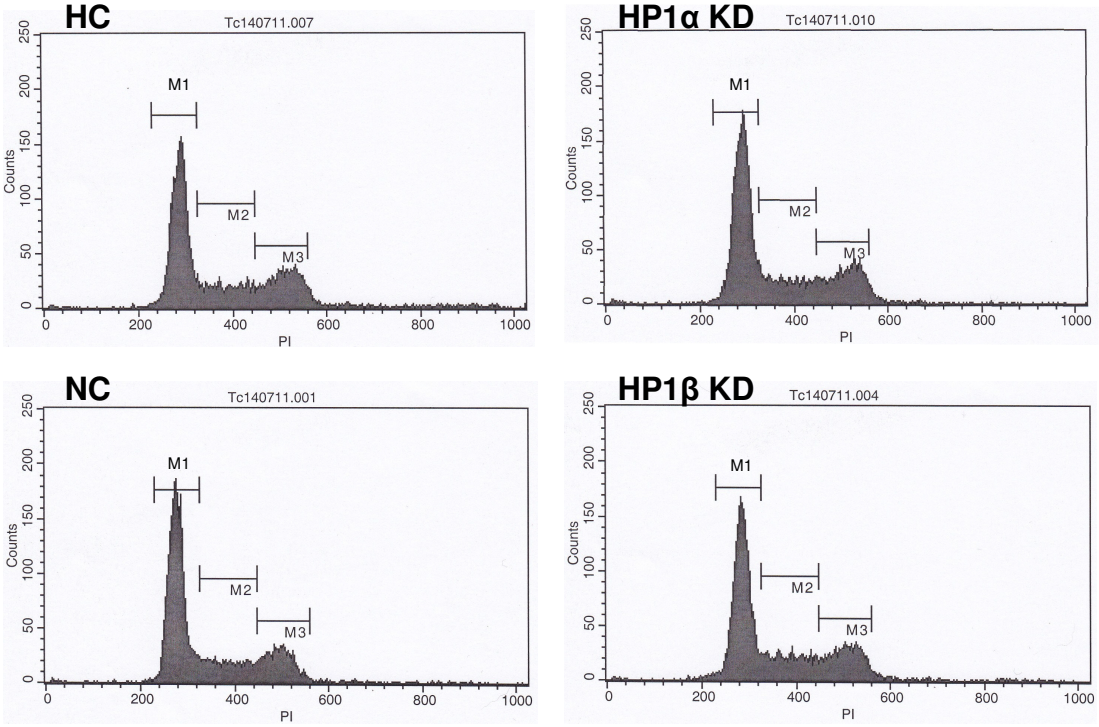

Figure 4.5 HP1α and HP1β knock-down MCF-7 cell lines have unchanged cell cycle profiles compared to control cell lines. Sub-confluent cells were harvested, fixed, stained with propidum iodide and sorted into G0/G1(M1), S(M2), and G2/M (M3) populations with a flow cytometer (method described in 2.2.21). Cell counts for each propidium iodide intensity were constructed into a graph for each cell line.

	Average % G0/G1 (M1) ± Std Dev	Average % S (M2) ± Std Dev	Average % G2/M (M3) ± Std Dev
HC	51.27±1.75	18.21±0.18	25.31±1.31
HP1α KD	57.75±1.36	18.14±0.28	19.81±0.86
NC	59.43±2.33	18.46±0.68	19.83±1.01
HP1β KD	55.34±0.44	19.4±0.19	22.68±0.64

Table 4.1 Proportions of HC, HP1α KD, NC and HP1β KD cells in G0/G1, S, and G2/M as determined by fluorescent activated cell sorting. Sub-confluent cells were harvested, fixed, stained with propidum iodide in triplicate and sorted into G0G1(M1), S(M2), and G2/M (M3) populations with a flow cytometer (method outlined in section 2.2.21).

different PI intensities in a similar pattern to the NC cells, with peaks at G0/G1 (M1) and G2/M (M3). Table 4.1 shows that the HP1β KD cells had similar percentages of G0/G1, S, and G2/M cells compared to the NC cells.

On the whole, these results indicate that decreasing HP1α or HP1β did not appear to influence the cell cycle of MCF-7 cells.

4.2.4 Acridine orange staining shows decreased chromatin compaction in HP1α KD and HP1β KD MCF-7 cells compared to control cell lines

As HP1 proteins can facilitate heterochromatin formation, it was investigated whether decreasing either HP1α or HP1β would alter global chromatin compaction in MCF-7 cells (Lachner *et al.*, 2001). To achieve this, the cells were fixed and stained with acridine orange, a stain that intercalates into DNA (McMaster and Carmichael, 1977). Cells with more globally open chromatin will incorporate more acridine orange than those with compacted DNA, and therefore give greater intensity of staining. After fixing and staining the cells according to the method described in section 2.2.23 six different images were taken of the cells using identical confocal microscope settings. Intensity plots were constructed from these images using Leica LAS AF software (Figure 4.6).

The HP1α KD cell line had greater fluorescence when compared to the HC cell line. Increased fluorescence is indicated by the presence of brighter orange cells in the photographs, and higher yellow peaks in the intensity plots. These peaks were present in the HP1α KD intensity plot, but absent in the HC intensity plot. Similarly, the HP1β KD cell line also exhibited greater fluorescence than the NC cell line. This was demonstrated by the presence of considerably more yellow peaks in the HP1β KD intensity plot compared to the NC intensity plot. The greater fluorescence seen in both the HP1α KD and HP1β KD cell lines indicates that these cell lines both have globally more open chromatin compared to the control cell lines. Hence, HP1α and HP1β may contribute to maintaining global chromatin compaction in MCF-7 cells.

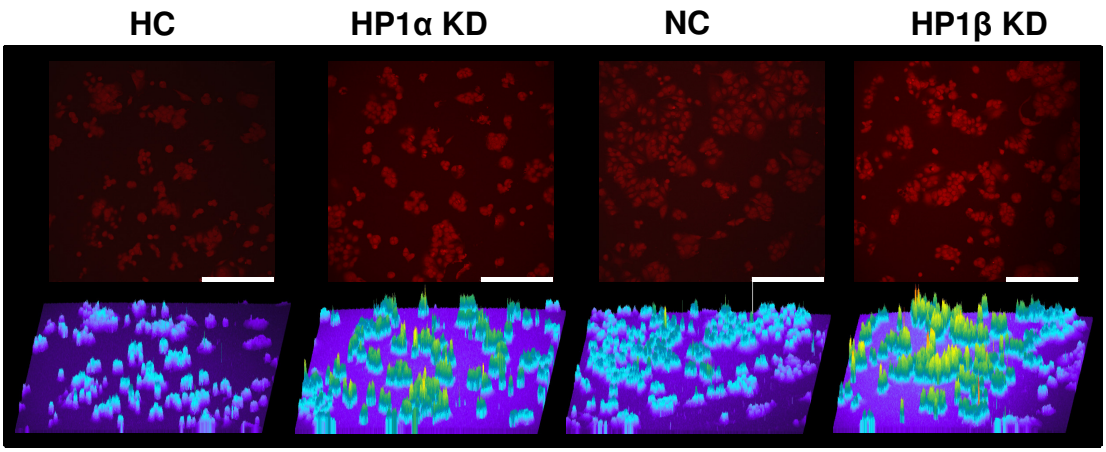

Figure 4.6 MCF-7 cells with HP1α or HP1β knock-down show decreased chromatin compaction compared to their respective control cell lines. HC, HP1α KD, NC and HP1β KD cell lines were fixed and stained with acridine orange as described in section 2.2.23. Six images were taken using identical conditions and intensity plots constructed from the pictures obtained. Increased staining intensity is indicated by the height of the peaks and also by the colour; intensity of staining increases moving from the purple/blue spectrum through to the yellow/red. Images are representative and scale bars (white) represent 250 μm.

4.3 Chapter discussion

MCF-7 cells with decreased expression of either HP1α or HP1β and their respective control cell lines were assayed for changes in proliferation, estrogen-dependent proliferation, cell cycle profile and chromatin compaction.

HP1α KD cells were found to have unaltered proliferation compared to the HC cells when examined with both the BrdU proliferation assay and real-time cell monitoring. This result agrees with the unchanged proliferation previously reported for MCF-7 cells with artificially reduced HP1α (Norwood *et al.*, 2006). Doubling times calculated from the real-time cell monitoring data were also the same, at around 25 hours. Additionally, real-time cell monitoring also showed that the HP1α KD cells had a similar increase in proliferation in response to β-estradiol treatment.

The HP1β KD MCF-7 cells also showed similar growth patterns to the NC cell line when analysed with the BrdU assay and real-time cell monitoring. Doubling times were 25 hours for the two cell lines, and an estrogen-dependent proliferation response was exhibited by both the HP1β KD and NC cell lines.

The HP1α KD cells were shown to have similar cell cycle profiles to the HC cells, with the percentages of cells sorted into G0/G1, S, or G2/M populations generally within 10% of each other for the two cell lines. There was slightly greater variation seen in the percentages of G2/M cells, but repeating this experiment with a higher of replicates may give percentages that are more similar may result in percentages that are more similar.

As with the HP1α KD cells, the HP1β KD cells also showed little variation in cell cycle profiles, and the sorted populations of cells were within 10% for the HP1β KD and NC cell lines. This result and the one given by the HP1α KD cells confirm the results of a study that examined cell cycle profiles of HeLa cells with HP1α or HP1β knockdown and also found them to be unchanged.

Both the HP1α KD and HP1β KD cell lines showed increased acridine orange staining

compared to their respective control cell lines. However, this result needs to be investigated in more depth and would benefit from the addition of a control to ensure that staining is even. However, an increase in acridine orange staining in the HP1α and HP1β KD cells compared to the control cell lines may indicate a decrease in global chromatin compaction.

5. Investigating *in vitro* metastatic potential of HP1α KD and HP1β KD MCF-7 cell lines

5.1 Introduction

To explore the *in vitro* metastatic potential of the HP1α KD and HP1β KD cell lines, assays were carried out to analyse invasive potential and anchorage independence. Increased invasive potential and anchorage independence are two properties acquired by cancer cells that allow them to detach from the primary tumour and move to another area of the body as the cells become metastatic (Huang and Ingber, 1999). An invasion assay was established to confirm whether the invasive potential of the HP1α KD cells was in agreement with previous studies, and also to explore the role of HP1β in invasion. A soft agar colony formation assay was also established to determine whether the cells could grow in an anchorage independent manner. This chapter describes the optimisation of these assays and their use to characterise the MCF-7 stable HP1α or HP1β knock-down cell lines.

5.2 Results

5.2.1 Investigating the invasive potential of MCF-7 HP1α and HP1β KD cell lines

Loss of HP1α has previously been identified as a causal factor in increasing the invasive potential of MCF-7 cells (Kirschmann *et al.*, 1999). However, whether decreased HP1β in MCF-7 cells alters invasive potential has not yet been explored. To investigate this, an assay was established to measure the invasive potential of the cells. In this assay, porous membranes coated with extracellular matrix proteins (ECM) are used to create upper and lower chambers in cell culture wells. The ECM is used to occlude the membrane pores and prevent indiscriminate migration. Cells are suspended in serum-free media and overlaid onto this membrane, while media containing FBS is used as a chemo-attractant in the lower chamber of the well. Cells that are capable of invasion are able to degrade the ECM proteins, pass through the membrane pores, and grow on the

underside of the membrane, where they are later fixed and stained in preparation for counting (Albini *et al.*, 1987).

Before the MCF-7 stable HP1 knock-down cell lines could be assayed for invasive potential, parameters including seeding density, the amount of ECM used in membrane coating, and the timespan of the assay needed to be optimised.

5.2.1.1 Optimisation of seeding density and ECM coating for MDA-MB-231 cells

An optimal seeding density will allow a sufficient number of invasive cells in the population to adhere the membrane for accurate counting. However, cell number seeded must not also be so high that the cells are able to degrade the membrane and invade due to over-growth of cells on the ECM layer.

Similarly, the amount of ECM used needed to be sufficient to provide a barrier to indiscriminate migration, but still result in a thin enough coating that the invasive cells could degrade it and pass through the membrane within the time constraints of the assay. Seeding density and the amount of ECM used in the invasion assay were consequently optimised with the MDA-MB-231 cell line, an invasive breast cancer cell line (Kirschmann *et al.*, 2000). Four different MDA-MB-231 seeding densities between $5x10^4$ cells/well and $2.5x10^5$ cells/well with three ECM coating amounts were assayed for invasive potential according to the prescribed method in section 2.2.18. Percentage invasion was calculated by multiplying the number of cells adhered to the bottom of the membrane in a field of specified size. This number was then extrapolated to area of the whole membrane to work out the total cell number of cells on the membrane. The total number of invading cells was then divided by the total number of cells that were seeded and finally multiplied by 100.

Figure 5.1A displays representative images of the invading MDA-MB-231 cells present on the underside of the membranes. Few cells are present at a seeding density at or below $1x10^5$ cells/well, but the number of invading cells has dramatically increased using a seeding density of $2.5x10^5$ cells/well. This indicates that a seeding density of

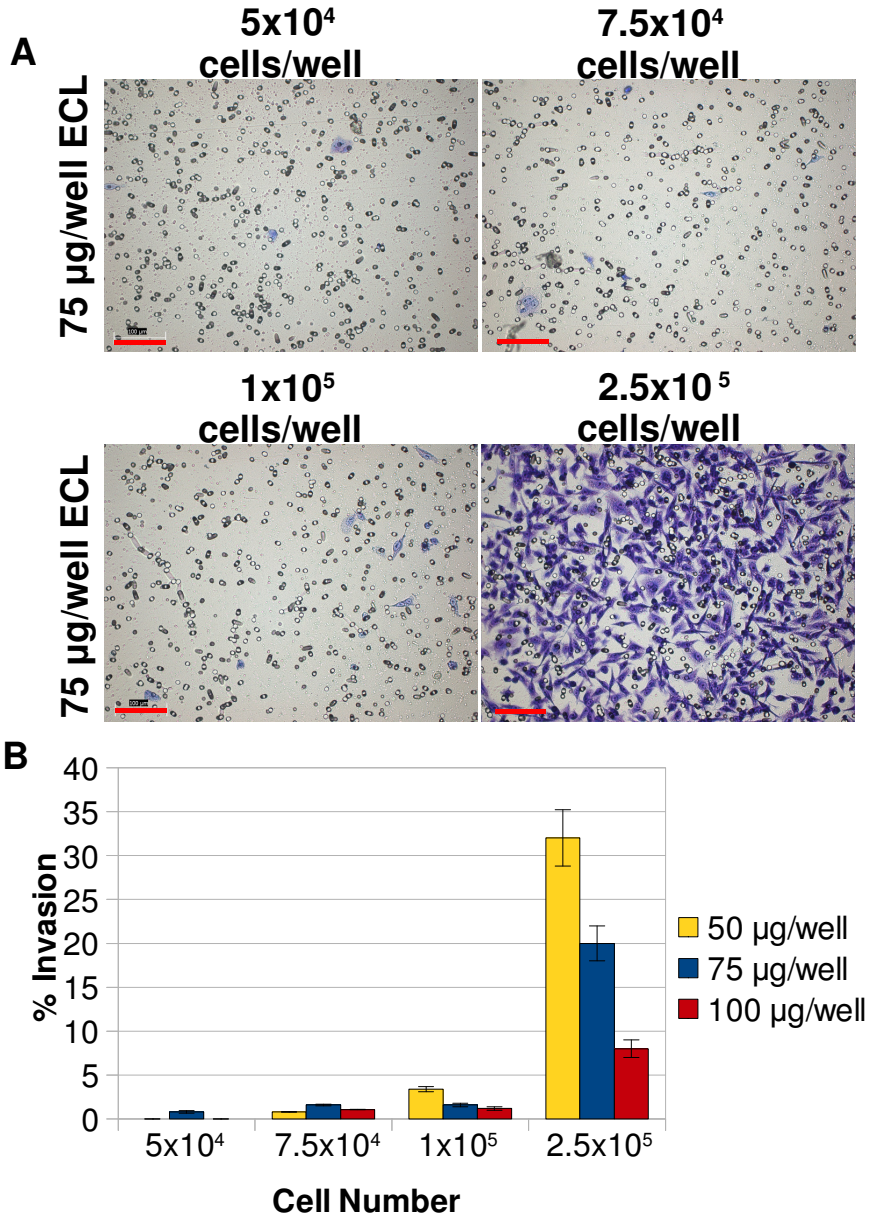

Figure 5.1 Optimising cell number and extracellular matrix coating amount for the invasion assay. The four different seeding densities of MDA-MB-231 cells shown above were seeded in duplicate onto membranes coated with either 50 µg, 75 µg or 100 µg of ECM and left to invade for 24 hours. At this point the cells were stained, imaged (**A**), counted (section 2.2.18) and the percentage invasion calculated and graphed (**B**). Error bars represent the standard error of the mean. Scale bars (red) represent 100 µm.

greater than $1x10^5$ cells/well is needed for MDA-MB-231 cells to achieve significant invasion. Figure 5.1B summarises the percentage invasion values of the MDA-MB-231 cells at a range of ECM and seeding densities. Cells seeded at less than $1x10^5$ cells/well achieved less than 1.6% invasion regardless of which ECM was used during seeding. Percent invasion rose to between 1.6% and 3.4% when the cells were seeded at $1x10^5$ cells/well onto one of the three ECM concentrations. A seeding density of $2.5x10^5$ cells/well had the highest percentage invasion across the three ECM amounts, with 32% invasion with 50 μg ECM/well, 20% invasion at 75 μg ECM/well and 8% invasion at 100 μg ECM/well. This indicates that an appropriate seeding density for MDA-MB-231 cells to achieve significant invasion was $2.5x10^5$ cells/well.

A seeding density of $2.5x10^5$ cells/well was also chosen for future invasion assays that were carried out with MCF-7 cells. While percentage invasion for the MDA-MB-231 cell line was greater than 7% at all three ECM amounts tested, MCF-7 cells are typically less invasive and therefore may not have been able to invade through 100 μg/well of ECM during the time constraints of this assay. Consequently, the 50 μg ECM/well and 75 μg ECM/well concentrations were both selected for further optimisation with the MCF-7 cells.

5.2.1.2 Optimisation of invasion assay length and ECM coating amount

Previous invasion assays with MCF-7 cells had been carried out using a variety of assay time lengths, ranging from just six hours to five days (Cos *et al.*, 1998; Fiucci *et al.*, 2002). Consequently, we needed to determine the optimal length of time needed for the MCF-7 HP1α and HP1β KD cells to invade through the membrane. The NC and HP1β KD MCF-7 cell lines were initially selected to optimise assay length and the amount of ECM required. These cells were suspended in FBS-free media and seeded at a density of $2.5x10^5$ cells/well onto membranes coated with either 50 μg/well and 75 μg/well of ECM. After incubation lasting either three or five days, the cells were stained, imaged and the percentage invasion calculated as in section 5.2.1.1.

Figure 5.2 summarises percentage invasion values obtained for the NC and HP1β KD

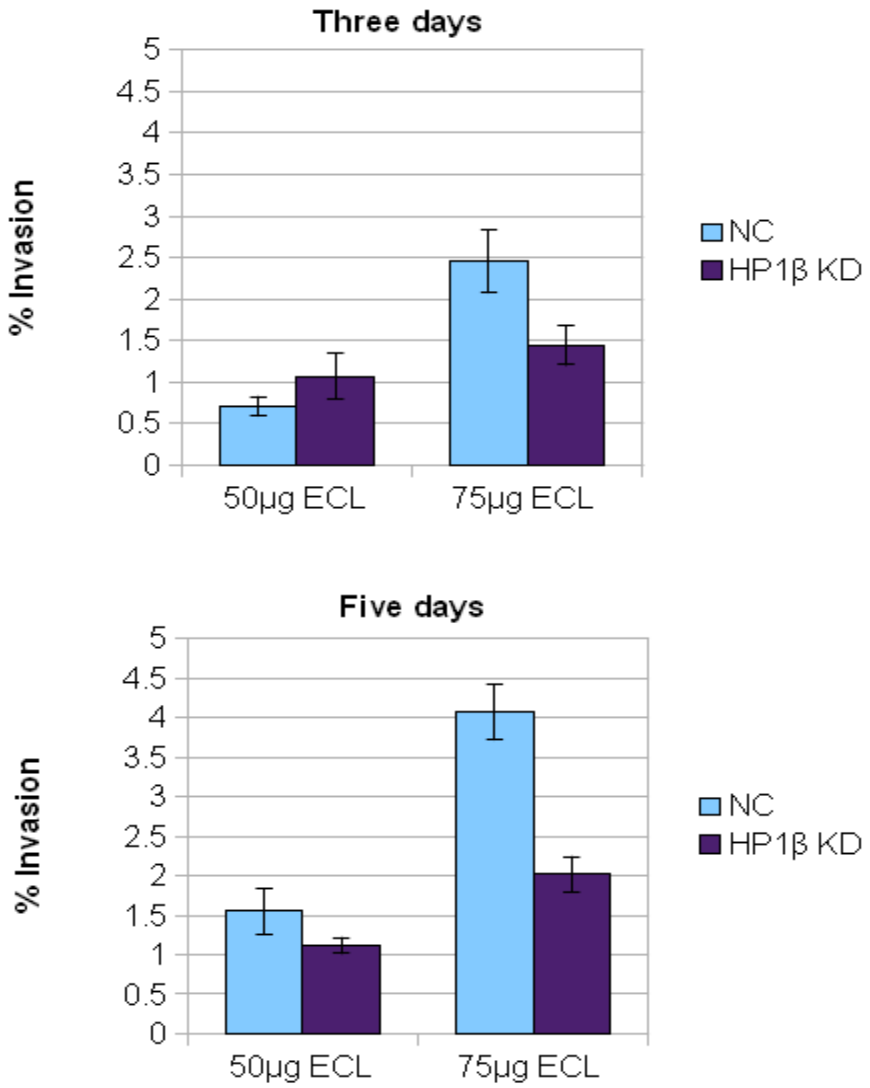

Figure 5.2 Optimising ECM amount and assay time length for NC and HP1β KD MCF-7 cell lines. Cells were seeded in duplicate onto membranes coated with either 50 µg or 75 µg of ECM and left to invade for either three days or five days. The membranes were then stained, imaged, counted and percentage invasion calculated as in 2.2.18. Error bars represent the standard error of the mean of duplicate wells.

cells. The two cell lines had similar percentages of invasion when 50 μg/well of ECM was used in either the three day or five day assays. Both cell lines showed higher percentage invasion using 75 μg/well of ECM at either three or five days compared to the 50 μg/well of ECM wells. However, when 75 μg/well of ECM was used the NC cells showed increased percentage invasion compared to the HP1β KD cells.

The final conditions selected to test the invasive potential of the HP1α KD and HP1β KD cell lines were five days, 50 μg/well of ECM and a $2.5x10^5$ cells/well seeding density. As the wells containing 75 μg/well of ECM did not dry as effectively as the 50 μg/well of ECM wells, there were concerns about about inconsistent ECM polymerisation in the 75 μg/well of ECM wells. Initially, a three day assay time was selected along with the same ECM amount and seeding density as this timespan did result in sufficient invading cells to calculate percentage invasion. However, no changes in invasion were seen amongst the four cell lines when the invasion assay was carried out using these conditions as all four cell lines exhibited between 0.5 and 0.6% invasion (Figure 5.3). Accordingly, the decision was made to proceed with the assay for five days instead, to ensure that differences in invasive potential amongst the cell lines would not become apparent when the cells were left to invade for longer.

5.2.1.3 Reduction of HP1α or HP1β levels does not alter invasive potential in MCF-7 cells

The conditions that were optimised in the previous assays described were used to measure the invasive potential of the HP1α KD and HP1β KD cells. Cells were suspended in FBS-free media and seeded onto membranes previously coated with 50 μg/well ECM. Migration controls, which demonstrated that the cells were capable of moving through an uncoated membrane, were provided by seeding the cells onto uncoated membranes with media containing FBS in the bottom well. This control also shows that invasion is inhibited by the presence of the ECM on the membrane. A control to demonstrate the chemo-attractive properties of the FBS media was created by seeding the cells onto an uncoated membrane with FBS-free media in the bottom well. The cells were incubated for five days, then the cells on the underside of the membrane

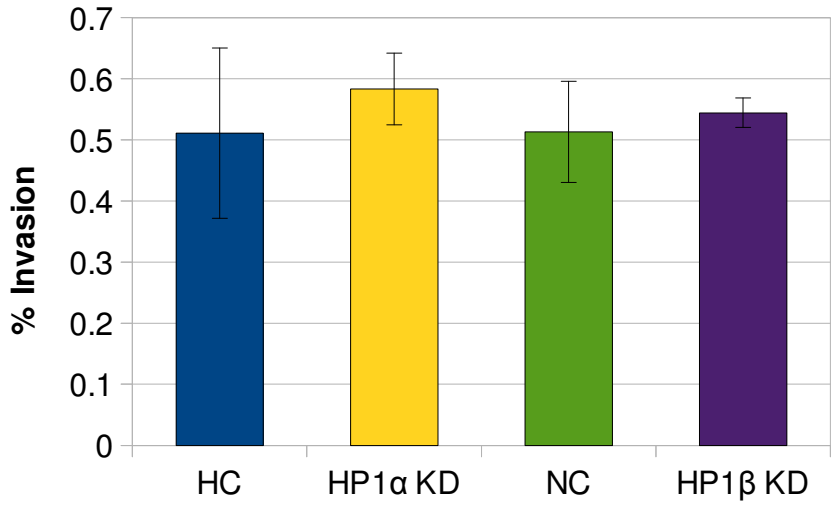

Figure 5.3 MCF-7 cells with HP1α or HP1β knock-down show no differences in invasive potential compared to their respective control cell lines after three days. The four MCF-7 cell lines were seeded onto either membranes coated with ECM with FBS as a chemo-attractant in the lower wells. After three days the cells were stained, imaged, counted and the percentage invasion calculated as in section 2.2.18. Error bars represent the standard error of the mean of triplicate wells.

were prepared and counted as described in 2.2.18. Percentage invasion was calculated as in section 5.2.1.1.

Figure 5.4 depicts the summarised results of the invasion assay using the four cell lines. Relative to the HC cell line, the HP1α KD cell lines had a very similar percentage invasion (Figure 5.4A). When the cells were tested in a migration control, however, the HP1α KD cell line had a lower percentage of migrated cells than the HC cell line (Figure 5.4B). This may have been due to an error in seeding density in the HC cells, as it would be expected that the migration of the HC and NC cell lines were more similar. The uncoated membrane/no FBS control resulted in both the HC and HP1α KD cell lines showing less than 0.3% invasion, which is the expected result as it demonstrates that the cells will not move through the membrane if there is no chemo-attractant present (Figure 5.4C).

The HP1β KD cell line was also found to have a similar percentage invasion compared to the NC cell line. The percentage of migrating cells was slightly lower in the HP1β KD cell line than in the NC cell line. As with the HC and HP1α KD cell line, the uncoated membrane/no FBS control also resulted in under 0.3% invasion.

Taken together, these results suggest that decreasing HP1α or HP1β does not impact the invasive potential of MCF-7 cells.

5.2.2 Examining anchorage independence of HP1α KD and HP1β KD MCF-7 cells

Characteristics of cancer cells include the ability to proliferate in the absence of ECM or cell-cell interactions (anchorage independence) and also the capacity to form three-dimensional colonies instead of a mono-layer (Assoian, 1997; Bissell and Radisky, 2001; Freedman and Shin, 1974). The ability of HP1α KD and HP1β KD cells to form anchorage-independent colonies was assayed using a soft agar colony formation assay. This involves mixing cells with low-melting temperature agarose combined with growth media and seeding them onto a layer of previously set agarose. The cells are then cultured for three weeks, stained, and the number of three dimensional round colonies

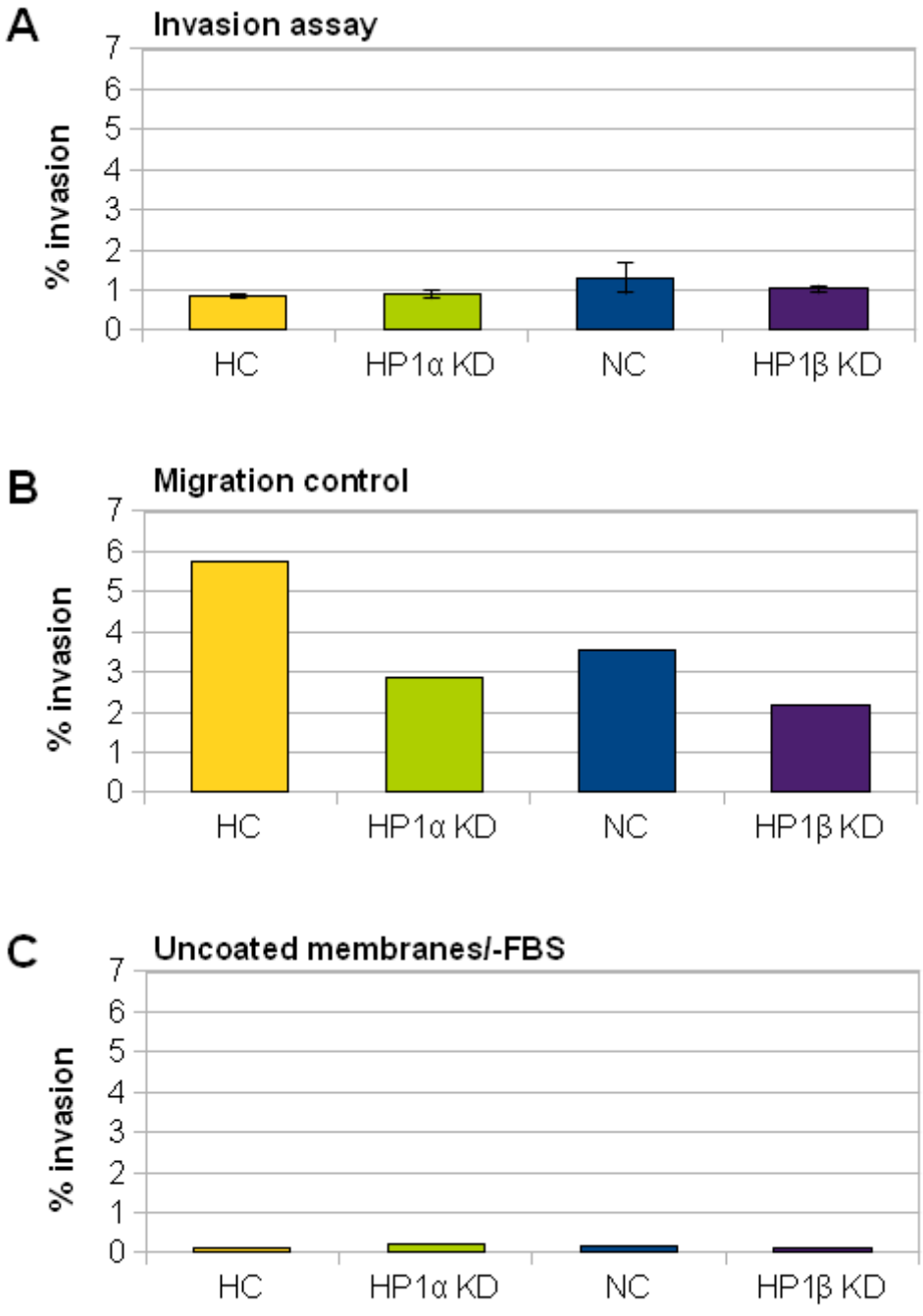

Figure 5.4 HP1α or HP1β KD MCF-7 cells displayed unaltered invasive potential compared to their respective control cell lines. The four MCF-7 cell lines were seeded onto either membranes coated with ECM with FBS as a chemo-attractant in the lower wells, or FBS free media as a control. After five days the cells were stained, imaged, counted and the percentage invasion calculated as in section 2.2.18. Error bars represent the standard error of the mean of triplicate wells.

are counted.

5.2.2.1 Optimising gelling time for the soft agar colony formation assay

An initial difficulty in establishing the soft agar colony formation assay came in the form of finding a suitable gelling time. Insufficiently gelled agarose, when placed in the incubator, will liquefy and the cells sink to the bottom of the plate. The NC and HP1β KD cell lines were used to optimise the agarose gelling time, as the length of time taken would remain constant regardless of which cell lines were used. Appropriate gelling time was determined by setting up agarose plates containing HP1β KD and NC cells as prescribed in 2.2.22. The plates of cells were then refrigerated for either five or ten minutes before placing the plates were relocated to the incubator. The cells were allowed to grow for three weeks before being stained, imaged and the spherical colonies were counted.

The plate incubated for five minutes resulted in the majority of the cells sinking to the bottom of the plate, and forming irregularly shaped flat patches. True colonies, spherical in shape and distinguishably three dimensional, were not in high abundance, with an average of just 18 colonies per well for the NC cells and 29 colonies per well for the HP1β KD cells (Figure 5.5A). The cells grown in the agarose that was allowed to gel for ten minutes gave many more spherical colonies; an average of 83 colonies per well for the NC cells and 225 colonies per well for the HP1β KD cells (Figure 5.5B). These results indicate that the ten minute gelling time was more suitable due to the increase in spherical colonies seen for both cell lines, and it was chosen for subsequent assays.

5.2.2.2 Decreasing HP1α or HP1β in MCF-7 cells alters anchorage independence

To assess their ability to grow anchorage independently and form three-dimensional colonies, the HP1α KD and HP1β KD were subjected to a soft agar colony formation assay. The cell lines were assayed in triplicate using the procedure outlined in 2.2.22 with at ten minute agarose gelling time. After three weeks' growth, the cells were stained, and the number of spherical three-dimensional colonies counted. This assay

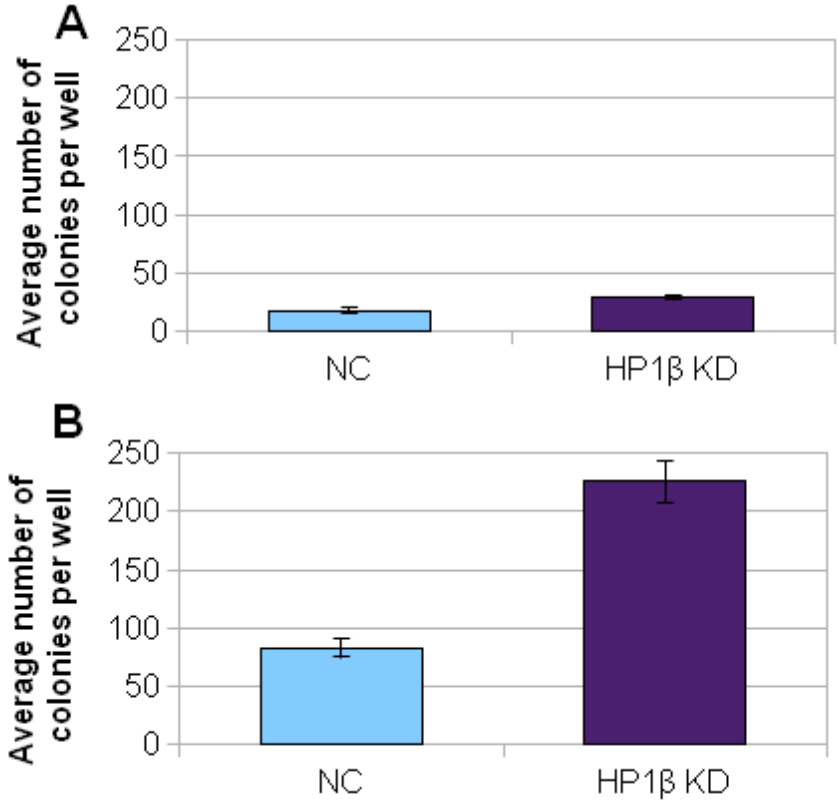

Figure 5.5 Optimisation of agarose gelling time for a soft agar colony formation assay. Soft agar colony formation assays were set up as described in section 2.2.22 using HP1β KD and NC cells. Gelling of the plated in the refrigerator was carried out for either five (**A**) or ten (**B**) minutes. After three weeks, the cells were stained with crystal violet, imaged, and the number of round three-dimensional colonies counted and graphed. Error bars represent the standard error of the mean of triplicate wells.

was repeated twice, and similar results were obtained each time.

Figure 5.6 summarises the results of this colony formation assay, and depicts representative images of the colonies obtained for each cell line. The HP1α KD cells formed on average, almost 200 colonies less than the HC cells, indicating that HP1α may be necessary for anchorage independence. This is also shown in the images of the cells, as there are fewer colonies present in the HP1α KD photograph compared to the HC photograph. In contrast, the HP1β KD cell line had just over 150 more colonies per well on average compared with the NC cell line. More colonies are also present in the image of the HP1β KD cells compared to the NC cells. This result may indicate that decreased HP1β permits enhanced anchorage-independent growth in MCF-7 cells.

5.3 Chapter discussion

Loss of HP1α has previously been observed in breast metastases compared to normal breast tissue (Kirschmann *et al.*, 2000), whereas HP1β protein levels have been shown to decrease in thyroid tumour progression (Contreras *et al.*, 2009). Consequently, the HP1α KD and HP1β KD MCF-7 cell lines were analysed *in vitro* for any changes in characteristics that contribute to metastasis. These were assayed using invasion assays and soft agar colony formation assays to examine invasive potential and anchorage independence respectively.

5.3.1 Does knock-down of HP1α or HP1β alter invasive potential of MCF-7 cells?

Although a previous study carried out by Norwood *et al.* (2006) reported an increase in invasive potential when HP1α was decreased in MCF-7 cells, the invasive potential of the HP1α KD cells examined in this study was unchanged. The differences seen between the results of the invasion assays for the HP1α KD cell lines presented here and those performed by Norwood *et al.* (2006) may be due to several factors. The HP1α KD cells used in this study were also found to have increased levels of HP1β, which was not reported by Norwood *et al.* (2006). Possible compensatory mechanisms between HP1α and HP1β levels with respect to invasive potential have not yet been investigated.

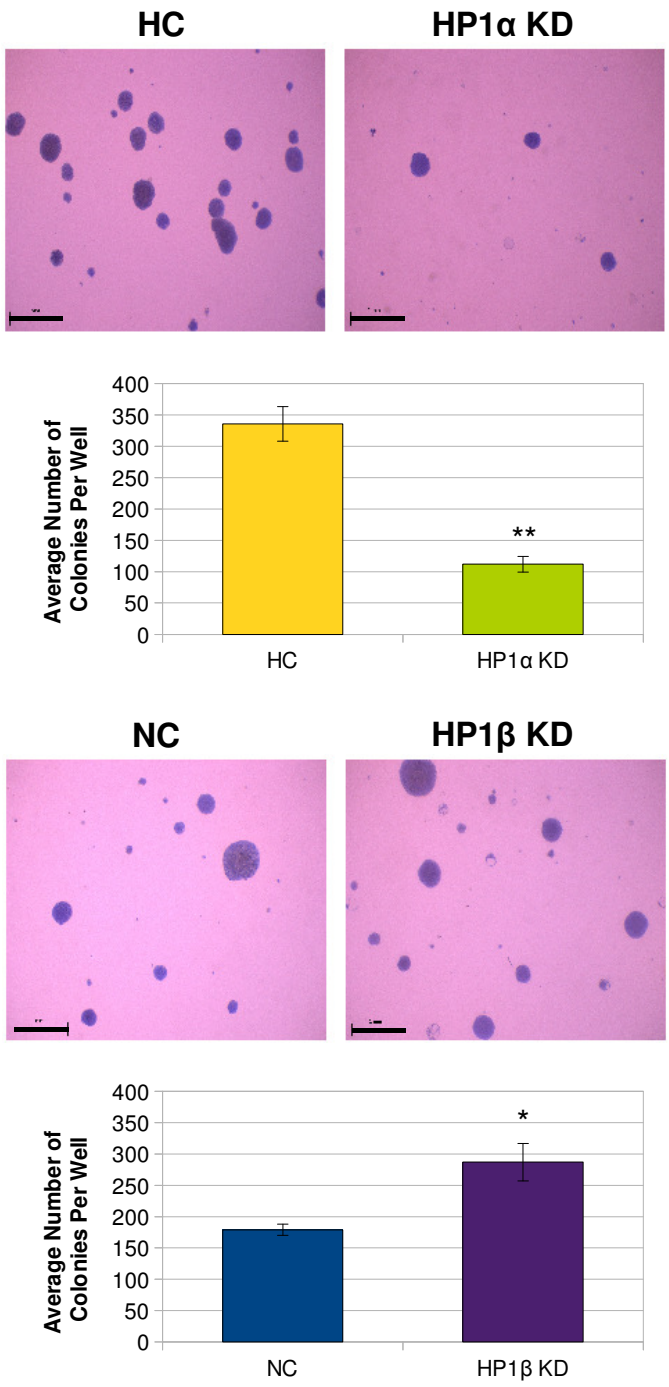

Figure 5.6 HP1 levels influence anchorage independence. Soft agar colony formation assays were performed in triplicate with the HP1α or HP1β knock-down MCF-7 cells and their respective control cell lines. Error bars represent the standard error of the mean, and * indicates that the p-value is less than 0.1 and a greater than 90% confidence that the data set is different to the respective control cell line data set. ** specifies a p-value of less than 0.05 and that there is a greater than 95% confidence that the data set is different to that of the control cells. Scale bars (black) represent 1 mm.

Secondly, although the assays used to measure invasive potential in this study and by Norwood *et al.* (2006) were based on the same method, there were some differences. The protein concentration of the ECM solution used by Norwood *et al.* (2006) was not specified, and may have been different to the one used in this study. Issues with ECM polymerisation and membrane coating are a limitation of this type of invasion assay. This could be addressed by carrying out a different type of invasion assay, which could involve culturing cells within layers of ECM proteins (Brekhman and Neufeld, 2009), or use specialised invasion plates adapted for the xCELLigence System™ (Bird and Kirstein, 2009).

This study also showed that decreased HP1β does not appear to influence invasive potential in MCF-7 cells, though this could also be corroborated by subjecting the HP1β KD cells to an alternative invasion assay. As mentioned before, further studies carried out with MDA-MB-231 cells may also be useful to further investigate the role of HP1β in invasion. In addition, the HP1β KD cell line did have a small decrease in HP1α, so it would also be important to repeat these assays using cells with HP1β knock-down only.

The migration control used in the invasion assay showed a slight decrease in migration for both the HP1α KD and HP1β KD cells compared to the controls. This result would appear to support the lack of increased invasion seen in either the HP1α KD or HP1β KD cells. However, as this assay was only carried out once it would need to be repeated to confirm this result.

5.3.2 How does knock-down of HP1α or HP1β impact anchorage independence in MCF-7 cells?

This study has potentially implicated HP1α and HP1β as having roles in anchorage independence in MCF-7 cells. In this study, MCF-7 cells with HP1α knock-down had decreased anchorage independence, which may suggest that it promotes anchorage independence. The HP1β KD cells, on the other hand, had increased anchorage independence, which could indicate that it suppresses anchorage independence. This is an interesting result which could be strengthened by characterising the other six HP1α

KD or HP1β KD MCF-7 cell lines described in Chapter 3 (CBX1/5 ID1, ID2, and ID4). This would ensure that the results given by the HP1α KD and HP1β KD cell lines examined were not just an anomaly particular to those cell lines. To confirm that HP1α and HP1β were important for anchorage independence in breast cancer cells in general and not just MCF-7 cells, different non-invasive cell lines such as T47D could be examined. This would involve creating HP1α or HP1β knock-down cell lines using the T47D and shRNA plasmids described in Chapter 3, then subjecting them to the same soft agar colony formation assays used in this study.

To ensure that the results obtained were not due to the method used, the HP1α KD and HP1β KD MCF-7 cells could be subjected to an alternative anchorage independence assay. Commercially available anchorage independence assays also culture cells in agarose, but instead of staining and counting the cells at the conclusion of the assay a cell quantification stain is used. After the cells have taken up this stain, a spectrophotometer is used to record the absorbance. This may be a more accurate method for quantifying the number of colonies as no counting would be required.

6. Creation of a MDA-MB-231 Tet-On HP1α-CFP inducible cell line

6.1 Introduction

Creating MCF-7 cell lines with reduced expression of HP1α allowed us to explore the effects of decreased HP1α on proliferation, invasive potential and anchorage independence. The invasive MDA-MD-231 human breast cell line has previously been found to have low expression of HP1α compared to MCF-7 cells (Kirschmann *et al.*, 1999). Once established, MDA-MB-231 cell lines with inducible HP1α expression could be examined for changes in proliferation, cell cycle profile, invasive potential and anchorage independence. The advantage of the MDA-MB-231 Tet-On cells is that assays can be performed with either high or low expression of HP1α, which is useful in determining the effects of different levels of HP1α protein on MDA-MB-231 cells.

To establish an MDA-MB-231 cell line with inducible expression of HP1α, we used the Tet-On Advanced System® (Clontech, Mountain View, CA). This system uses doxycycline to tightly control expression of the gene of interest. This will enable the examination of the effects that various levels of HP1α expression have on MDA-MB-231 cells. This chapter describes the creation of the cell line mentioned above.

6.2 Results

6.2.1 qRT-PCR determination of HP1α levels in MDA-MB-231 and MCF-7 cells

Prior to establishing the MDA-MB-231 Tet-On HP1α-CFP cell line it was confirmed that MDA-MB-231 cells have decreased levels of HP1α mRNA compared to MCF-7 cells (Kirschmann *et al.*, 2000; Thomsen *et al.*, 2011). Total RNA was isolated from MCF-7 and MDA-MB-231 cells, reverse transcribed and qRT-PCR performed using primers designed to specifically amplify HP1α or β-actin cDNA (outlined in section 2.2.11). Figure 6.1 is a graph summarising qRT-PCR results, this highlights that levels of HP1α normalised to β-actin in the MDA-MB-231 cells were around 50% of that seen in the MCF-7 cells. This confirmed that endogenous levels of HP1α are greatly reduced

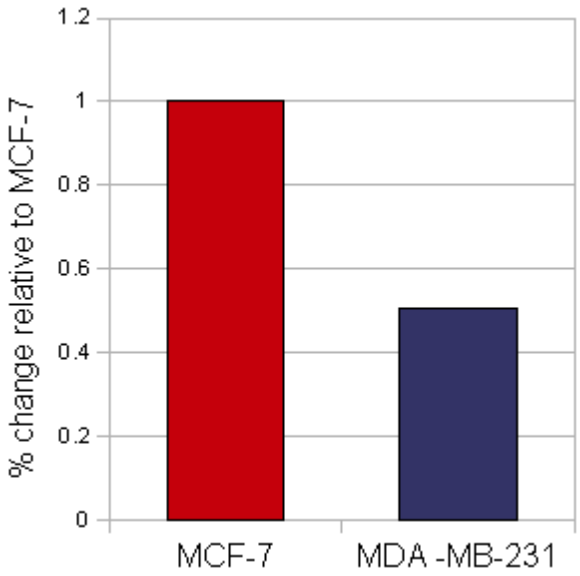

Figure 6.1 MDA-MB-231 cells show decreased HP1α expression compared to MCF-7 cells. Quantitative RT-PCR was performed in triplicate to determine levels of HP1α mRNA (outlined in section 2.2.11) HP1α mRNA levels were normalised to β-actin levels. MDA-MB-231 HP1α levels are shown relative to MCF-7 HP1α mRNA levels.

in MDA-MB-231 cells compared to MCF-7 cells used in this study.

6.2.2 MDA-MB-231 Tet-On cell line development

The Tet-On Advanced® system requires the stable uptake of two plasmids, the first is the Tet-On Advanced plasmid encoding a transcriptional transactivator and a gene which confers resistance to geneticin. The second plasmid, pTre-Tight, contains a modified Tet-responsive element upstream of a CMV promoter, and the of the gene of interest (in this case, HP1α with a CFP tag) is cloned downstream. When both plasmids are successfully integrated into a mammalian cell, expression of the gene of interest can be induced with doxycycline. Doxycycline binds to the transcriptional transactivator, which in turn activates expression of the gene of interest through an interaction with the Tet-responsive element in the promoter (Figure 6.2).

The first step in the creation of an inducible MDA-MB-231 Tet-On cell line was to establish a MDA-MB-231 cell line that stably expressed the transcriptional transactivator protein. This was accomplished by transfecting MDA-MB-231 cells with the pTet-On Advanced® vector, as described in Methods section 2.2.3. Transfected cells were selected for using 400 μg/mL of geneticin and eleven clones were obtained after 15-25 days. These clones were then tested for inducibility by a transient transfection with the pTre-Tight-Luc reporter plasmid (described in section 2.2.5). This pTre-Tight-Luc plasmid has the firefly luciferase reporter gene under the control of a promoter containing the tet-responsive element. A renilla luciferase plasmid was co-transfected to monitor transfection efficiency. Expression of firefly luciferase was induced with 1 μg/mL of doxycycline, and the cell lysates were assayed for firefly and renilla luciferase activity (described in section 2.2.6), which were both recorded as Relative Light Units (RLU). Firefly luciferase activity was normalised against renilla luciferase activity and the results are summarised in Figure 6.3.

Of the 11 clones tested, only three (H2, A1 and I6) were found to have increased normalised luciferase activity when treated with 1 μg/mL of doxycycline and each clone had low luciferase activity in the absence of doxycycline. Normalised firefly RLU of the

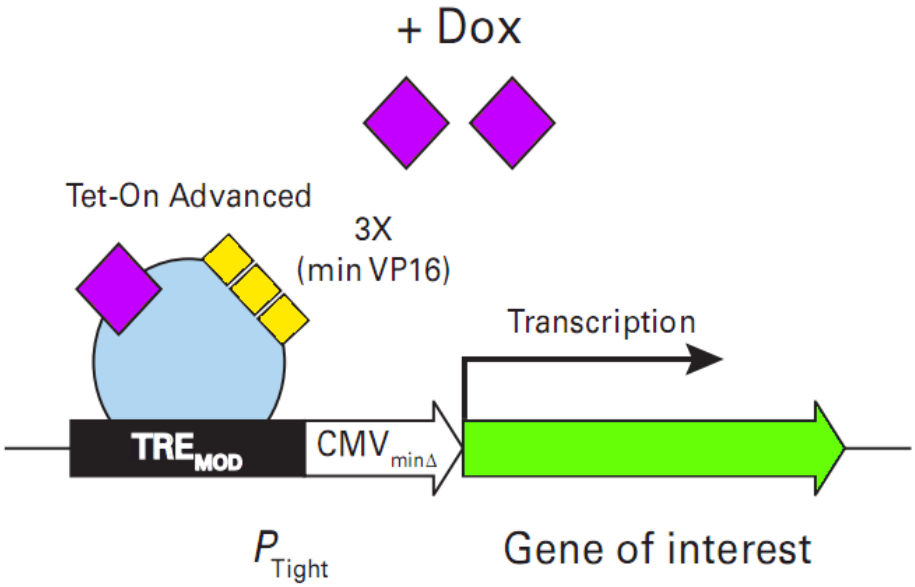

Figure 6.2 Overview of doxycycline induced expression in the Tet-On Advanced System™. Doxycycline (purple) binds to a mutant version of the E.coli Tet repressor protein (blue), which is joined to three minimal transcription activation domains from the herpes simplex virus (HSV) VP16 protein (yellow) to give a transcriptional transactivator. When doxycycline is bound, the transcriptional transactivator binds to the tetracycline response element (TRE_{MOD}) in the pTRE-Tight promoter and activates transcription of the gene of interest (green) through a minimal CMV promoter (adapted from Clontechniques, 2003).

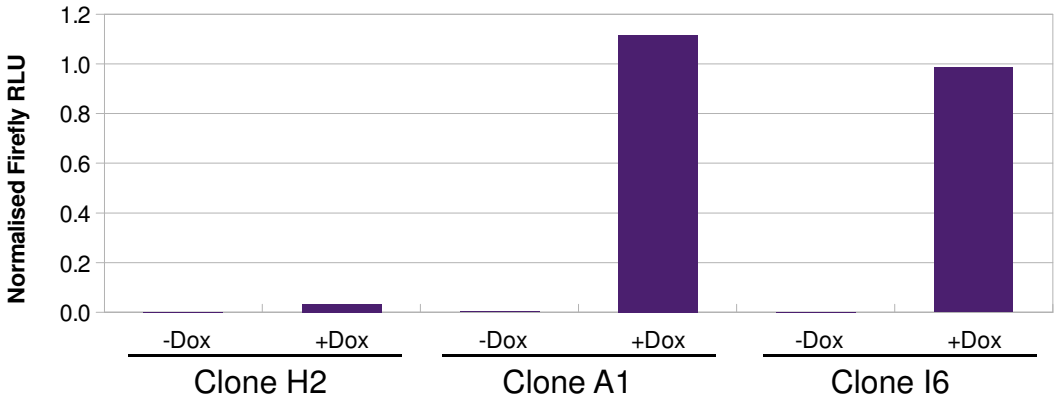

Figure 6.3 Clones stably transfected with pTet-On show varying inducibility. H2, A1 and I6 pTet-On stably transfected MDA-MB-231 clones were transfected with the pTre-Tight-Luc plasmid and pCMV renilla plasmid as described in Methods section 2.2.8. After 48 hours of induction with 1 μg/mL of doxycycline or being left untreated whole-cell lysates from these cells were prepared and assayed for luciferase activity as described in section 2.2.6.

H2, A1 and I6 clones were 0.03, 1.1 and 0.98 respectively when induced with doxycycline. Conversely, the normalised luciferase RLU readings of the cells not treated with doxycycline were $1x10^{-3}$ or less for each of these three clones. The other eight cell lines did not show increased luciferase activity when treated with doxycycline (data not shown). Testing for inducibility ensured that the pTet-On Advanced® vector had incorporated into a region of the genome that was transcriptionally active. Additionally, it also ensured that the resulting transcriptional transactivator produced was able to both respond to doxycycline and bind to the Tet-responsive elements present in a pTre-Tight promoter.

For a clone to be considered suitable for stable transfection with the pTre-Tight plasmid, it must express the transcriptional TetR transactivator at sufficient levels to be able to bind to the Tet-responsive element and strongly activate expression through the pTre-Tight promoter when doxycycline is present. Conversely, the transcriptional transactivator must not be able to bind to the Tet-responsive element when doxycycline is not present. This is to ensure that that leaky expression of the gene under the control of the pTre-Tight promoter cannot occur. The fold induction of a clone is calculated by dividing the normalised firefly RLU of the induced cells by the normalised firefly RLU of the uninduced cells. The fold induction should be at least 20 fold when the cells are induced with 1 µg/mL doxycycline, according to the manufacturer's recommendations. The H2 clone had a calculated fold induction of $1.9x10^{2}$, whereas the A1 and I6 clones were found to have $2.8x10^{2}$ and $3.6x10^{5}$ fold inductions respectively.

6.2.2.1 Doxycycline titration to identify variable expression of the TetR transactivator in MDA-MB-231 clones

Once potential clones that were inducible with 1 µg/mL of doxycycline were identified, it was determined whether the expression of firefly luciferase could be modulated in these clones using different concentrations of doxycycline. The I6 and A1 cell lines (shown to have the highest fold inductions in Figure 6.3) were again transiently transfected with pTre-tight-luc and pCMV-Renilla. Luciferase expression was then induced with a range of five doxycycline concentrations between $1x10^{-5}$ and 1 µg/mL

for 48 hours, and the resulting lysates were assayed for luciferase activity. Figure 6.4 summarises the fold inductions calculated for the A1 and I6 clones at five doxycycline concentrations. The fold inductions for both cell lines are progressively higher as doxycycline concentration increases, though the fold inductions of the I6 clone are consistently higher than those of the A1 clone. Thus, the A1 clone proved more sensitive to doxycycline than the I6 clone.

A1 cells that were not treated with doxycycline had a normalised firefly luciferase RLU reading of $2x10^{-4}$, whereas the I6 uninduced cells had a higher normalised firefly luciferase RLU reading of $6.4x10^{-3}$. Luciferase expression should be as low as possible in uninduced cells, as this shows that the transcriptional transactivator cannot effectively activate expression of the gene of interest in the absence of doxycycline. This minimises undesirable expression of the gene of interest when doxycycline is not present. As the A1 clone had lower uninduced firefly luciferase expression than the I6 clone and thus had higher fold induction, it was chosen to create the inducible HP1α-CFP cell line.

6.2.3 MDA-MB-231 Tet-On HP1α-CFP stable cell line development

6.2.3.1 Transient expression of pTre-Tight-HP1α-CFP in a MDA-MB-231 Tet-On cell line

After an inducible MDA-MB-231 Tet-On cell line was selected, it was necessary to ensure that the HP1α-CFP protein could be expressed in this cell line in response to induction with doxycycline. This was initially achieved by transiently transfecting the pTre-Tight-HP1α-CFP vector (assembly of a HP1α-CFP construct and cloning of it into the pTre-Tight vector had previously been carried out by Dr Tracy Hale) into the MDA-MB-231 Tet-On A1 cell line, as described in section 2.2.5. The cells were treated with five doxycycline concentrations ($1x10^{-4}$, $1x10^{-3}$, 0.01, 0.1 and 1 μg/mL) or left untreated for 48 hours, then HP1α-CFP expression was examined by immunoblot analysis with an antibody against HP1α (outlined in sections 2.2.14-2.2.16). As endogenous HP1α was expected to be the same across all samples, an internal loading control such as tubulin was not used. Figure 6.5 is an image of the immunoblot showing that the cells that were

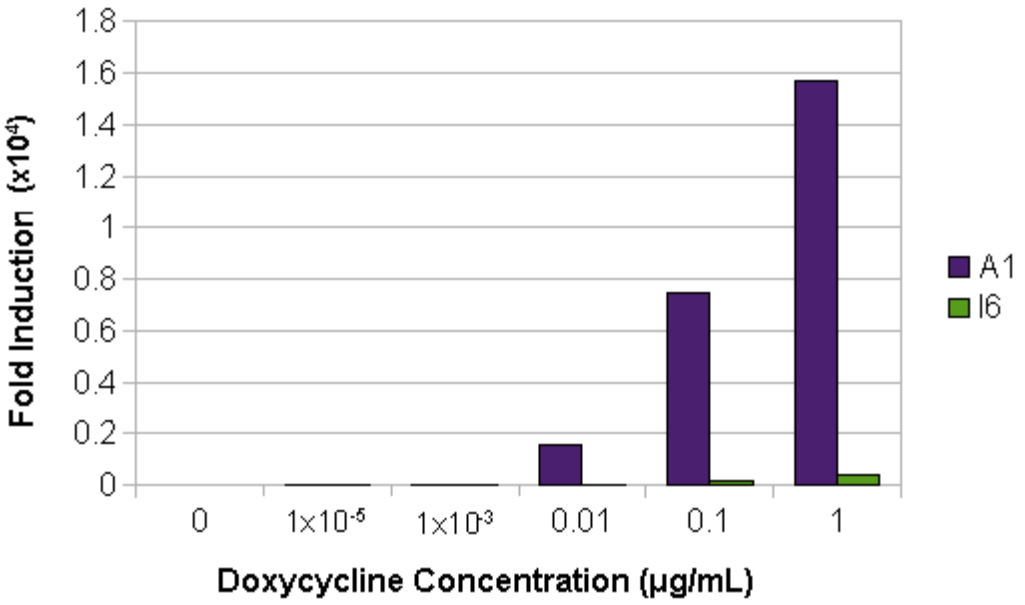

Figure 6.4 Modulation of doxycycline levels results in tunable p-Tre-Tight induction**.** A1 and I6 stably transfected pTet-on MDA-MB-21 clones were transiently transfected with 0.95 µg of pTre-Tight-Luc plasmid and 0.05 µg of pCMV renilla plasmid. After 48 hours in the presence of media containing either no doxycycline or 1, 0.1, 0.01, $1x10^{-3}$ or $1x10^{-5}$ µg/mL of doxycycline, whole cell lysates were prepared and assayed for luciferase activity. Fold induction is calculated by dividing normalised firefly RLU of doxycycline-induced cells by normalised firefly RLU of uninduced cells.

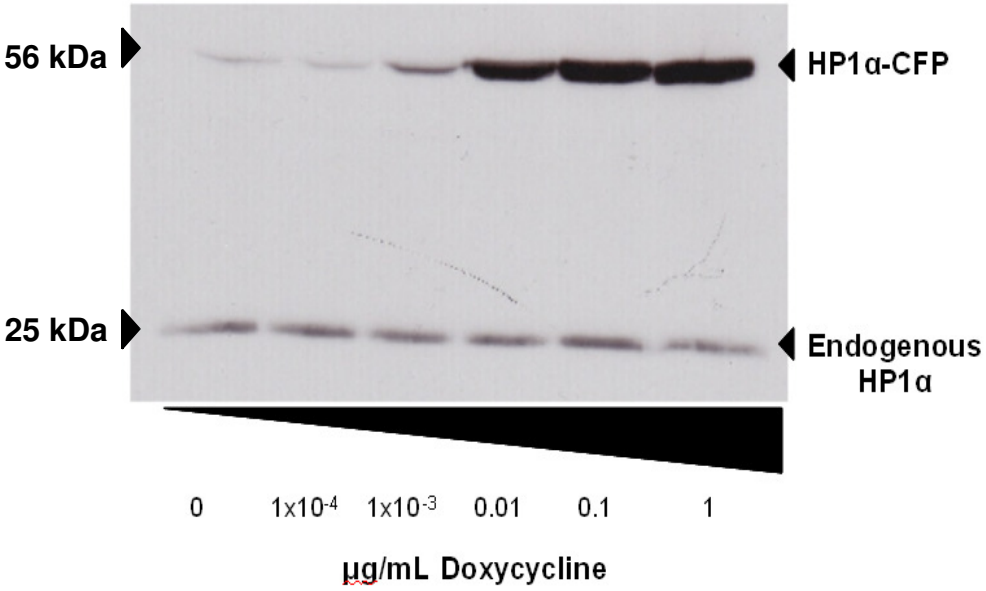

Figure 6.5 pTre-Tight-HP1α-CFP is expressed in response to doxycycline in a dose-dependent manner**.** Cells stably expressing pTet-on were transfected with pTre-Tight-HP1α-CFP (outlined in Methods section 2.2.5), and treated with one of five doxycycline concentrations or left untreated. Equal amounts of whole cell lysates were subjected to immunoblot analysis as described in Methods sections 2.2.14-2.2.16 using an antibody against HP1α.

not treated with doxycycline or with $1x10^{-4}$ μg/mL of doxycycline had low expression of the 56 kDa HP1α-CFP protein. However, with each increasing doxycycline concentration from $1x10^{-3}$ μg/mL, the amount of HP1α-CFP protein also increased. Expression of the 25 kDa endogenous HP1α protein were similar across all samples. This shows that expression of the HP1α-CFP protein could be modulated by varying doxycycline concentrations, and also that the expression of this protein did not appear to affect expression of endogenous HP1α protein.

6.2.3.2 Identifying a MDA-MB-231 Tet-On stable cell line with inducible HP1α-CFP expression

Creation of the stable cell line with inducible HP1α-CFP expression was accomplished by co-transfecting 1 μg of pTre-Tight-HP1α-CFP and 0.05 μg of a linear hygromycin marker into the MDA-MB-231 Tet-On A1 cell line (carried out as in section 2.2.4). Stable transfection was maintained with 600 μg/mL of hygromycin until nine clones were established between 14-21 days later. To identify a clone that expressed HP1α-CFP in a doxycycline dose-dependent manner, three clones (D1, H1 and E2) were grown in the presence of either 0, 0.01, 0.1 or 1 μg/mL of doxycycline. Lysates were prepared from these cells 48 hours after induction and levels of HP1α-CFP protein expression determined by immunoblot analysis using an antibody against HP1α.

Figure 6.6 is an immunoblot showing that the H1 clone successfully expressed HP1α-CFP protein relative to the increasing doxycycline concentration. The most HP1α-CFP protein was present in the cells induced with 1 μg/mL of doxycycline. Importantly, little expression of HP1α-CFP was seen when the H1 cells were not exposed to doxycycline. Endogenous HP1α does not appear to vary greatly for samples from each clone. Five clones (D1 and E2 can be seen in Figure 6.6) displayed little to no expression of HP1α-CFP even in the presence of doxycycline. Collectively, this indicated that the H1 clone could be propagated and used as a stable MDA-MB-231 cell line with inducible HP1α-CFP expression in the presence of doxycycline.

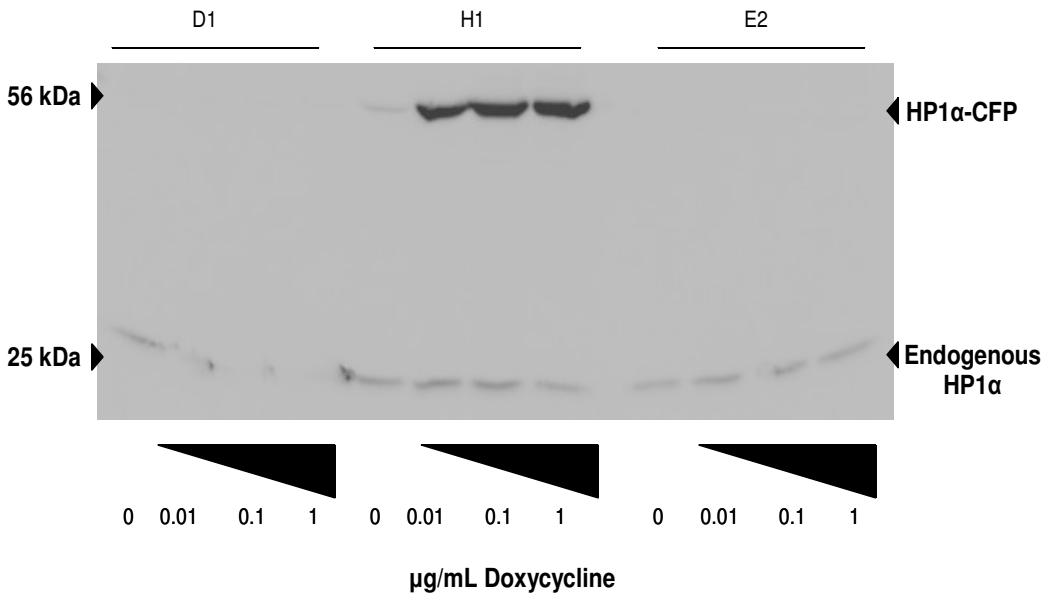

Figure 6.6 Expression of stably transfected pTre-Tight-HP1α-CFP in a MDA-MB-231 Tet-On clone. MDA-MB-231 cells stably expressing pTet-On were transfected with pTre-Tight-HP1α-CFP as described in Methods section 2.2.4, and the resulting clones induced with either 0.01, 0.1, or 1 µg/mL of doxycycline or left uninduced. Equal amounts of whole cell lysate were subjected to SDS-PAGE and immunoblot using an antibody against HP1α, as outlined in Methods section 2.2.15-2.2.16.

6.3 Chapter summary

A MDA-MB-231 cell line with inducible expression of HP1α-CFP was created to enable future work regarding the role of HP1α protein levels in breast cancer progression. Of three MDA-MB-231 clones, the A1 clone was chosen to create the inducible HP1α-CFP cell line. This was due to its responsiveness to doxycycline induction, and also to its ability to maintain minimal pTre-Tight promoter activity in the absence of doxycycline.

Transient transfection of the MDA-MB-231 Tet-On A1 clone with pTre-Tight-HP1α-CFP resulted in successful expression of the HP1α-CFP protein, which had increased levels at higher doxycycline concentrations. Upon stable transfection of the MDA-MB-231 Tet-On (A1 clone) with pTre-Tight-HP1α-CFP, a clone (H1) was obtained that gave similar HP1α-CFP expression increases with doxycycline titration to the transient transfection. This clone also had suitably low levels of uninduced HP1α-CFP expression, indicating that expression of the gene encoding HP1α-CFP was tightly regulated by the TetR transactivator.

Although the functional analysis of the effects of HP1α over-expression in MDA-MB-231 cells was not carried out during this study, the establishment of this cell line can be used in future studies exploring the role of HP1α in processes such as invasion and anchorage independence.

7. Discussion and future work

Work to date is yet to clarify the role of HP1α in breast cancer, or address any involvement of HP1β. In this study, MCF-7 cell lines with knock-down of either HP1α or HP1β were established and characterised to investigate the roles of these proteins in breast cancer progression.

Reduction of HP1α in MCF-7 cells did not alter proliferation rates or cell cycle profiles (refer to Figures 4.2, 4.3 and 4.5) in asynchronous cells. This is in agreement with with studies published previously, which found that decreasing HP1α did not impact proliferation in MCF-7 cells (Norwood *et al.*, 2006) or the cell cycle profiles of HeLa cells (De Koning *et al.*, 2009). Collectively, these results suggest that HP1α is not essential for proliferation or the cell cycle, and that a previously reported decrease in HP1α levels upon cells entering the quiescent phase is not essential for the cell cycle to proceed (De Koning *et al.*, 2009).

Reduction of HP1β in MCF-7 cells did not appear to alter proliferation rates or cell cycle profiles (refer to Figures 4.2, 4.3 and 4.5). Unchanged cell cycle profiles were also seen in HeLa cells with HP1β knock-down (De Koning *et al.*, 2009), which together with the results of this study indicates that HP1β levels do not affect the cell cycle or proliferation. However, the consequences of loss of HP1α or HP1β in MCF-7 cells could be examined further by investigating proteins that are known to interact with HP1α and HP1β and which are also involved in cell division. Such proteins include the lamin B receptor, which has implicated the HP1 proteins in roles in nuclear envelope re-assembly (Kourmouli *et al.*, 2000; Ye and Worman, 1996). Any changes in the localisation of the lamin B receptor or the nuclear envelope resulting from decreased HP1α or HP1β could be examined through visualising the nuclear envelope and the lamin B receptor using immunofluorescence.

MCF-7 cells express estrogen receptors and therefore are able to proliferate at an increased rate in response to β-estradiol (Wiese *et al.*, 1992). The response of MCF-7 cells with reduced HP1α to β-estradiol was unaltered (refer to Figure 4.4). This result

implies that HP1α levels do not affect the pathways that govern the estrogen-dependent proliferation response in MCF-7 cells.

Like the HP1α KD cells, the HP1β KD cells showed no changes in estrogen-dependent proliferation (see Figure 4.4) indicating that levels of HP1β do not impact the pathways that facilitate estrogen-dependent proliferation in MCF-7 cells. A microarray containing cDNAs of genes encoding proteins involved in the estrogen-dependent proliferation response (such as AKT1) could be used to distinguish any alterations in the expression of these genes when either HP1α or HP1β is present or absent (Ahmad *et al.*, 1999). This would confirm whether HP1α or HP1β was involved in regulating the expression of proteins that facilitate the estrogen response.

The HP1α knock-down MCF-7 cells were found to show no changes in invasive potential (refer to Figure 5.4). However, this result conflicts with a previous study, where MCF-7 cells with HP1α knock-down were found to have increased invasion (Norwood *et al.*, 2006). Additionally, an aggressive breast cell line has been found to have decreased invasive potential when HP1α was artificially over-expressed (Kirschmann *et al.*, 2000). Collectively, this suggests that further work using alternative methods of measuring invasive potential may be needed to definitively establish the role of HP1α in invasion.

MCF-7 cells with decreased HP1β were also found to have unaltered invasive potential (refer to Figure 5.4), which suggests that levels of HP1β do not impact on the pathways that lead to increased invasion in MCF-7 cells. However, as with the HP1α KD cells, these results could be further explored using a different assay to investigate invasive potential.

This study also found that both the HP1α KD and HP1β KD MCF-7 cell lines may have decreased global chromatin compaction (refer to Figure 4.6). Given the role that the HP1 proteins have in heterochromatin maintenance, it is possible that their loss during cancer progression contributes to the heterochromatin instability often seen in cancer (Jones and Baylin, 2002). Further investigation is needed to establish if knock-down of

HP1α or HP1β affects chromatin compaction and levels of heterochromatin. This could be achieved by examining levels of histone marks that are typically associated with either heterochromatin or euchromatin. An increase in global histone acetylation levels may indicate a decrease in heterochromatin (Strahl and Allis, 2000), which may also be shown by a decrease in DNA methylation (Jaenisch, 1997). However, altered heterochromatin levels may not be the only contributor to chromatin instability in HP1α KD or HP1α KD cells. Given that HP1α and HP1β have been implicated in roles in several different DNA repair pathways (Luijsterburg *et al.*, 2009; Song *et al.*, 2001), decreases in levels either of these proteins is likely to result in an increase in DNA lesions. This could be investigated through examining levels of markers of DNA damage, such as the histone variant H2AX, which is phosporylated at serine 139 in response to DNA double-strand breaks (Mah *et al.*, 2010).

In non-cancerous cells, detachment from the ECM or other cells will usually result in a form of programmed cell death known as anoikis (Gilmore, 2000). This occurs because signalling from the ECM, which is mediated through proteins such as integrins, is necessary for normal cell growth. In cancer cells, however, pathways that mediate anoikis can become de-regulated, and cells gain the ability to escape apoptosis when they lose contact with the ECM and other cells (Gilmore, 2000). As cancer cells are able to survive independently of ECM attachment, they are capable of detaching from the primary tumour and metastasising to other areas of the body. Consequently, a cancer cell's ability to survive without attachment to the ECM or other cells is one predictor of its metastatic potential.

While loss of either HP1α or HP1β has been previously associated with advanced tumour samples (Contreras *et al.*, 2009; Kirschmann *et al.*, 2000), it was unknown how decreased levels of these proteins may contribute to metastatic potential. MCF-7 cells with HP1α knock-down were found to have decreased anchorage independence (see Figure 5.6). This indicates that HP1α has a role in promoting anchorage independence in MCF-7 cells. However, as the HP1α KD cells used in this study also had increased HP1β, it raises the question of whether decreased HP1α or increased HP1β inhibits anchorage independence. This could be addressed by over-expressing HP1α or HP1β in

MCF-7 cells; it would be expected that anchorage independence would increase if HP1α enhanced this process. Although the possible role of HP1α as an enhancer of anchorage independence in MCF-7 cells does need to be further investigated, this study supports the idea presented by De Koning *et al.* (2009) that increased levels of HP1α are detrimental in breast cancer progression and may be associated with metastasis.

In contrast, the HP1β knock-down MCF-7 cells were shown to have increased anchorage independence (refer to Figure 5.6). This result suggests that HP1β may have a role in suppressing anchorage independence in MCF-7 cells, and that the loss of HP1β may enhance the metastatic ability of breast cancer cells. The relationship between levels of HP1β and anchorage independence could be further defined by establishing breast cancer cell lines that over-express HP1β. If HP1β did act to inhibit anchorage independence, it would be expected that cells with increased HP1β levels may show a decrease in anchorage independence.

Exactly how HP1α or HP1β are involved in regulating anchorage independence is yet to be determined. However, one possible way that HP1β may inhibit anchorage independence is by suppressing pathways necessary for overcoming RAS induced apoptosis. Over-expression of the RAS protein will normally lead to activation of pathways that result in apoptosis, such as the caspase-9 phosphorylation cascade (Cardone *et al.*, 1998). However, MCF-7 cells with HP1β knock-down have been observed to show an increased ability to escape apoptosis when K-RAS is over-expressed (Tracy Hale, personal communication). This may indicate that decreased levels of HP1β permit increased expression or activity of proteins in signal transduction pathways that counteract apoptosis. The Ras-related C3 botulinum toxin substrate 1 (Rac1) GTPase is activated by RAS through the Rac GDP-GTP exchange factors, and in turn participates in signal cascades that regulate processes such as cell proliferation and transcriptional transactivation through the transcription factor NF-κB (Joneson and Bar-Sagi, 1999). The activation of these pathways in the HP1β KD cells as a means to overcome apoptosis induced by anchorage independence could be investigated by examining the levels the proteins involved, such as Rac1 and NF-κB.

Given that the HP1 isoforms have been implicated in transcriptional regulation and heterochromatic silencing (Bachman *et al.*, 2001; Fuks *et al.*, 2003; Vassallo and Tanese, 2002), it is possible that they regulate expression of genes encoding proteins that participate in anchorage independence or anti-apoptosis pathways. To identify genes that are either up-regulated or down-regulated in the HP1α KD or HP1β KD MCF-7 cells, whole cell mRNA could be extracted and subjected to transcriptome analysis using Next Generation Sequencing. By comparing the knock-down and control cell lines, genes with altered expression that correlated with decreased HP1α or HP1β could be identified. To further implicate HP1α or HP1β in the regulation of any genes identified, the same transcriptome analysis could be carried out in MCF-7 cell lines with induced over-expression of HP1α or HP1β. Evidence of direct regulation of target genes by HP1α or HP1β could be obtained through subjecting the cells to chromatin-immunoprecipitation sequencing using antibodies against HP1α or HP1β respectively.

The HP1 proteins have been implicated in chromosome segregation, and HP1α has been suggested to be a facilitator of mitosis (De Koning *et al.*, 2009; Kellum, 2003). HeLa cells with HP1α knock-down were shown to have an increased incidence of chromosome bridges and misalignments, though increased mitotic defects were not reported in the HP1β KD cells (De Koning *et al.*, 2009). This is surprising given HP1β has been shown to be important for normal chromosome segregation in mice (Aucott *et al.*, 2008). Further investigation of mitotic HP1α KD or HP1β KD MCF-7 cells is needed to establish the importance of these isoforms in regulating mitosis. As the HP1α KD and HP1β KD MCF-7 cell lines established in this study are polyclonal, not all cells will be expected to have the same level of HP1α or HP1β knock-down. Therefore using immunofluorescence to examine staining of HP1α or HP1β concurrently with the chromosomal staining would be important to identify which cells had decreased expression, and whether this correlated with any mitotic defects seen.

The HP1 isoforms have each have unique localisation patterns on chromosomes (Bartkova *et al.*, 2011; Dialynas *et al.*, 2007). Distribution of HP1β in the HP1α KD cells (and vice versa) could be compared to the control cell line, which could provide information about whether any changes in HP1β localisation had taken place in

response to the decreased HP1α levels. This may help to establish whether HP1α or HP1β show any compensatory change in chromosomal distribution when levels of the other isoform are decreased.

This study has focused on the role of HP1α and HP1β in breast cancer, but HP1γ may also be involved. Altered HP1γ levels have been observed in tumours such as seminomas and also in some ovarian cancer cell lines (Bartkova *et al.*, 2011; Maloney *et al.*, 2007). While HP1γ mRNA levels have been shown to differ little between non-invasive and invasive breast cell lines (Kirschmann *et al.*, 2000), it is unknown what role, if any, it may play in breast cancer progression. MCF-7 cell lines with HP1γ knock-down could therefore be created and characterised in the same way as the HP1α KD and HP1β KD cell lines to investigate this further.

Several drugs used to treat breast malignancy target DNA to achieve cell death. Cisplatin and its derivatives are examples of these drugs, and activate apoptosis via the DNA repair pathway by binding to nucleotides and cross-linking DNA (Kelland, 2007). These drugs are effective because cancer cells often possess defective DNA repair pathways as the genes encoding DNA repair pathway proteins, such as p53 or BRCA2, are mutated or silenced (Khanna and Jackson, 2001; Lane, 1992). Consequently, the cells are unable to repair DNA injuries and apoptosis is induced (Hoeijmakers, 2001). As mentioned earlier, HP1α has been shown to associate with two proteins involved in the non-homologous end-joining and homologous recombination repair pathways respectively (Maul *et al.*, 1998; Song *et al.*, 2001). Additionally, HP1α and HP1β are both recruited to UV-induced DNA lesions (Luijsterburg *et al.*, 2009). Given these interactions, it is possible that decreasing levels of HP1α or HP1β would lead to a reduced capacity for DNA repair. Therefore, the sensitivity of HP1α or HP1β MCF-7 cells to chemotherapy drugs that induce DNA damage may be increased. In the future, information gained about the sensitivity of HP1α KD or HP1β KD breast cancer cells to specific drugs may allow for the selection of more effective treatment regimes.

Previous studies have produced contradictory reports of HP1α expression in primary breast tumour samples, and it is unclear if HP1α is increased or decreased (De Koning

et al., 2009; Kirschmann *et al.*, 2000). A large scale investigation of HP1α levels in breast tumours is needed to clarify how HP1α levels change as breast cancer progresses. Additionally, HP1β levels have not yet been investigated in breast tumours. Examining breast tumour samples for a loss of HP1β in either concurrently with loss of HP1α or alone will aid in determining whether loss of HP1β is important in breast cancer progression. The results presented in this thesis suggest that loss of HP1β loss may be important in breast cancer progression, particularly in anchorage independence, but a decrease in HP1β staining in breast metastases would support this. A breast tumour tissue array with corresponding data on patient outcomes would also confirm whether loss of HP1α or HP1β could be useful as a prognostic marker.

Overall, the results presented in this study do not indicate that a decrease in HP1α is important in breast cancer progression, but instead that increased HP1α may play a role. Although additional experiments using different HP1α knock-down cell lines or cells over-expressing HP1α would be required to confirm these results, our studies indicate that decreased HP1α inhibits anchorage independence and does not alter invasive potential.

The findings of this study also indicate that loss of HP1β is an important step in breast cancer progression, and a novel function for HP1β as a potential suppressor of anchorage independence has been identified. As a result, breast cancer cells with decreased HP1β may have an increased metastatic potential. Further investigation is needed to establish if this correlation between decreased HP1β and increased metastatic potential holds true for other breast cancer cell lines or for breast tumour samples. Nonetheless, we have identified HP1β as a possible marker of metastasis in breast cancer and have found an avenue of enquiry that may lead to increased understanding of the mechanisms of metastasis in breast cancer. This has the potential to bring about the development of new drugs and more effective treatment regimes, resulting in improved patient outcomes.

References

Ahmad, S., Singh, N., and Glazer, R.I. (1999). Role of AKT1 in 17β-estradiol- and insulin-like growth factor I (IGF-I)-dependent proliferation and prevention of apoptosis in MCF-7 breast carcinoma cells. Biochemical Pharmacology *58*, 425-430.

Ainsztein, A.M., Kandels-Lewis, S.E., Mackay, A.M., and Earnshaw, W.C. (1998). INCENP centromere and spindle targeting: Identification of essential conserved motifs and involvement of heterochromatin protein HP1. Journal of Cell Biology *143*, 1763-1774.

Albini, A., Iwamoto, Y., Kleinman, H.K., Martin, G.R., Aaronson, S.A., Kozlowski, J.M., and McEwan, R.N. (1987). A rapid invitro assay for quantitating the invasive potential of tumor-cells. Cancer Research *47*, 3239-3245.

Assoian, R.K. (1997). Anchorage-dependent Cell Cycle Progression. The Journal of Cell Biology *136*, 1-4.

Atienzar, F.A., Tilmant, K., Gerets, H.H., Toussaint, G., Speeckaert, S., Hanon, E., Depelchin, O., and Dhaluin, S. (2011). The Use of Real-Time Cell Analyzer Technology in Drug Discovery: Defining Optimal Cell Culture Conditions and Assay Reproducibility with Different Adherent Cellular Models. Journal of Biomolecular Screening *16*, 575-587.

Aucott, R., Bullwinkel, J., Yu, Y., Shi, W., Billur, M., Brown, J.P., Menzel, U., Kioussis, D., Wang, G.Z., Reisert, I.*, et al.* (2008). HP1-beta is required for development of the cerebral neocortex and neuromuscular junctions. Journal of Cell Biology *183*, 597-606.

Bachman, K.E., Rountree, M.R., and Baylin, S.B. (2001). Dnmt3a and Dnmt3b are transcriptional repressors that exhibit unique localization properties to heterochromatin. Journal of Biological Chemistry *276*, 32282-32287.

Ball, L.J., Murzina, N.V., Broadhurst, R.W., Raine, A.R.C., Archer, S.J., Stott, F.J., Murzin, A.G., Singh, P.B., Domaille, P.J., and Laue, E.D. (1997). Structure of the chromatin binding (chromo) domain from mouse modifier protein 1. EMBO J *16*, 2473-2481.

Bannister, A.J., Zegerman, P., Partridge, J.F., Miska, E.A., Thomas, J.O., Allshire, R.C.,

and Kouzarides, T. (2001). Selective recognition of methylated lysine 9 on histone H3 by the HP1 chromo domain. Nature *410*, 120-124.

Bartkova, J., Moudry, P., Hodny, Z., Lukas, J., Rajpert-De Meyts, E., and Bartek, J. (2011). Heterochromatin marks HP1 gamma, HP1 alpha and H3K9me3, and DNA damage response activation in human testis development and germ cell tumours. International Journal of Andrology *34*, E103-E113.

Bartova, E., Pachernik, J., Kozubik, A., and Kozubek, S. (2007). Differentiation-specific association of HP1 alpha and HP1 beta with chromocentres is correlated with clustering of TIF1 beta at these sites. Histochemistry and Cell Biology *127*, 375-388.

Bird, A. (1992). The essentials of DNA methylation. Cell *70*, 5-8.

Bird, A. (2002). DNA methylation patterns and epigenetic memory. Genes & Development *16*, 6-21.

Bird, C., and Kirstein, S. (2009). Real-time, label-free monitoring of cellular invasion and migration with the xCELLigence system. Nature Methods *6*.

Bissell, M.J., and Radisky, D. (2001). Putting tumours in context. Nat Rev Cancer *1*, 46-54.

Bos, J.L. (1989). Ras oncogenes in human cancer - a review. Cancer Research *49*, 4682-4689.

Bradbury, E.M. (1992). Reversible histone modifications and the chromosome cell cycle. Bioessays *14*, 9-16.

Brasher, S.V., Smith, B.O., Fogh, R.H., Nietlispach, D., Thiru, A., Nielsen, P.R., Broadhurst, R.W., Ball, L.J., Murzina, N.V., and Laue, E.D. (2000). The structure of mouse HP1 suggests a unique mode of single peptide recognition by the shadow chromo domain dimer. EMBO J *19*, 1587-1597.

Brekhman, V., and Neufeld, G. (2009). A novel asymmetric 3D in-vitro assay for the study of tumor cell invasion. Bmc Cancer *9*.

Bromberg, J.F. (2001). Activation of STAT proteins and growth control. Bioessays *23*, 161-169.

Bustin, S.A. (2000). Absolute quantification of mRNA using real-time reverse

transcription polymerase chain reaction assays. Journal of Molecular Endocrinology *25*, 169-193.

Campisi, J. (2005). Senescent cells, tumor suppression, and organismal aging: Good citizens, bad neighbors. Cell *120*, 513-522.

Cantley, L.C., Auger, K.R., Carpenter, C., Duckworth, B., Graziani, A., Kapeller, R., and Soltoff, S. (1991). Oncogenes and signal transduction. Cell *64*, 281-302.

Cardone, M.H., Roy, N., Stennicke, H.R., Salvesen, G.S., Franke, T.F., Stanbridge, E., Frisch, S., and Reed, J.C. (1998). Regulation of cell death protease caspase-9 by phosphorylation. Science *282*, 1318-1321.

Chambers, A.F., Groom, A.C., and MacDonald, I.C. (2002). Dissemination and growth of cancer cells in metastatic sites. Nat Rev Cancer *2*, 563-572.

Chiu, Y.L., and Rana, T.M. (2003). siRNA function in RNAi: A chemical modification analysis. RNA-Publ RNA Soc *9*, 1034-1048.

Clarke, M., Collins, R., Davies, C., Godwin, J., Gray, R., Peto, R., and Early Breast Cancer Trialists Collaborative, G. (1998). Tamoxifen for early breast cancer: An overview of the randomised trials. Lancet *351*, 1451-1467.

Contreras, A., Kroll, T., and Tretiakova, M. (2009). Epigenetic Regulation of Chromatin Structure in Tumorigenesis: Polycomb Group Protein EZH2 and Heterochromatin Protein 1 Expression in Malignant Thyroid Lesions. Modern Pathology *22*, 246A-246A.

Cos, S., Fernandez, R., Guezmes, A., and Sanchez-Barcelo, E.J. (1998). Influence of melatonin on invasive and metastatic properties of MCF-7 human breast cancer cells. Cancer Research *58*, 4383-4390.

Cowieson, N.P., Partridge, J.F., Allshire, R.C., and McLaughlin, P.J. (2000). Dimerisation of a chromo shadow domain and distinctions from the chromodomain as revealed by structural analysis. Current Biology *10*, 517-525.

De Koning, L., Savignoni, A., Boumendil, C., Rehman, H., Asselain, B., Sastre-Garau, X., and Almouzni, G. (2009). Heterochromatin protein 1 alpha: a hallmark of cell proliferation relevant to clinical oncology. Embo Molecular Medicine *1*, 178-191.

De Lange, R., Burtscher, H., Jarsch, M., and Weidle, U.H. (2001). Identification of

metastasis-associated genes by transcriptional profiling of metastatic versus non-metastatic colon cancer cell lines. Anticancer Res *21*, 2329-2339.

de Lange, T. (2005). Shelterin: the protein complex that shapes and safeguards human telomeres. Genes & Development *19*, 2100-2110.

Debies, M.T., and Welch, D.R. (2001). Genetic basis of human breast cancer metastasis. Journal of Mammary Gland Biology and Neoplasia *6*, 441-451.

Dernburg, A.F., Sedat, J.W., and Hawley, R.S. (1996). Direct evidence of a role for heterochromatin in meiotic chromosome segregation. Cell *86*, 135-146.

Dialynas, G.K., Terjung, S., Brown, J.P., Aucott, R.L., Baron-Luhr, B., Singh, P.B., and Georgatos, S.D. (2007). Plasticity of HP1 proteins in mammalian cells. Journal of Cell Science *120*, 3415-3424.

Dutrillaux, B., Gerbaultseureau, M., and Zafrani, B. (1990). Characterisation of chromosomal-anomalies in human breast cancer-a comparison of 30 paradiploid cases with few chromosome changes. Cancer Genetics and Cytogenetics *49*, 203-217.

Eissenberg, J.C., and Elgin, S.C.R. (2000). The HP1 protein family: getting a grip on chromatin. Current Opinion in Genetics & Development *10*, 204-210.

Eissenberg, J.C., James, T.C., Fosterhartnett, D.M., Hartnett, T., Ngan, V., and Elgin, S.C.R. (1990). Mutation in a heterochromatin-specific chromosomal protein is associated with suppression of position-effect variegation in *Drosophila-melanogaster*. Proceedings of the National Academy of Sciences of the United States of America *87*, 9923-9927.

Fanti, L., Giovinazzo, G., Berloco, M., and Pimpinelli, S. (1998). The Heterochromatin protein 1 prevents telomere fusions in Drosophila. Mol Cell *2*, 527-538.

Feinberg, A.P., and Vogelstein, B. (1983). Hypomethylation distinguishes genes of some human cancers from their normal counterparts. Nature *301*, 89-92.

Felsenfeld, G., and McGhee, J.D. (1986). Structure of the 30 nm chromatin fiber. Cell *44*, 375-377.

Fiucci, G., Ravid, D., Reich, R., and Liscovitch, M. (2002). Caveolin-1 inhibits anchorage-independent growth, anoikis and invasiveness in MCF-7 human breast

cancer cells. Oncogene *21*, 2365-2375.

Fraga, M.F., Ballestar, E., Villar-Garea, A., Boix-Chornet, M., Espada, J., Schotta, G., Bonaldi, T., Haydon, C., Ropero, S., Petrie, K.*, et al.* (2005). Loss of acetylation at Lys16 and trimethylation at Lys20 of histone H4 is a common hallmark of human cancer. Nature Genetics *37*, 391-400.

Freedman, V.H., and Shin, S. (1974). Cellular tumorigenicity in nude mice - correlation with cell-growth in semisolid medium. Cell *3*, 355-359.

Friend, S.H., Horowitz, J.M., Gerber, M.R., Wang, X.F., Bogenmann, E., Li, F.P., and Weinberg, R.A. (1987). Deletions of a dna-sequence in retinoblastomas and mesenchymal tumors - organization of the sequence and its encoded protein. Proceedings of the National Academy of Sciences of the United States of America *84*, 9059-9063.

Fujimoto, N., Yeh, S.Y., Kang, H.Y., Inui, S., Chang, H.C., Mizokami, A., and Chang, C.S. (1999). Cloning and characterization of androgen receptor coactivator, ARA55, in human prostate. Journal of Biological Chemistry *274*, 8316-8321.

Fuks, F., Hurd, P.J., Deplus, R., and Kouzarides, T. (2003). The DNA methyltransferases associate with HP1 and the SUV39H1 histone methyltransferase. Nucleic Acids Research *31*, 2305-2312.

Gilmore, A.P. (2000). Anoikis. Cell Death Differ *12*, 1473-1477.

Gratzner, H.G. (1982). Monoclonal-antibody to 5-bromodeoxyuridine and 5-iododeoxyuridine - a new reagent for detection of DNA-replication. Science *218*, 474-475.

Grewal, S.I.S., and Jia, S.T. (2007). Heterochromatin revisited. Nat Rev Genet *8*, 35-46.

Hackett, A.J., Smith, H.S., Springer, E.L., Owens, R.B., Nelsonrees, W.A., Riggs, J.L., and Gardner, M.B. (1977). 2 syngeneic cell lines from human breast-tissue - aneuploid mammary epithelial (HS578t) and diploid myoepithelial (HS578BST) cell lines. J Natl Cancer Inst *58*, 1795-1806.

Hanahan, D., and Weinberg, R.A. (2000). The hallmarks of cancer. Cell *100*, 57-70.

Harvey, J.M., Clark, G.M., Osborne, C.K., and Allred, D.C. (1999). Estrogen receptor

status by immunohistochemistry is superior to the ligand-binding assay for predicting response to adjuvant endocrine therapy in breast cancer. J Clin Oncol *17*, 1474-1481.

Hayakawa, T., Haraguchi, T., Masumoto, H., and Hiraoka, Y. (2003). Cell cycle behavior of human HP1 subtypes: distinct molecular domains of HP1 are required for their centromeric localization during interphase and metaphase. Journal of Cell Science *116*, 3327-3338.

Hendzel, M.J. (1997). Mitosis-specific phosphorylation of histone H3 initiates primarily within pericentromeric heterochromatin during G2 and spreads in an ordered fashion coincident with mitotic chromosome condensation. Chromosoma *106*, 348-360.

Hoeijmakers, J.H.J. (2001). Genome maintenance mechanisms for preventing cancer. Nature *411*, 366-374.

Hollstein, M., Sidransky, D., Vogelstein, B., and Harris, C.C. (1991). P53 mutations in human cancers. Science *253*, 49-53.

Huang, S., and Ingber, D.E. (1999). The structural and mechanical complexity of cell-growth control. Nat Cell Biol *1*, E131-E138.

Hunter, K.W., Broman, K.W., Le Voyer, T., Lukes, L., Cozma, D., Debies, M.T., Rouse, J., and Welch, D.R. (2001). Predisposition to efficient mammary tumor metastatic progression is linked to the breast cancer metastasis suppressor gene Brms1. Cancer Research *61*, 8866-8872.

Hurlin, P.J., Fry, D.G., Maher, V.M., and McCormick, J.J. (1987). Morphological Transformation, Focus Formation, and Anchorage Independence Induced in Diploid Human Fibroblasts by Expression of a Transfected H-ras Oncogene. Cancer Research *47*, 5752-5757.

Jaenisch, R. (1997). DNA methylation and imprinting: Why bother? Trends in Genetics *13*, 323-329.

James, T.C., and Elgin, S.C.R. (1986). Identification of a nonhistone chromosomal protein associated with heterochromatin in *Drosophila melanogaster* and its gene. Molecular and Cellular Biology *6*, 3862-3872.

Jenuwein, T., and Allis, C.D. (2001). Translating the histone code. Science *293*, 1074-

1080.

Jones, P.A., and Baylin, S.B. (2002). The fundamental role of epigenetic events in cancer. Nat Rev Genet *3*, 415-428.

Jones, P.A., and Baylin, S.B. (2007). The epigenomics of cancer. Cell *128*, 683-692.

Joneson, T., and Bar-Sagi, D. (1999). Suppression of Ras-induced apoptosis by the Rac GTPase. Molecular and Cellular Biology *19*, 5892-5901.

Karpen, G.H., Le, M.H., and Le, H. (1996). Centric heterochromatin and the efficiency of achiasmate disjunction in Drosophila female meiosis. Science *273*, 118-122.

Kaufman, P.D., Kobayashi, R., Kessler, N., and Stillman, B. (1995). The P150 and P60 subunits of chromatin assembly factor-i - a molecular link between newly synthesized histones and DNA-replication. Cell *81*, 1105-1114.

Kelland, L. (2007). The resurgence of platinum-based cancer chemotherapy. Nat Rev Cancer *7*, 573-584.

Kellum, R. (2003). HP1 complexes and heterochromatin assembly. In Protein Complexes That Modify Chromatin (Berlin, Springer-Verlag Berlin), pp. 53-77.

Kellum, R., and Alberts, B.M. (1995). Heterochromatin protein-1 is required for correct chromosome segregation in Drosophila embryos. Journal of Cell Science *108*, 1419-1431.

Khanna, K.K., and Jackson, S.P. (2001). DNA double-strand breaks: signaling, repair and the cancer connection. Nature Genetics *27*, 247-254.

Kirschmann, D.A., Lininger, R.A., Gardner, L.M.G., Seftor, E.A., Odero, V.A., Ainsztein, A.M., Earnshaw, W.C., Wallrath, L.L., and Hendrix, M.J.C. (2000). Down-regulation of HP1(Hs alpha) expression is associated with the metastatic phenotype in breast cancer. Cancer Research *60*, 3359-3363.

Kirschmann, D.A., Seftor, E.A., Nieva, D.R.C., Mariano, E.A., and Hendrix, M.J.C. (1999). Differentially expressed genes associated with the metastatic phenotype in breast cancer. Breast Cancer Res Treat *55*, 127-136.

Komitowski, D., and Janson, C. (1990). Quantitative Features of Chromatin Structure in the Prognosis of Breast-Cancer. Cancer *65*, 2725-2730.

Komitowski, D.D., Hart, M.M., and Janson, C.P. (1993). Chromatin organization and breast-cancer prognosis - 2-dimensional and 3-dimensional image-analysis. Cancer *72*, 1239-1246.

Koshland, D., and Strunnikov, A. (1996). Mitotic chromosome condensation. Annu Rev Cell Dev Biol *12*, 305-333.

Kourmouli, N., Theodoropoulos, P.A., Dialynas, G., Bakou, A., Politou, A.S., Cowell, I.G., Singh, P.B., and Georgatos, S.D. (2000). Dynamic associations of heterochromatin protein 1 with the nuclear envelope. EMBO J *19*, 6558-6568.

Kouzarides, T. (2007). Chromatin modifications and their function. Cell *128*, 693-705.

Lachner, M., O'Carroll, N., Rea, S., Mechtler, K., and Jenuwein, T. (2001). Methylation of histone H3 lysine 9 creates a binding site for HP1 proteins. Nature *410*, 116-120.

Laemmli, U.K., Beguin, F., and Gujerkel.G (1970). A factor preventing major head protein of bacteriophage T4 from random aggregation. Journal of Molecular Biology *47*, 69-&.

Lane, D.P. (1992). CANCER - P53, GUARDIAN OF THE GENOME. Nature *358*, 15-16.

Lechner, M.S., Begg, G.E., Speicher, D.W., and Rauscher, F.J. (2000). Molecular determinants for targeting heterochromatin protein 1-mediated gene silencing: Direct chromoshadow domain-KAP-1 corepressor interaction is essential. Molecular and Cellular Biology *20*, 6449-6465.

Levine, A.J., Momand, J., and Finlay, C.A. (1991). The P53 tumor suppressor gene. Nature *351*, 453-456.

Li, Y.H., Kirschmann, D.A., and Wallrath, L.L. (2002). Does heterochromatin protein 1 always follow code? Proceedings of the National Academy of Sciences of the United States of America *99*, 16462-16469.

Lieberthal, J.G., Kaminsky, M., Parkhurst, C.N., and Tanese, N. (2009). The role of YY1 in reduced HP1 alpha gene expression in invasive human breast cancer cells. Breast Cancer Res *11*.

Little, C.D., Nau, M.M., Carney, D.N., Gazdar, A.F., and Minna, J.D. (1983).

Amplification and expression of the c-myc oncogene in human-lung cancer cell-lines. Nature *306*, 194-196.

Lomberk, G., Wallrath, L.L., and Urrutia, R. (2006). The Heterochromatin Protein 1 family. Genome Biology *7*.

Lorentz, A., Ostermann, K., Fleck, O., and Schmidt, H. (1994). Switching gene SWI6, involved in repression of silent mating-type loci in fission yeast, encodes a homolog of chromatin-associated proteins from *Drosophila* and mammals. Gene *143*, 139-143.

Lu, B.Y., Emtage, P.C.R., Duyf, B.J., Hilliker, A.J., and Eissenberg, J.C. (2000). Heterochromatin protein 1 is required for the normal expression of two heterochromatin genes in Drosophila. Genetics *155*, 699-708.

Luger, K., Mader, A.W., Richmond, R.K., Sargent, D.F., and Richmond, T.J. (1997). Crystal structure of the nucleosome core particle at 2.8 angstrom resolution. Nature *389*, 251-260.

Luijsterburg, M.S., Dinant, C., Lans, H., Stap, J., Wiernasz, E., Lagerwerf, S., Warmerdam, D.O., Lindh, M., Brink, M.C., Dobrucki, J.W., *et al.* (2009). Heterochromatin protein 1 is recruited to various types of DNA damage. Journal of Cell Biology *185*, 577-586.

Luijsterburg, M.S., and van Attikum, H. (2011). Chromatin and the DNA damage response: The cancer connection. Molecular Oncology *5*, 349-367.

M.O.H (2004). *Cancer: New Registrations and Deaths 2000: Revised Edition*, M.o. Health, ed. (Wellington, New Zealand Health Information Service).

Mah, L.J., El-Osta, A., and Karagiannis, T.C. (2010). gamma H2AX: a sensitive molecular marker of DNA damage and repair. Leukemia *24*, 679-686.

Maison, C., and Almouzni, G. (2004). HP1 and the dynamics of heterochromatin maintenance. Nature Reviews Molecular Cell Biology *5*, 296-304.

Maloney, A., Clarke, P.A., Naaby-Hansen, S., Stein, R., Koopman, J.O., Akpan, A., Yang, A., Zvelebil, M., Cramer, R., Stimson, L., *et al.* (2007). Gene and protein expression profiling of human ovarian cancer cells treated with the heat shock protein 90 inhibitor 17-allylamino-17-demethoxygeldanamycin. Cancer Research *67*, 3239-

3253.

Mateescu, B., Bourachot, B., Rachez, C., Ogryzko, V., and Muchardt, C. (2008). Regulation of an inducible promoter by an HP1 beta-HP1 gamma switch. Embo Reports *9*, 267-272.

Maul, G.G., Jensen, D.E., Ishov, A.M., Herlyn, M., and Rauscher, F.J. (1998). Nuclear redistribution of BRCA1 during viral infection. Cell Growth Differ *9*, 743-755.

McGhee, J.D., and Felsenfeld, G. (1980). Nucleosome structure. Annu Rev Biochem *49*, 1115-1156.

McMaster, G.K., and Carmichael, G.G. (1977). Analysis of single-stranded and double-stranded nucleic-acids on polyacrylamide and agarose gels by using glyoxal and acridine-orange. Proceedings of the National Academy of Sciences of the United States of America *74*, 4835-4838.

Minc, E., Allory, V., Worman, H.J., Courvalin, J.C., and Buendia, B. (1999). Localization and phosphorylation of HP1 proteins during the cell cycle in mammalian cells. Chromosoma *108*, 220-234.

Minc, E., Courvalin, J.C., and Buendia, B. (2000). HP1 gamma associates with euchromatin and heterochromatin in mammalian nuclei and chromosomes. Cytogenet Cell Genet *90*, 279-284.

Murzina, N., Verreault, A., Laue, E., and Stillman, B. (1999). Heterochromatin dynamics in mouse cells: Interaction between chromatin assembly factor 1 and HP1 proteins. Mol Cell *4*, 529-540.

Nielsen, A.L., Ortiz, J.A., You, J., Oulad-Abdelghani, M., Khechumian, R., Gansmuller, A., Chambon, P., and Losson, R. (1999). Interaction with members of the heterochromatin protein 1 (HP1) family and histone deacetylation are differentially involved in transcriptional silencing by members of the TIF1 family. Embo Journal *18*, 6385-6395.

Norwood, L.E., Grade, S.K., Cryderman, D.E., Hines, K.A., Furiasse, N., Toro, R., Li, Y.H., Dhasarathy, A., Kladde, M.R., Hendrix, M.J.C., *et al.* (2004). Conserved properties of HP1(Hs alpha). Gene *336*, 37-46.

Norwood, L.E., Moss, T.J., Margaryan, N.V., Cook, S.L., Wright, L., Seftor, E.A., Hendrix, M.J.C., Kirschmann, D.A., and Wallrath, L.L. (2006). A requirement for dimerization of HP1(Hs alpha) in suppression of breast cancer invasion. Journal of Biological Chemistry *281*, 18668-18676.

Oberman, H.A. (1987). Metaplastic carcinoma of the breast - a clinicopathological study of 29 patients. American Journal of Surgical Pathology *11*, 918-929.

Obuse, C., Iwasaki, O., Kiyomitsu, T., Goshima, G., Toyoda, Y., and Yanagida, M. (2004). A conserved Mis12 centromere complex is linked to heterochromatic HP1 and outer kinetochore protein Zwint-1. Nat Cell Biol *6*, 1135-U1137.

Page, D.L., Dupont, W.D., Rogers, L.W., and Rados, M.S. (1985). Atypical hyperplastic lesions of the female breast - a long-term follow-up-study. Cancer *55*, 2698-2708.

Paget, S. (1989). Stephen Paper reproduced from the Lancet, 1889. Cancer and Metastasis Reviews *8*, 98-101.

Paro, R., and Hogness, D.S. (1991). The polycomb protein shares a homologous domain with a heterochromatin-associated protein of *Drosophila*

Proceedings of the National Academy of Sciences of the United States of America *88*, 263-267.

Peng, J.C., and Karpen, G.H. (2007). H3K9 methylation and RNA interference regulate nucleolar organization and repeated DNA stability. Nat Cell Biol *9*, 25-U24.

Peng, J.C., and Karpen, G.H. (2009). Heterochromatic Genome Stability Requires Regulators of Histone H3 K9 Methylation. PLoS Genet *5*, e1000435.

Peters, A., O'Carroll, D., Scherthan, H., Mechtler, K., Sauer, S., Schofer, C., Weipoltshammer, K., Pagani, M., Lachner, M., Kohlmaier, A.*, et al.* (2001). Loss of the Suv39h histone methyltransferases impairs mammalian heterochromatin and genome stability. Cell *107*, 323-337.

Platero, J.S., Hartnett, T., and Eissenberg, J.C. (1995). Functional-analysis of the chromo domain of HP1. Embo Journal *14*, 3977-3986.

Polakis, P. (2000). Wnt signaling and cancer. Genes & Development *14*, 1837-1851.

Pomeroy, S.L., Tamayo, P., Gaasenbeek, M., Sturla, L.M., Angelo, M., McLaughlin,

M.E., Kim, J.Y.H., Goumnerova, L.C., Black, P.M., Lau, C.*, et al.* (2002). Prediction of central nervous system embryonal tumour outcome based on gene expression. Nature *415*, 436-442.

Popova, E.Y., Claxton, D.F., Lukasova, E., Bird, P.I., and Grigoryev, S.A. (2006). Epigenetic heterochromatin markers distinguish terminally differentiated leukocytes from incompletely differentiated leukemia cells in human blood. Experimental Hematology *34*, 453-462.

Rakha, E.A., Reis, J.S., Baehner, F., Dabbs, D.J., Decker, T., Eusebi, V., Fox, S.B., Ichihara, S., Jacquemier, J., Lakhani, S.R.*, et al.* (2010). Breast cancer prognostic classification in the molecular era: the role of histological grade. Breast Cancer Res *12*.

Reuter, G., and Wolff, I. (1981). Isolation of dominant suppressor mutations for position-effect variegation in *Drosophila-melanogaster*. Molecular & General Genetics *182*, 516-519.

Ritou, E., Bai, M., and Georgatos, S.D. (2007). Variant-specific patterns and humoral regulation of HP1 proteins in human cells and tissues. Journal of Cell Science *120*, 3425-3435.

Rogenhofer, S., Kahl, P., Holzapfel, S., Von Ruecker, A., Mueller, S.C., and Ellinger, J. (2012). Decreased Levels of Histone H3K9me1 Indicate Poor Prognosis in Patients with Renal Cell Carcinoma. Anticancer Res *32*, 879-886.

Saunders, W.S., Chue, C., Goebl, M., Craig, C., Clark, R.F., Powers, J.A., Eissenberg, J.C., Elgin, S.C.R., Rothfield, N.F., and Earnshaw, W.C. (1993a). Molecular-cloning of a human homolog of Drosophila heterochromatin protein HP1 using anicentromere antibodies with anti-chromo specificity. Journal of Cell Science *104*, 573-582.

Saunders, W.S., Chue, C., Goebl, M., Craig, C., Clark, R.F., Powers, J.A., Eissenberg, J.C., Elgin, S.C.R., Rothfield, N.F., and Earnshaw, W.C. (1993b). Molecular-cloning of a human homolog of *Drosophila* heterochromatin protein HP1 using anticentromere autoantibodies with anti-chromo specificity. Journal of Cell Science *104*, 573-582.

Schmiedeberg, L., Weisshart, K., Diekmann, S., Hoerste, G.M.Z., and Hemmerich, P. (2004). High- and low-mobility populations of HP1 in heterochromatin of mammalian cells. Molecular Biology of the Cell *15*, 2819-2833.

Schneider, A.C., Heukamp, L.C., Rogenhofer, S., Fechner, G., Bastian, P.J., von Ruecker, A., Muller, S.C., and Ellinger, J. (2011). Global histone H4K20 trimethylation predicts cancer-specific survival in patients with muscle-invasive bladder cancer. BJU Int *108*, E290-E296.

Schottenfeld, D., Nash, A.G., Robbins, G.F., and Beattie, E.J. (1976). 10-year results of treatment of primary operable breast carcinoma - summary of 304 patients evaluated by TNM system. Cancer *38*, 1001-1007.

Serrano, M., Lin, A.W., McCurrach, M.E., Beach, D., and Lowe, S.W. (1997). Oncogenic ras provokes premature cell senescence associated with accumulation of p53 and p16(INK4a). Cell *88*, 593-602.

Shapiro, E., Huang, H.Y., Ruoff, R., Lee, P., Tanese, N., and Logan, S.K. (2008). The heterochromatin protein 1 family is regulated in prostate development and cancer. Journal of Urology *179*, 2435-2439.

Sharma, G.G., Hwang, K.K., Pandita, R.K., Gupta, A., Dhar, S., Parenteau, J., Agarwal, M., Worman, H.J., Wellinger, R.J., and Pandita, T.K. (2003). Human heterochromatin protein 1 isoforms HP1(Hs alpha) and HP1(Hs beta) interfere with hTERT-telomere interactions and correlate with changes in cell growth and response to ionizing radiation. Molecular and Cellular Biology *23*, 8363-8376.

Shi, S., Calhoun, H.C., Xia, F., Li, J.H., Le, L., and Li, W.X. (2006). JAK signaling globally counteracts heterochromatic gene silencing. Nature Genetics *38*, 1071-1076.

Shiota, M., Song, Y., Yokomizo, A., Tada, Y., Kuroiwa, K., Eto, M., Oda, Y., Inokuchi, J., Uchiumi, T., Fujimoto, N.*, et al.* (2010). Human heterochromatin protein 1 isoform HP1 beta enhances androgen receptor activity and is implicated in prostate cancer growth. Endocrine-Related Cancer *17*, 455-467.

Silverstein, M.J., Poller, D.N., Waisman, J.R., Colburn, W.J., Barth, A., Gierson, E.D., Lewinsky, B., Gamagami, P., and Slamon, D.J. (1995). Prognostic classification of breast ductal carcinoma-in-situ. Lancet *345*, 1154-1157.

Sinclair, D.A.R., Mottus, R.C., and Grigliatti, T.A. (1983). Genes which suppress position-effect variegation in *Drosophila-melanogaster* are clustered. Molecular & General Genetics *191*, 326-333.

Singh, P.B., Miller, J.R., Pearce, J., Kothary, R., Burton, R.D., Paro, R., James, T.C., and Gaunt, S.J. (1991a). Sequence motif found in a *Drosophila* heterochromatin protein is conserved in animals and plants. Nucleic Acids Research *19*, 789-794.

Singh, P.B., Miller, J.R., Pearce, J., Kothary, R., Burton, R.D., Paro, R., James, T.C., and Gaunt, S.J. (1991b). A sequence motif found in a Drosophila heterochromatin protein is conserved in animals and plants. Nucleic Acids Research *19*, 789-794.

Singletary, S.E., Allred, C., Ashley, P., Bassett, L.W., Berry, D., Bland, K.I., Borgen, P.I., Clark, C.G., Edge, S.B., Hayes, D.F.*, et al.* (2002). Revision of the American Joint Committee on Cancer staging system for breast cancer. J Clin Oncol *20*, 3628-3636.

Slamon, D.J., Clark, G.M., Wong, S.G., Levin, W.J., Ullrich, A., and McGuire, W.L. (1987). HUMAN-BREAST CANCER - CORRELATION OF RELAPSE AND SURVIVAL WITH AMPLIFICATION OF THE HER-2 NEU ONCOGENE. Science *235*, 177-182.

Slamon, D.J., Godolphin, W., Jones, L.A., Holt, J.A., Wong, S.G., Keith, D.E., Levin, W.J., Stuart, S.G., Udove, J., Ullrich, A.*, et al.* (1989). Human-breast cancer - correlation of relapse and survival with amplification of the HER-2 neu oncogene. Science *244*, 707-712.

Slamon, D.J., Leyland-Jones, B., Shak, S., Fuchs, H., Paton, V., Bajamonde, A., Fleming, T., Eiermann, W., Wolter, J., Pegram, M.*, et al.* (2001). Use of chemotherapy plus a monoclonal antibody against HER2 for metastatic breast cancer that overexpresses HER2. New England Journal of Medicine *344*, 783-792.

Song, K.Y., Jung, Y.S., Jung, D.H., and Lee, I. (2001). Human Ku70 interacts with heterochromatin protein 1 alpha. Journal of Biological Chemistry *276*, 8321-8327.

Steeg, P.S. (2006). Tumor metastasis: mechanistic insights and clinical challenges. Nature Medicine *12*, 895-904.

Strahl, B.D., and Allis, C.D. (2000). The language of covalent histone modifications. Nature *403*, 41-45.

Tavassoli, F.A.D. (2003). World Health Organisation Classification of Tumours: Pathology and Genetics of Tumours of the Breast and Female Genital Organs (WHO), pp. 9-19.

Thiru, A., Nietlispach, D., Mott, H.R., Okuwaki, M., Lyon, D., Nielsen, P.R., Hirshberg, M., Verreault, A., Murzina, N.V., and Laue, E.D. (2004). Structural basis of HP1/PXVXL motif peptide interactions and HP1 localisation to heterochromatin. EMBO J *23*, 489-499.

Thomsen, R., Christensen, D.B., Rosborg, S., Linnet, T.E., Blechingberg, J., and Nielsen, A.L. (2011). Analysis of HP1 alpha Regulation in Human Breast Cancer Cells. Molecular Carcinogenesis *50*, 601-613.

Toguchida, J., Ishizaki, K., Sasaki, M.S., Ikenaga, M., Sugimoto, M., Kotoura, Y., and Yamamuro, T. (1988). Chromosomal reorganization for the expression of recessive mutation of retinoblastoma susceptibility gene in the development of osteo-sarcoma. Cancer Research *48*, 3939-3943.

Tomari, Y., and Zamore, P.D. (2005). Perspective: machines for RNAi. Genes & Development *19*, 517-529.

Trojer, P., and Reinberg, D. (2007). Facultative heterochromatin: Is there a distinctive molecular signature? Mol Cell *28*, 1-13.

Vassallo, M.F., and Tanese, N. (2002). Isoform-specific interaction of HP1 with human TAF(II)130. Proceedings of the National Academy of Sciences of the United States of America *99*, 5919-5924.

Wasenius, V.M., Hemmer, S., Kettunen, E., Knuutila, S., Franssila, K., and Joensuu, H. (2003). Hepatocyte growth factor receptor, matrix metalloproteinase-11, tissue inhibitor of metalloproteinase-1, and fibronectin are up-regulated in papillary thyroid carcinoma: A cDNA and tissue microarray study. Clinical Cancer Research *9*, 68-75.

Wei, Y., Yu, L., Bowen, J., Gorovsky, M.A., and Allis, C.D. (1999). Phosphorylation of histone H3 is required for proper chromosome condensation and segregation. Cell *97*, 99-109.

Weidner, N., Folkman, J., Pozza, F., Bevilacqua, P., Allred, E.N., Moore, D.H., Meli, S., and Gasparini, G. (1992). Tumor angiogenesis - a new significant and independent prognostic indicator in early-stage breast-carcinoma. J Natl Cancer Inst *84*, 1875-1887.

Weidner, N., Semple, J.P., Welch, W.R., and Folkman, J. (1991). TUMOR ANGIOGENESIS AND METASTASIS - CORRELATION IN INVASIVE BREAST-

CARCINOMA. New England Journal of Medicine *324*, 1-8.

Wiese, T.E., Kral, L.G., Dennis, K.E., Butler, W.B., and Brooks, S.C. (1992). Optimization of estrogen growth-response in MCF-7 cells. In Vitro Cellular & Developmental Biology-Animal *28A*, 595-602.

Wilfinger, W.W., Mackey, K., and Chomczynski, P. (1997). Effect of pH and ionic strength on the spectro-photometric assessment of nucleic acid purity. Biotechniques *22*, 474-&.

Wustmann, G., Szidonya, J., Taubert, H., and Reuter, G. (1989). The genetics of position-effect variegation modifying loci in *Drosophila-melanogaster*. Molecular & General Genetics *217*, 520-527.

Wyckoff, J.B., Jones, J.G., Condeelis, J.S., and Segall, J.E. (2000). A critical step in metastasis: In vivo analysis of intravasation at the primary tumor. Cancer Research *60*, 2504-2511.

Xia, Z.G., Dickens, M., Raingeaud, J., Davis, R.J., and Greenberg, M.E. (1995). Opposing effects of ERK and JNK-p38 map kinases on apoptosis. Science *270*, 1326-1331.

Yamauchi, H., Stearns, V., and Hayes, D.F. (2001). When is a tumor marker ready for prime time? A case study of c-erbB-2 as a predictive factor in breast cancer. J Clin Oncol *19*, 2334-2356.

Yan, S.J., Lim, S.J., Shi, S., Dutta, P., and Li, W.X. (2011). Unphosphorylated STAT and heterochromatin protect genome stability. Faseb J *25*, 232-241.

Yang, J., Mani, S.A., Donaher, J.L., Ramaswamy, S., Itzykson, R.A., Come, C., Savagner, P., Gitelman, I., Richardson, A., and Weinberg, R.A. (2004). Twist, a master regulator of morphogenesis, plays an essential role in tumor metastasis. Cell *117*, 927-939.

Yasuhara, J.C., and Wakimoto, B.T. (2006). Oxymoron no more: the expanding world of heterochromatic genes. Trends in Genetics *22*, 330-338.

Ye, Q., and Worman, H.J. (1996). Interaction between an integral protein of the nuclear envelope inner membrane and human chromodomain proteins homologous to

Drosophila HP1. Journal of Biological Chemistry *271*, 14653-14656.

Zou, Z.Q., Anisowicz, A., Hendrix, M.J.C., Thor, A., Neveu, M., Sheng, S.J., Rafidi, K., Seftor, E., and Sager, R. (1994). Maspin, a serpin with tumor-suppressing activity in human mammary epithelial-cells. Science *263*, 526-529.

Appendix 1

Primers used to amplify regions of the HP1α, HP1β, HP1γ and β-actin cDNA

Primer target	**Forward primer sequence 5' to 3'**	**Reverse primer sequence 5' to 3'**
***CBX5* (HP1α)**	CTCAAACAGTGCCGATGACA	AACAGTGCCGATGACATCAAA
***CBX1* (HP1β)**	AAAACAAGAAAGTAGAGGAGGTGC	CAGATGTGACAGGGGCTGG
***CBX3* (HP1γ)**	CAGCAGTGGAGAATTGATGTT	CTGGACAAGAATGCCAAGTTA
β-actin	ATGTGGCCGAGGACTTTGATT	AGTGGGGTGGCTTTTAGGATG

Appendix 2

Chromatogram obtained from sequencing the PCR product of the HP1α primers

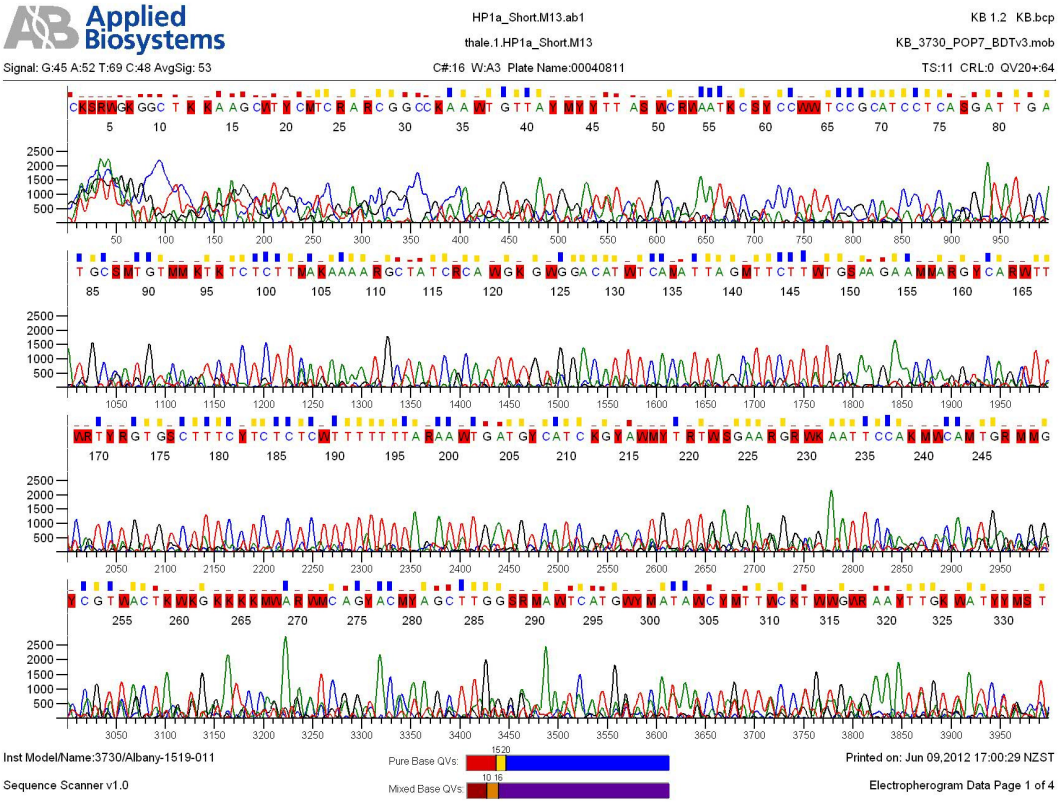

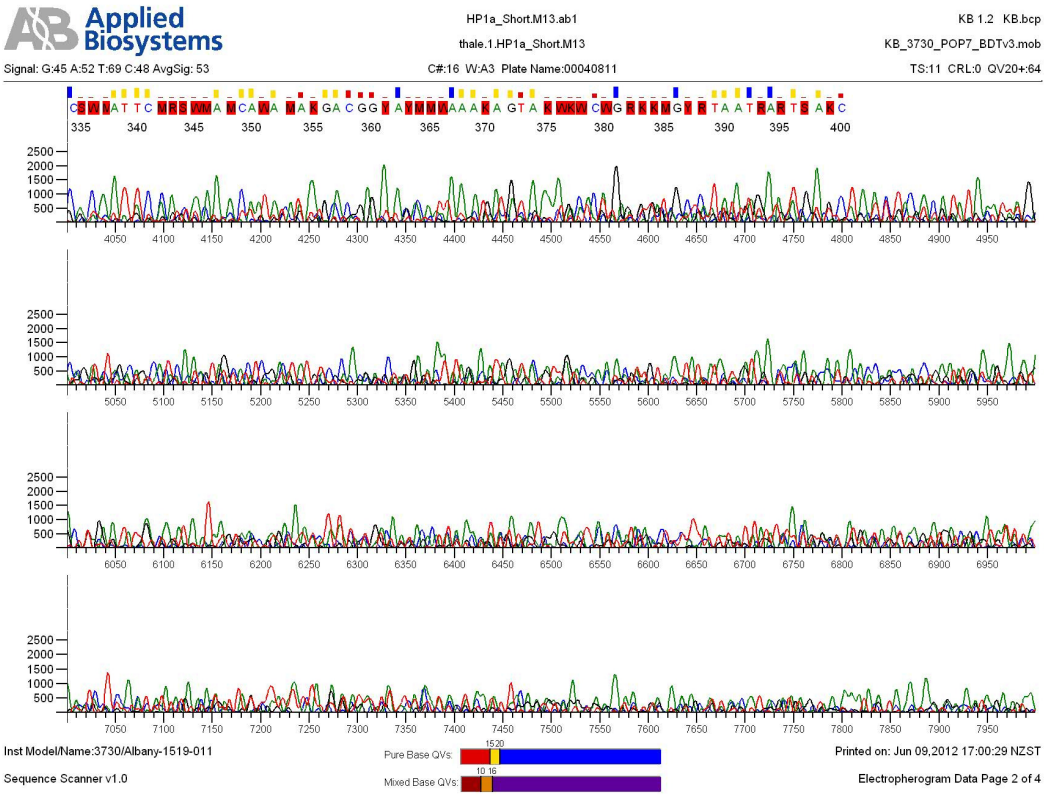

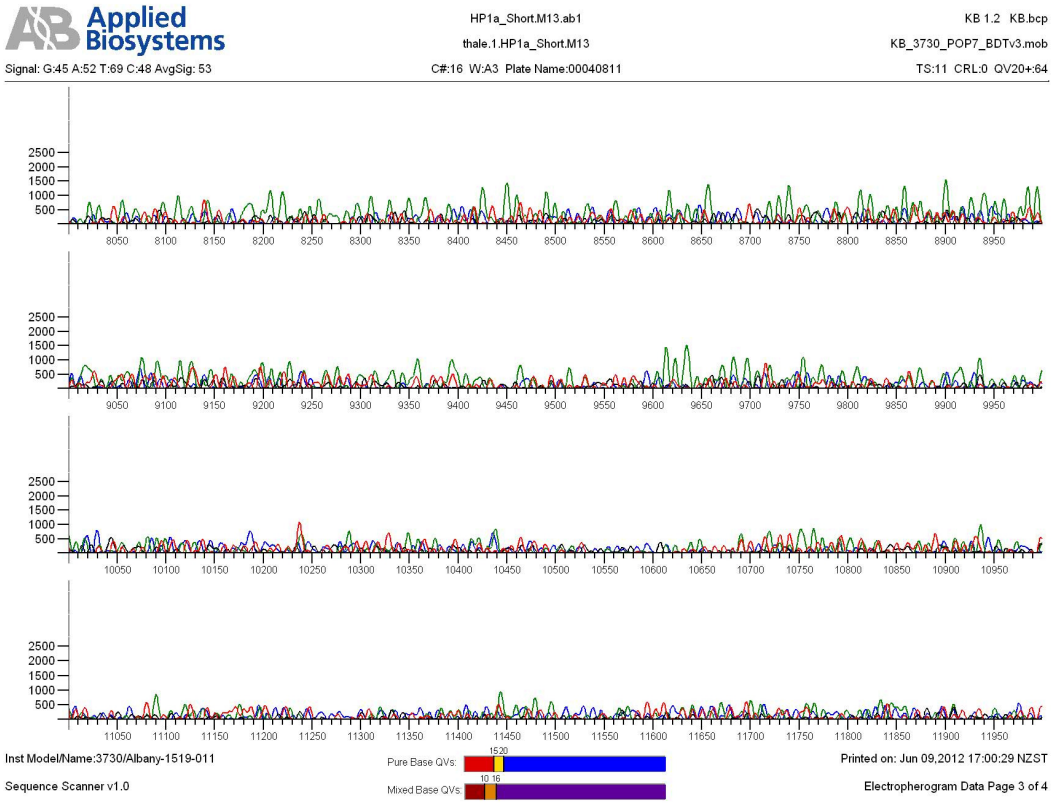
Applied Biosystems
HP1a_Short.M13.ab1
KB 1.2 KB.bcp
thale.1.HP1a_Short.M13
KB_3730_POP7_BDTv3.mob
Signal: G:45 A:52 T:69 C:48 AvgSig: 53
C#:16 W:A3 Plate Name:00040811
TS:11 CRL:0 QV20+:64
Inst Model/Name:3730/Albany-1519-011
Sequence Scanner v1.0
Pure Base QVs:
Mixed Base QVs:
Printed on: Jun 09,2012 17:00:29 NZST
Electropherogram Data Page 3 of 4

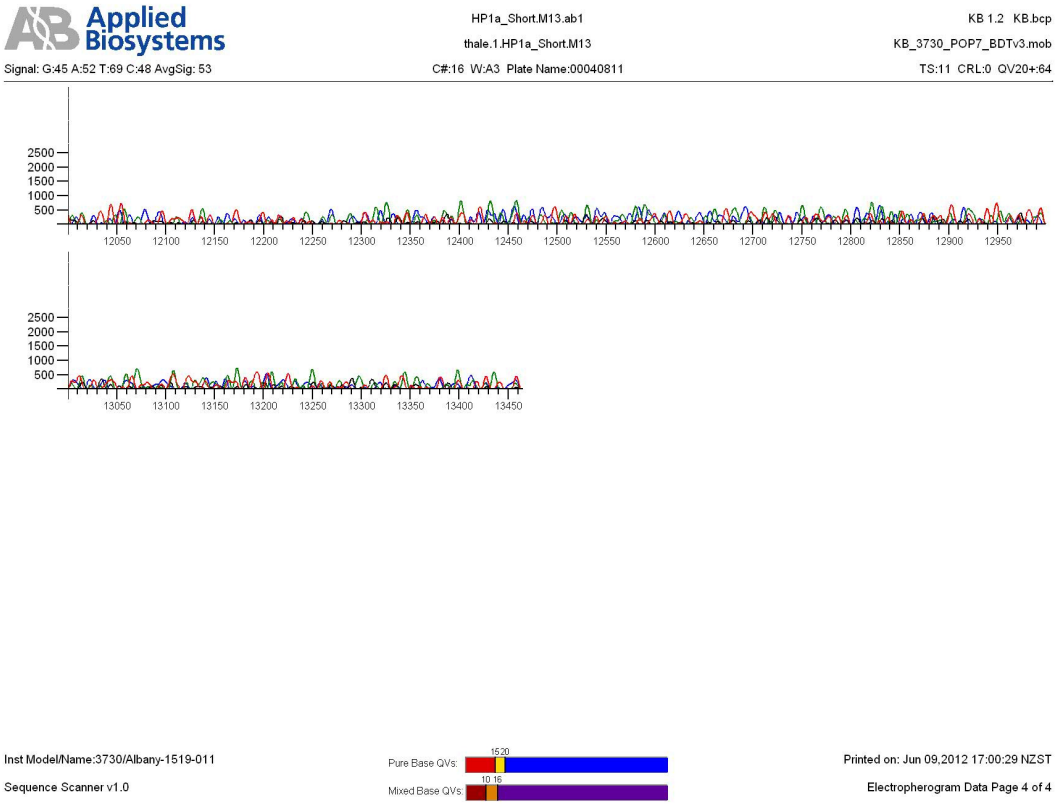
Applied Biosystems
HP1a_Short.M13.ab1
KB 1.2 KB.bcp
thale.1.HP1a_Short.M13
KB_3730_POP7_BDTv3.mob
Signal: G:45 A:52 T:69 C:48 AvgSig: 53
C#:16 W:A3 Plate Name:00040811
TS:11 CRL:0 QV20+:64
Inst Model/Name:3730/Albany-1519-011
Sequence Scanner v1.0
Pure Base QVs:
Mixed Base QVs:
Printed on: Jun 09,2012 17:00:29 NZST
Electropherogram Data Page 4 of 4

Chromatogram obtained from sequencing the PCR product of the HP1β primers

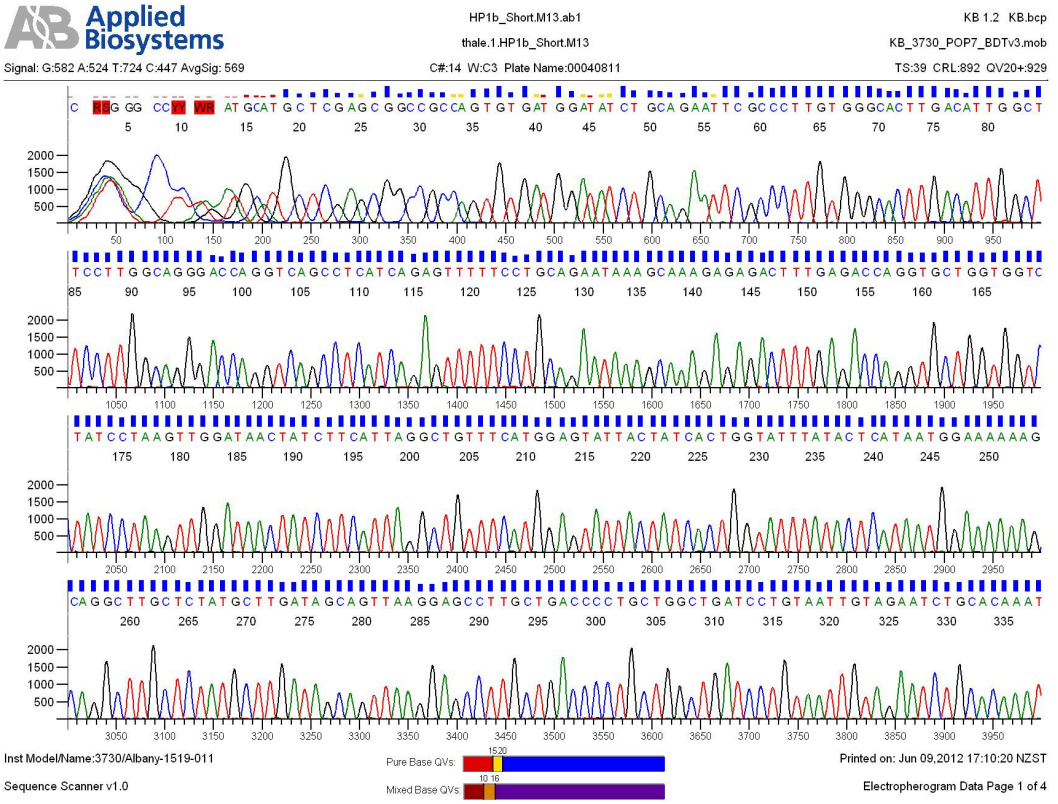

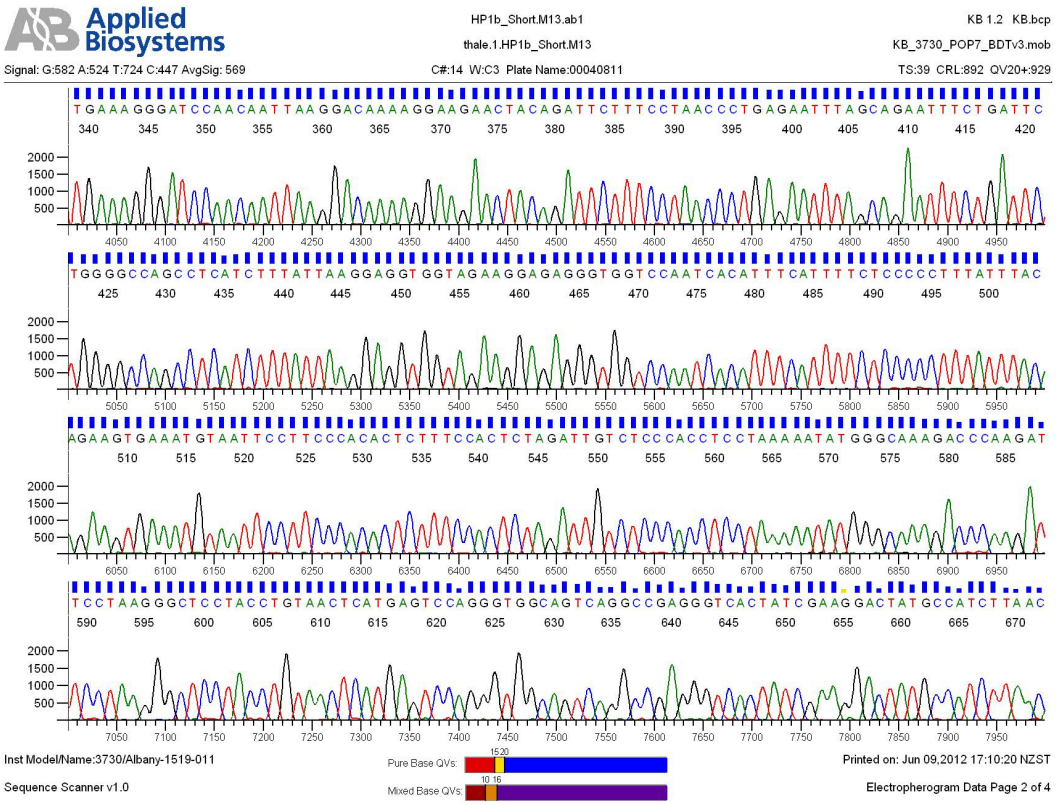

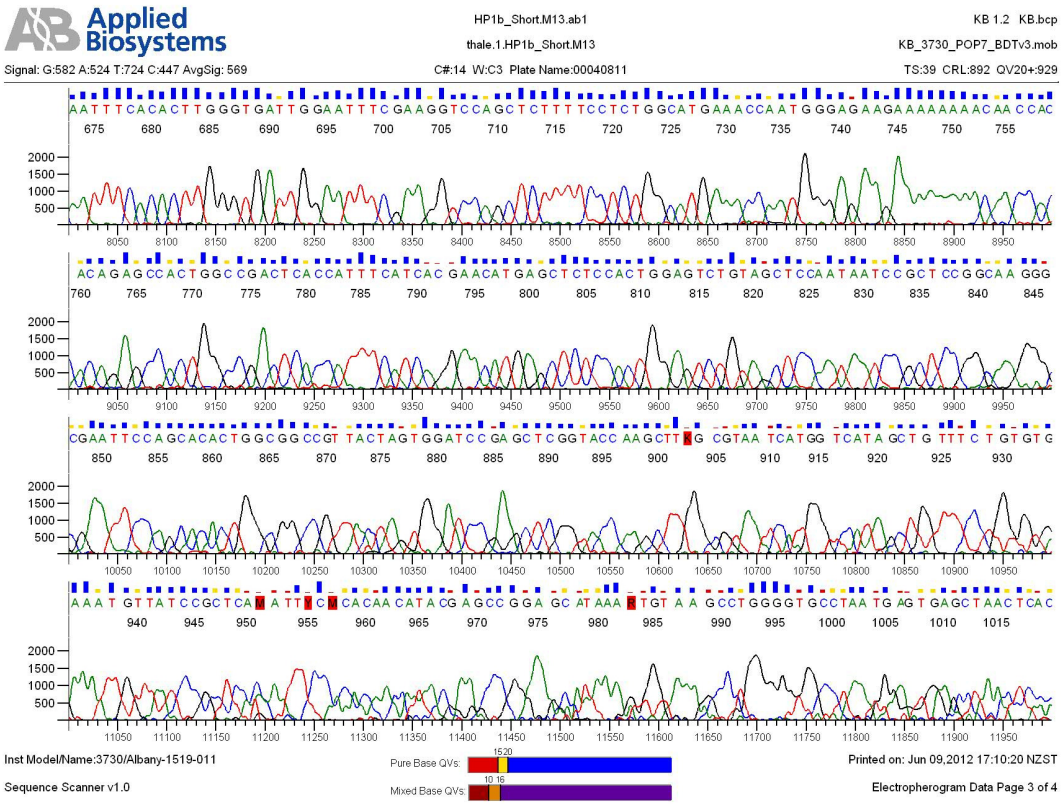
Applied Biosystems
HP1b_Short.M13.ab1
KB 1.2 KB.bcp
thale.1.HP1b_Short.M13
KB_3730_POP7_BDTv3.mob
Signal: G:582 A:524 T:724 C:447 AvgSig: 569
C#:14 W:C3 Plate Name:00040811
TS:39 CRL:892 QV20+:929
Inst Model/Name:3730/Albany-1519-011
Sequence Scanner v1.0
Pure Base QVs:
Mixed Base QVs:
Printed on: Jun 09,2012 17:10:20 NZST
Electropherogram Data Page 3 of 4

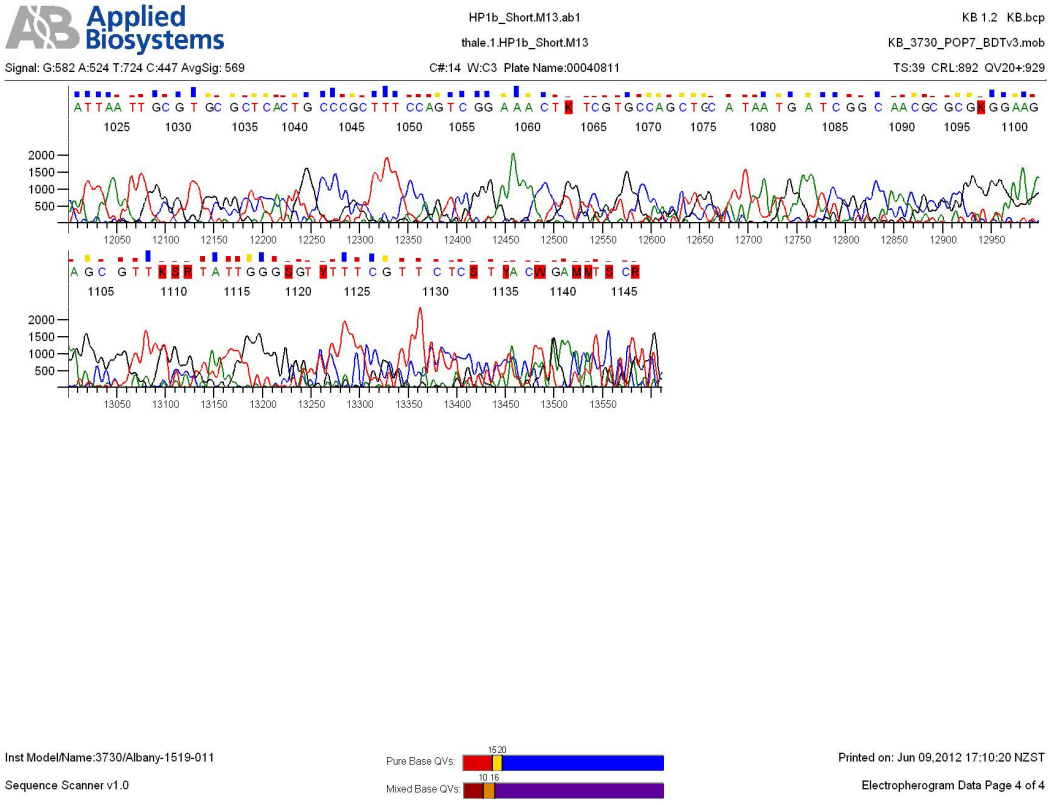
Applied Biosystems
HP1b_Short.M13.ab1
KB 1.2 KB.bcp
thale.1.HP1b_Short.M13
KB_3730_POP7_BDTv3.mob
Signal: G:582 A:524 T:724 C:447 AvgSig: 569
C#:14 W:C3 Plate Name:00040811
TS:39 CRL:892 QV20+:929
Inst Model/Name:3730/Albany-1519-011
Sequence Scanner v1.0
Pure Base QVs:
Mixed Base QVs:
Printed on: Jun 09,2012 17:10:20 NZST
Electropherogram Data Page 4 of 4

Chromatogram obtained from sequencing the PCR product of the HP1γ primers

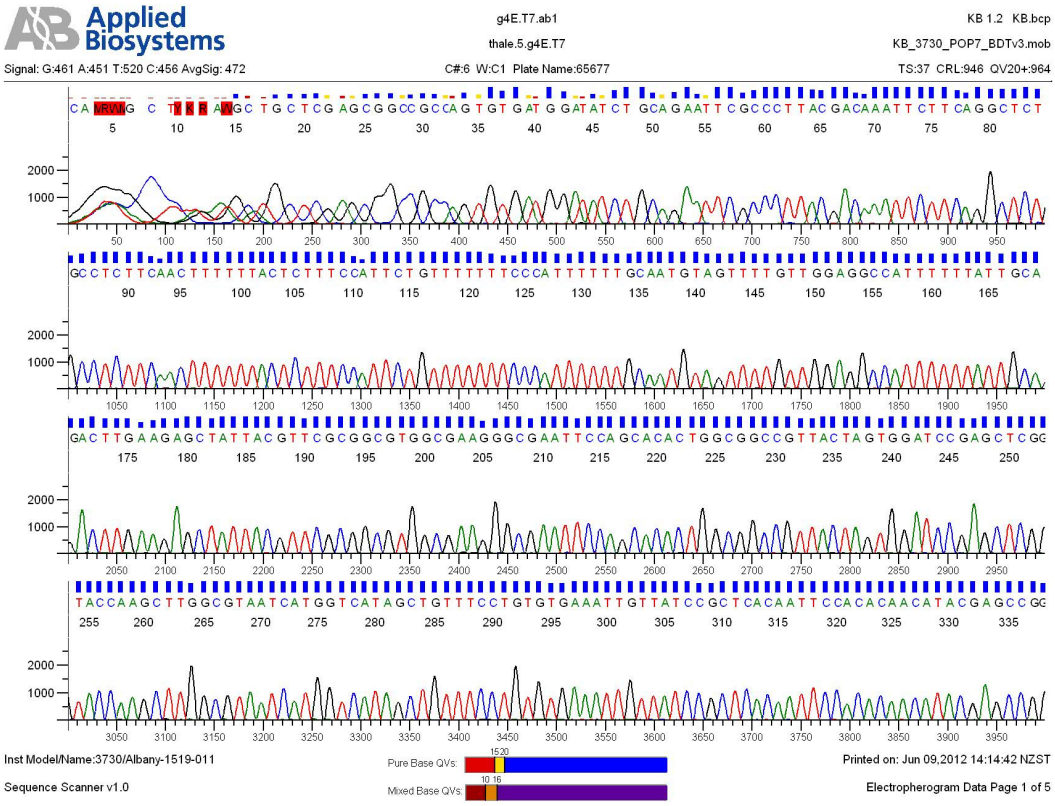

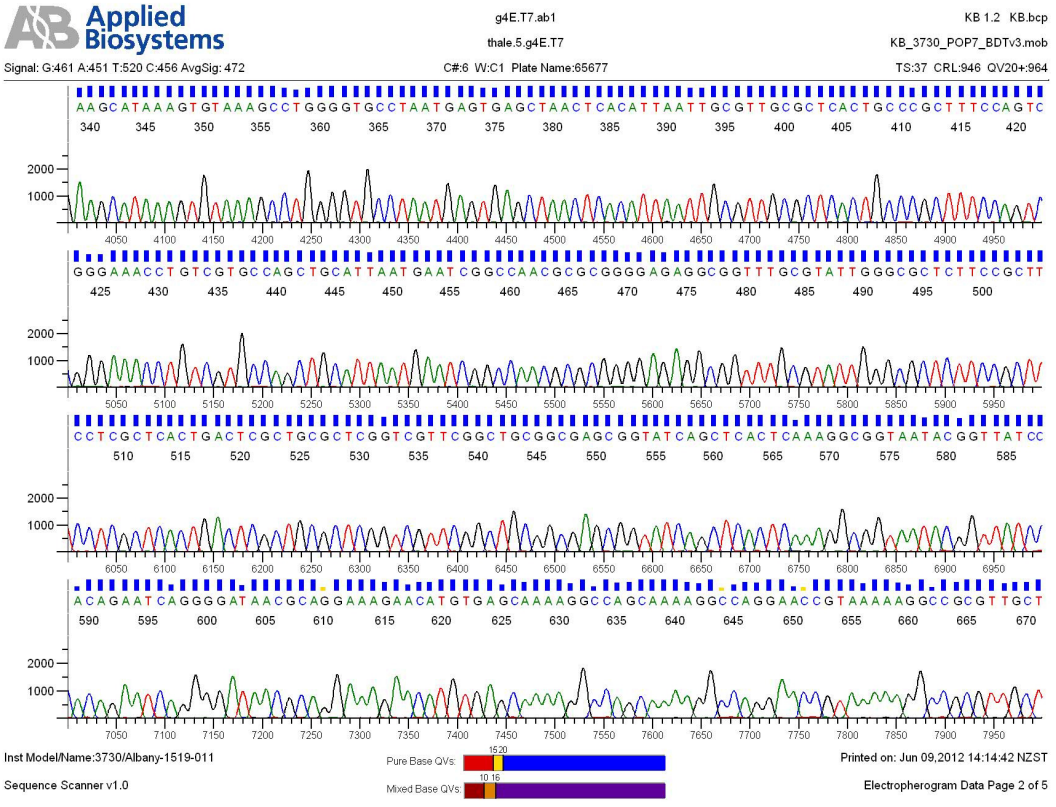

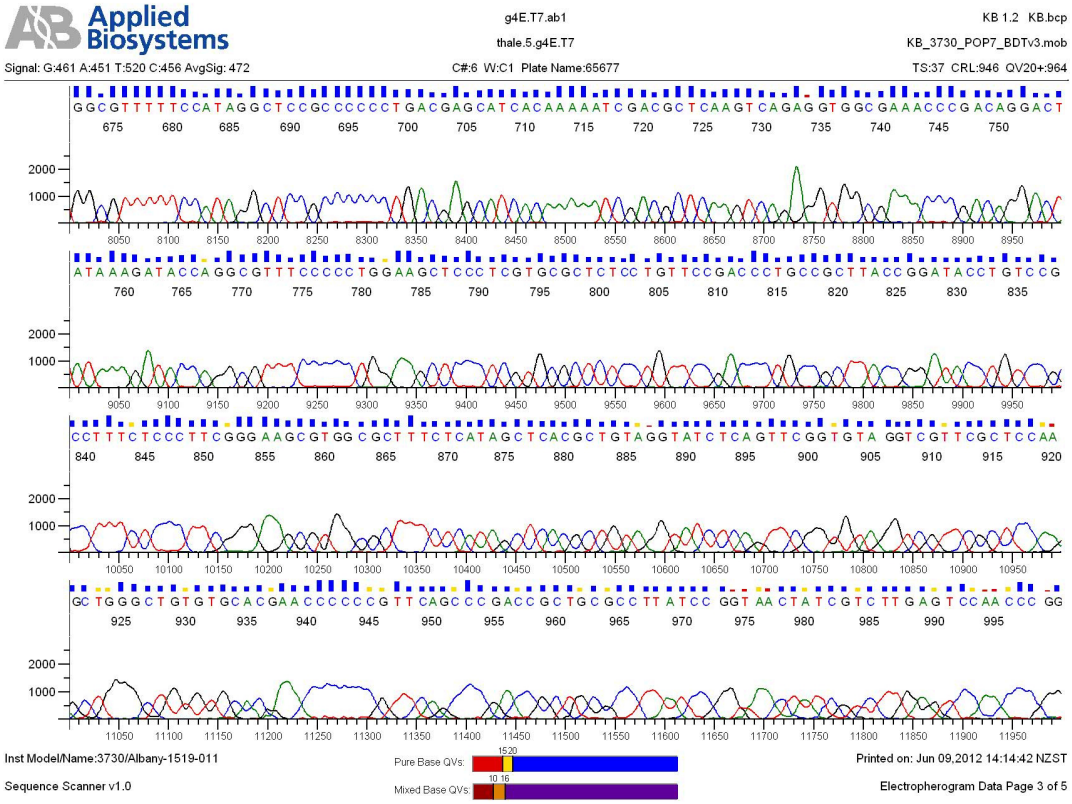
Applied Biosystems
g4E.T7.ab1
thale.5.g4E.T7
KB 1.2 KB.bcp
KB_3730_POP7_BDTv3.mob
Signal: G:461 A:451 T:520 C:456 AvgSig: 472
C#:6 W:C1 Plate Name:65677
TS:37 CRL:946 QV20+:964
Inst Model/Name:3730/Albany-1519-011
Sequence Scanner v1.0
Pure Base QVs:
Mixed Base QVs:
Printed on: Jun 09,2012 14:14:42 NZST
Electropherogram Data Page 3 of 5

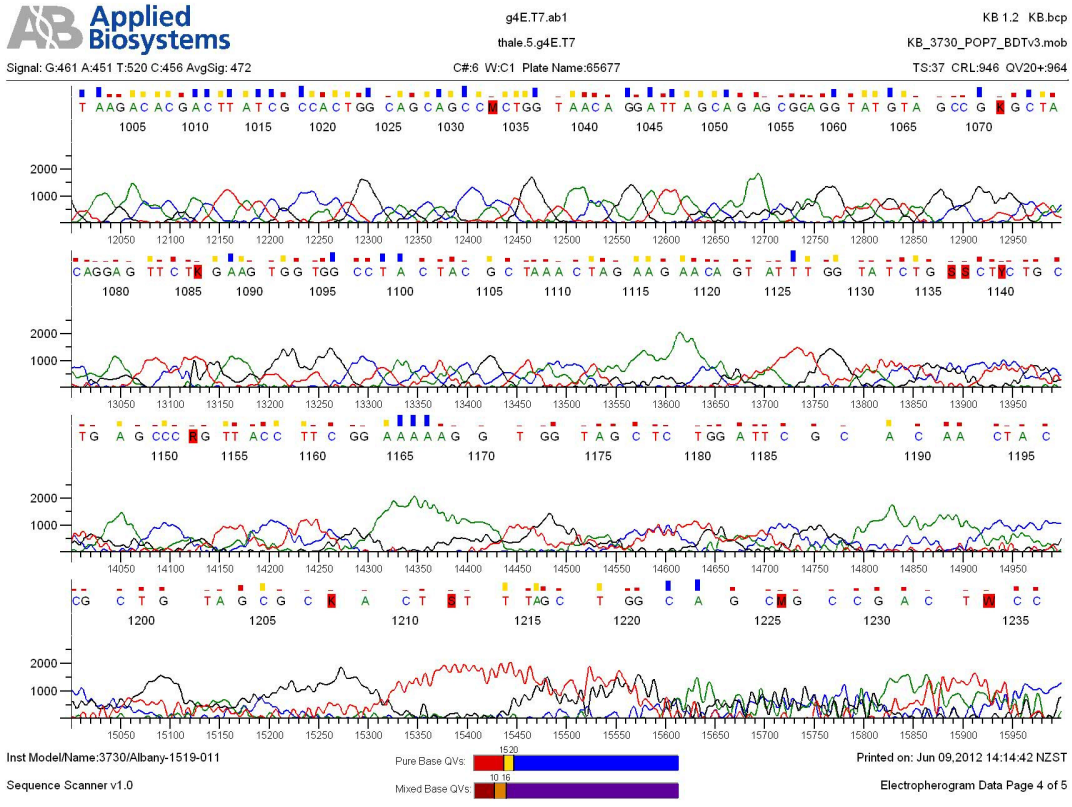
Applied Biosystems
g4E.T7.ab1
thale.5.g4E.T7
KB 1.2 KB.bcp
KB_3730_POP7_BDTv3.mob
Signal: G:461 A:451 T:520 C:456 AvgSig: 472
C#:6 W:C1 Plate Name:65677
TS:37 CRL:946 QV20+:964
Inst Model/Name:3730/Albany-1519-011
Sequence Scanner v1.0
Pure Base QVs:
Mixed Base QVs:
Printed on: Jun 09,2012 14:14:42 NZST
Electropherogram Data Page 4 of 5

Applied Biosystems

g4E.T7.ab1 | KB 1.2 KB.bcp

thale.5.g4E.T7 | KB_3730_POP7_BDTv3.mob

Signal: G:461 A:451 T:520 C:456 AvgSig: 472 | C#:6 W:C1 Plate Name:65677 | TS:37 CRL:946 QV20+:964

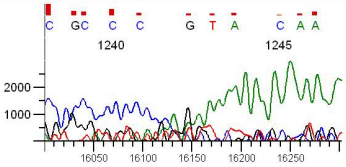

Inst Model/Name:3730/Albany-1519-011

Sequence Scanner v1.0

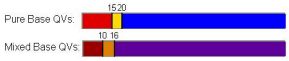

Printed on: Jun 09,2012 14:14:42 NZST

Electropherogram Data Page 5 of 5

Chromatogram obtained from sequencing the PCR product of the β-actin primers

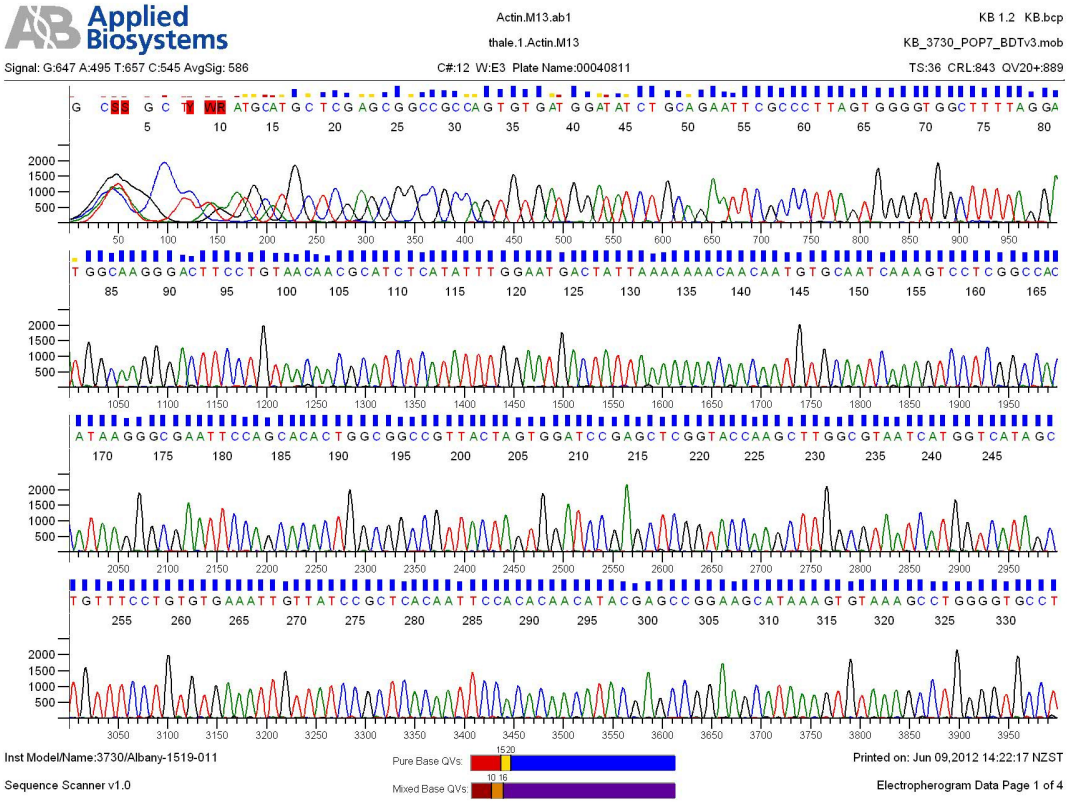

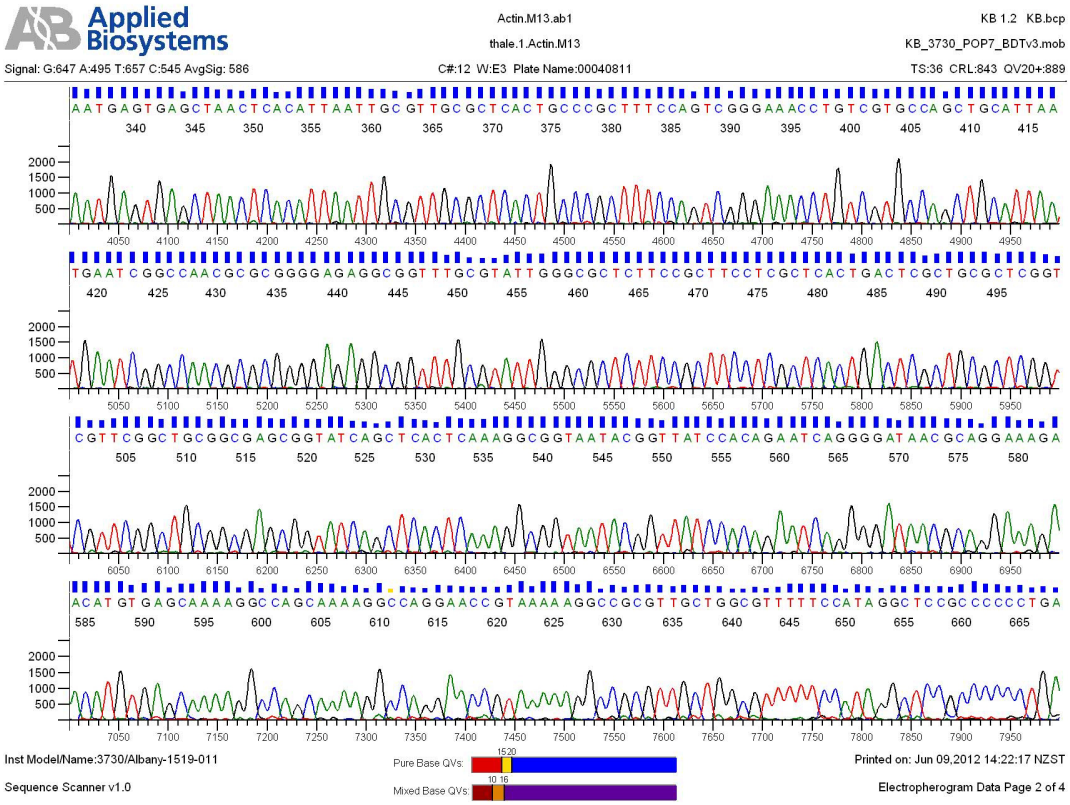

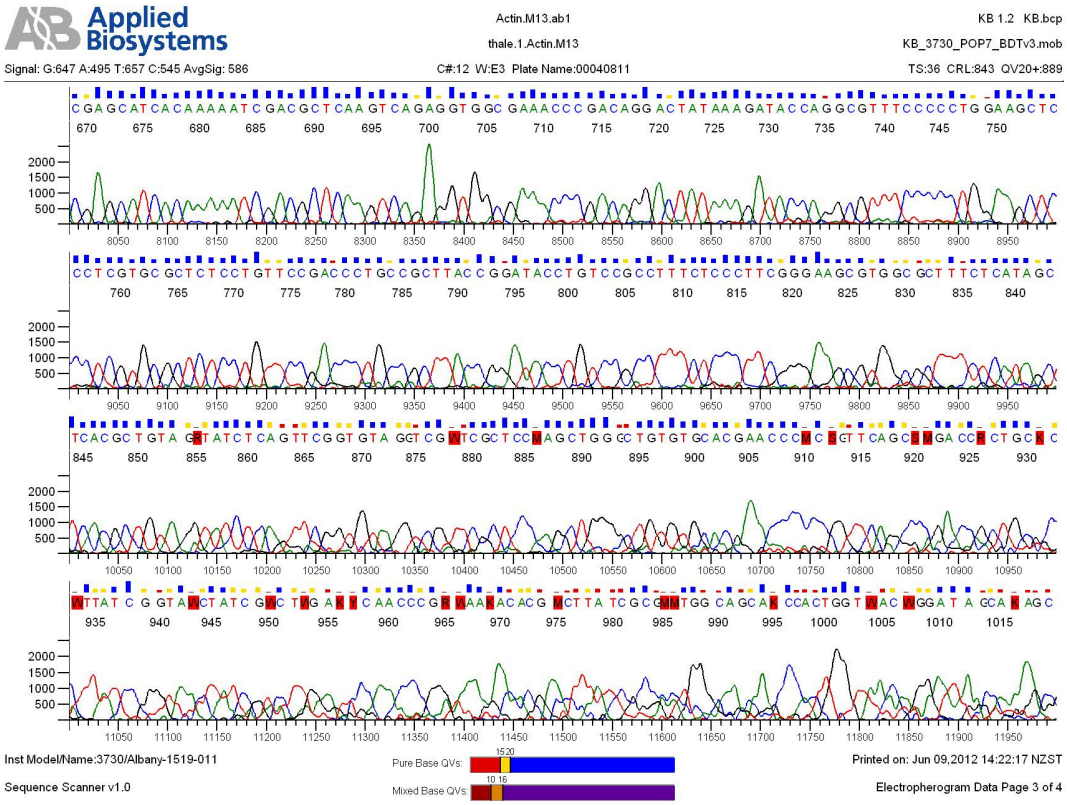
Applied Biosystems
Actin.M13.ab1
thale.1.Actin.M13
KB 1.2 KB.bcp
KB_3730_POP7_BDTv3.mob
Signal: G:647 A:495 T:657 C:545 AvgSig: 586
C#:12 W:E3 Plate Name:00040811
TS:36 CRL:843 QV20+:889
Inst Model/Name:3730/Albany-1519-011
Sequence Scanner v1.0
Pure Base QVs:
Mixed Base QVs:
Printed on: Jun 09,2012 14:22:17 NZST
Electropherogram Data Page 3 of 4

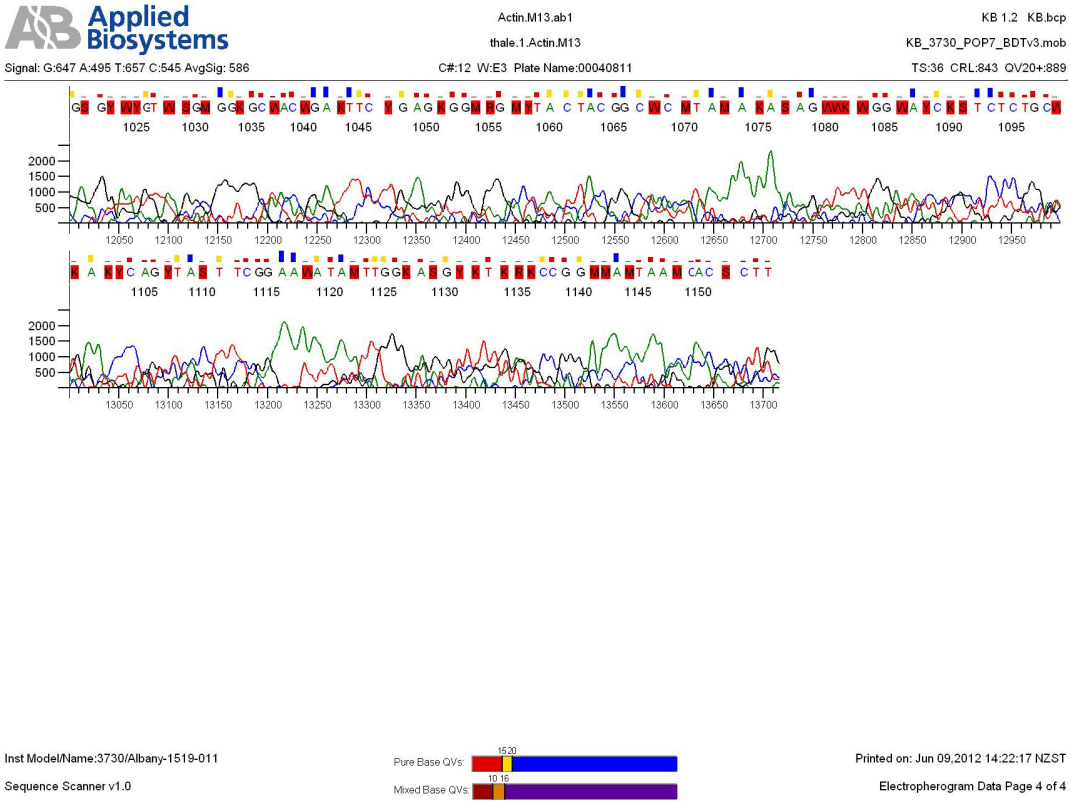
Applied Biosystems
Actin.M13.ab1
thale.1.Actin.M13
KB 1.2 KB.bcp
KB_3730_POP7_BDTv3.mob
Signal: G:647 A:495 T:657 C:545 AvgSig: 586
C#:12 W:E3 Plate Name:00040811
TS:36 CRL:843 QV20+:889
Inst Model/Name:3730/Albany-1519-011
Sequence Scanner v1.0
Pure Base QVs:
Mixed Base QVs:
Printed on: Jun 09,2012 14:22:17 NZST
Electropherogram Data Page 4 of 4